UNDERSTANDING CHAPERONE INTERACTIONS IN DISEASE

by

Nitika

A dissertation submitted to the faculty of
The University of North Carolina at Charlotte
in partial fulfillment of the requirements
for the degree of Doctor of Philosophy in
Biological Sciences

Charlotte

2021

Approved by:

_____
Dr. Andrew Truman

_____
Dr. Christine Richardson

_____
Dr. Shan Yan

_____
Dr. Richard Chi

_____
Dr. Mehdi Mollapour

_____
Dr. Kirill Afonin

ABSTRACT
NITIKA. Understanding Chaperone interactions in disease.
(Under the direction of DR. ANDREW W. TRUMAN)

The correct folding of proteins after synthesis and stress-promoted denaturation is critical for cell viability in all organisms. The Hsp70 molecular chaperone is a key player in proteostasis, deciding which proteins are foldable and which are too badly damaged and need to be targeted for degradation. Hsp70 plays an important role as a drive of cancer, stabilizing key mutated oncoproteins such as HER2, p53, RNR, SHR and MUC1. This importance of Hsp70 in basic cell functions as well as human illness prompted us to examine novel ways to characterize Hsp70 genetic and physical interactors. In this thesis, we decided to tackle three main roadblocks in studying chaperone interactions; 1) purification of chaperone complexes at native stoichiometry in mammalian cells, 2) understanding the roles of co-chaperones in cancer 3) teasing apart bridged vs direct chaperone interactions. To solve the issue of native stoichiometry purification, we have utilized CRISPR-Cas9 genome engineering to insert epitope tags into the N-terminus of Hsp70 in mammalian cells. This tagged chaperone is present as the only Hsp70 in cells, is stable without the use of any selectable marker and allows expression of Hsp70 at native levels. To understand co-chaperone function in cancer, we used a novel chemogenomic screening technology on WT and DNAJA1 knockout HAP1 cells. In doing so, we have uncovered a dependence of a large proportion of approved oncology drugs on DNAJA1 status. Finally, we have used cross-linking mass spectrometry to define for the first time the direct interactors of Hsp70 in yeast. Our data reveals a wealth of information of fundamental Hsp70 function including discovery of active Hsp70 dimers, client binding

throughout Hsp70 and a huge number of novel PTM-associated Hsp70 interactions. Overall, aside from gaining fundamental insight into the workings of Hsp70, this thesis provides a roadmap and tools for the chaperone community to explore novel biologically relevant Hsp70 interactions.

DEDICATION

In the loving memory of my dad who wanted me to be a doctor,

my mom, for sending me thousands of miles away to pursue my dreams

my brother, for always supporting me

and our loving dog, Jerry

Thanks for being there for me every step of the way.

ACKNOWLEDGEMENTS

First and foremost, I would like to thank my mentor, Dr. Andrew Truman. This journey began with my first email to you for joining your lab as a graduate student when you replied "You have exactly the right experience I am looking for! I think you would be very well suited for working in my lab." Those words of encouragement touched my heart, and that is when I knew that I wanted to join your lab. Words can't express enough gratitude for being the most amazing mentor I could ever ask. You have always supported and encouraged me even with my crazy experimental ideas. You taught me what it takes to be a scientist. Your optimistic nature and enthusiasm for science and research is infectious. I have learned a lot under your mentorship ranging from our daily scientific discussions to critiquing research articles, presenting research and publishing. Not only have you been a fantastic mentor to me, but you have taught me how to mentor other people. Thank you for being such a great role model. I owe all my success to you. Truly I have been lucky to have you as my PI. I will remain forever grateful to you. I will miss my times in the Truman Lab.

To my committee members Dr. Christine Richardson, Dr. Shan Yan, Dr. and Dr. Mehdi Mollapour, Dr. Richard Chi and Dr. Kirill Afonin, thank you all for your support and feedback throughout my graduate research. Additionally, to Dr. Richardson, you have always helped me whether its training on FACS ARIA, degree requirements or with recommendations for fellowships, I thank you for always being there. Dr. Shan Yan, thank you for your Cell Biology class, endless recommendation letters and insightful advice on

my career. Thank you, Dr. Mehdi Mollapour, for inspirational research and always being supportive. Thanks to Dr. Richard Chi for your teachings in Advanced Cell Biology class, one of the best classes of my coursework and always being helpful and supportive whenever I needed help with some experiments or lab reagents. Thanks to Dr. Didier Dreau for training me on FACS FORTESSA, helping me with my cancer cell line/spheroid experiments and making the department a fun place to work even during the crazy covid times and holidays. I will miss the pranks, fun banter, life discussions and your valuable advice. Thanks to Dr. Adam Reitzel for hiring me as an RA on your project and helping me with my CPT and graduate school related work. Thanks to Dr. Pinku Mukherjee and Dr. Valery Grdzelishvili for their valuable advice and support during my graduate studies. Thanks to Dr. Paola Lopez-Duarte for letting me use the Leica microscope and buying the YFP filter for my experiments.

I would like to thank the many undergraduates and graduates, past and current, members of Truman lab including Jill Waller, Jackob Blackman, Megan Ward, Lizbeth Saa, Siddhi Paranjape, Jade Takakuwa, Alexandria Szalanscy, Stephanie Delgado, Neha Galla and Victoria. Thanks to Dr. Bo Zheng for helping me out with my experiments. Thanks to Courtney Shrader for the amazing baked goods you made and cheering me up.

I would like to extend special thanks to my lab mate Dr. Laura Knighton. You have been such a great friend over these years giving me advice, from our outings, exploring and trying out new things, you have always been there for me whenever I needed some help.

Special thanks to Isaac Sluder, Monserrat Cuevas, Bryant Maldonado, Elvira An and Devin Clegg who made me feel at home when I first joined the lab. I can’t express enough

gratitude to you guys for your kind and big hearts. From our late-night lab experiments to dinners, movies, competitive badminton games, and pushing me to try new things, you guys are and will always be part of my American family! I love you guys!

Thanks to all the Chi lab members past and present Trey Grissom, Jonathan Taylor and Henry Weaver for making our shared lab space a fun place to work at.

Thanks to all the labs in the department form which I have borrowed lab reagents for my experiments.

Thanks to Dr. Ken Piller, Dr. Abhishek Dey, Dr. Sebastien Felt, Dr. Christian Bressy, Dr. Ru Zhou, Dr. Michelle Pass and Dr. Brittany Johnson for their valuable advice over the years.

Thanks to all my friends in department over the years, Dr. Priyanka Grover who is always there for me and helps me solve my problems. Thanks for always being there for me.

Thanks to Shreya Goyal for being my sous chef in cooking/baking for de-stressing, paint and sip sessions and the moral support without which I might have gone crazy in past few years of graduate school. Thanks to Dr. Austin Jefferies and Sara Seegers for always listening to me and being great friends.

Thank you to David Gray for helping me whenever any equipment broke down in the department.

Thank you to all the faculty and staff here in the Department of Biological Sciences specially Ruthie Moser, Brendan Bishop, Andrea Strong and the Graduate school.

Thanks to my friends in Upstate University specially Fiza Hashmi and Mark Woodford for being supportive and my cheerleaders. Thanks to Deepa Kumari from Brodsky lab to provide me reagents and boosting my moral.

Thanks to Professor K. Muralidhar for his valuable advice and being a great mentor, which got me where I am today.

Thanks to Professor Vani Brahmachari for training me in her lab and developing critical thinking in me.

Thanks to all my friends Shah Hussain, Harsimrut Kaur, Amjad Ali, Shweta Mendiratta Soni, Kartik Soni, Jayant Maini, Gunjan Kak, Mohsin Raza, Hina Khushboo, Vikrant Goswami, Alok Rout for their valuable scientific advice, discussions and cheering me up whenever I needed moral support during this journey.

I owe my family a huge amount of gratitude for always supporting me no whatever what.

To my mom, Sucksham, thanks for your valuable teachings, always encouraging and supporting me.

To my brother Sidharth, thanks for making me laugh, helping me out navigating difficult times and being there for me always.

TABLE OF CONTENTS

LIST OF FIGURES xii

LIST OF ABBREVIATIONS xiv

CHAPTER 1: INTRODUCTION 1

CHAPTER 2: ENDOGENOUS EPITOPE TAGGING OF HEAT SHOCK PROTEIN ISOFROM HSC70 USING CRISPR/CAS9 41

2.1 Introduction 41

2.2 Materials and Methods 43

2.3 Results 48

2.4 Discussion 52

2.5 Figures 56

2.6 References 61

CHAPTER 3: CHEMOGENOMIC SCREENING IDENTIFIES THE HSP70 CO-CHAPERONE DNAJA1 AS A HUB FOR ANTICANCER DRUG RESISTANCE 64

3.1 Introduction 64

3.2 Materials and Methods 66

3.3 Results 69

3.4 Discussion 74

3.5 Figures and Tables 80

3.6 Reference 87

CHAPTER 4: AN ATLAS OF BIOLOGICALLY IMPORTANT PTM-ASSOCIATED HSP70 INTERACTIONS UNCOVERED THROUGH CROSSLINKING PROTEOMICS 90

4.1 Introduction 90

4.2 Materials and Methods 92

4.3 Results 102

4.4 Discussion 111

4.5 Figures and Tables 117

4.6 References 141

CHAPTER 5: CONCLUSIONS 146

REFERENCES 149

APPENDIX 161

Publications

Contributions, Honors, and Awards

LIST OF FIGURES

CHAPTER 1

Figure 1. The post-translational modifications of mammalian Hsp70, Hsc70, BiP and yeast Ssa1-4. 37

Figure 2. Locations of PTMs on the Hsp70 structure. 38

Figure 3. Conservation of Hsp70 PTMs and surrounding sequence between Hsp70 isoforms. 39

Figure 4. The hallmarks of Hsp70 regulation. 40

CHAPTER 2

Figure 5. Design of a tandem HIS-FLAG epitope suitable for endogenous tagging of Hsc70. 56

Figure 6. Expression of Cas9-2A-GFP in HEK293T cells transfected Hsc70-gRNA-pX458. 56

Figure 7. Determining CRISPR-mediated cleavage using SURVEYOR assay. 57

Figure 8. Schematic and results of a PCR-based assay (in-out PCR). 57

Figure 9. Western Blot analysis of single-cell-derived HEK293T clones. 58

Figure 10. CRISPR-mediated tagging of Hsc70 is isoform specific. 59

Figure 11. Validation of known Hsc70 interactions in HEK293THIS-FLAG-Hsc70 cells. 60

CHAPTER 3

Figure 12. DNAJA1 is altered in cancer. 80

Figure 13. Sensitivity of WT and DNAJA1 knockout cells to the NIH Approved Oncology Collection. 81

Figure 14. Drug interaction between 116-9e (DNAJA1 inhibitor) and selected hits. 82

Figure 15. Effect of combination treatments on prostate cancer spheroids. 83

Figure 16. Expression of various chaperone/co-chaperone proteins in HAP1 WT/DNAJA1 knockout cells. 84

Figure 17. Effects of selected FDA-approved drugs on LnCaP cells. 85

CHAPTER 4

Figure 17. Cross-linking mass spectrometry of Ssa1 complexes. 117

Figure 18. A proportion of Ssa1 exists as dimer. 118

Figure 19. Novel clients and post translationally modified clients identified on yeast Hsp70 based on XL-MS. 119

Figure 20. HIR complex is a novel client of Hsp70 in yeast and humans. 120

Figure 21. Pim1 phosphorylation regulates mitochondrial clearance in an Ssa1-dependent manner. 121

Figure 22. Mtw1 is a client of Hsp70 and is regulated by phosphorylation. 122

Figure 23. Ste11 dimethylation impacts the osmotic stress response in an Ssa1-dependent manner. 123

Figure 24. Supplementary 1 124

Figure 25. Supplementary 2 125

Figure 26. Supplementary 3 126

LIST OF ABBREVIATIONS

Hsp70 – Heat Shock Protein 70

Hsc70 - Heat Shock Cognate 70

BiP – Binding Protein

NBD - Nucleotide-binding domain

SBD - Substrate-binding domain

NTD – N terminal domain

CTD - C-terminal domain

PTM – Post Translational Modification

CRISPR/Cas9 – Clustered regularly interspaced short palindromic repeats

AP-MS/MS - Affinity Purification Mass Spectrometry

IP - Immunoprecipitation

sgRNA – short guide Ribonucleic acid

FACS – Flow Cytometry Associated Cell Sorting

CRPC - Castration-Resistant Prostate Cancer Cell

NEF - Nucleotide Exchange Factors

JDP – J domain Proteins

HTS - High-Throughput Drug Screening

DMSO- Dimethyl Sulfoxide

CI – Combination Index

XL-MS – Cross linking Mass Spectrometry

DSSO - Disuccinimidyl Sulfoxide

LC-MS – Liquid chromatography mass spectrometry

GO - Gene ontology

BiFC – Bimolecular fluorescence complementation

Hir – Histone regulation

GFP – Green fluorescent protein

Mtw1 – Mis twelve like

Mis12 – Mis twelve

Lonp1 – Lon Protease

BZ - Bortezomib

NLS – Nuclear localization signaling

CHAPTER 1: INTRODUCTION

This chapter has been published:

Nitika[1,#], Corey M. Porter[2,#], Andrew W. Truman[1,†,*] and Matthias C. Truttmann[2,3, †,*] Hsp70 post-translational modifications: Expanding the chaperone code.

General introduction

The heat shock protein 70 (Hsp70) family consists of well-conserved yet functionally diverse molecular chaperones that are critical for nascent protein folding (1), clearance of misfolded/unfolded proteins (2), prevention of stress-induced protein aggregation (3), disaggregation of existing protein deposits, protein degradation (4), and chaperone-mediated autophagy (5). Mutations in genes encoding components of the Hsp70 system are linked to several human diseases, including Parkinson's disease (6-9), diabetes mellitus (10), colorectal cancer (2, 11) and cardiomyopathy (12, 13). As an integral part of the cellular proteostasis machinery, Hsp70s are critical for maintaining cell viability in response to a large variety of cellular stresses, including high temperature, nutrient starvation, osmotic shock, oxidative stress, and DNA damage (2). Historically, studies on Hsp70s have primarily focused on intrinsic folding activity driven by the binding and hydrolysis of ATP, interaction with helper co-chaperones, and inducibility of expression under stress. More recently, evidence has accumulated that Hsp70s are highly modified at the post-translational level (14-18). These modifications fine-tune chaperone function, altering chaperone activity, localization, and selectivity. In the same way that modifications on histones are collectively called the “histone code,” we now refer to the complex array of post-translational modifications (PTMs) on chaperones as the “chaperone code.” In this review, we summarize in detail the current knowledge of how PTMs contribute to the

regulation of Hsp70 family chaperones. We further offer a perspective on future directions and challenges the field may encounter in establishing and integrating the physiological impact of the Hsp70 chaperone code.

The Hsp70 family of proteins is evolutionarily conserved and found in archaebacteria, prokaryotes, and eukaryotes (including plants and animals), establishing it as a crucial protein family in the phylogenetic tree of life (19-21). Hsp70s have been widely studied both *in vitro* and *in vivo*, using a combination of purified recombinant proteins, tissue culture setups, and model organism such as *Saccharomyces cerevisiae* (budding yeast). A testament to the high level of functional conservation is the ability of Hsp70s from diverse organisms (human, sea anemone, and plant) to maintain the cell viability of budding yeast when expressed as the sole cytosolic Hsp70 (22). *S. cerevisiae* contains seven cytosolic Hsp70 isoforms: the four canonical chaperones Ssa1, Ssa2, Ssa3, and Ssa4 and the three ribosome-associated chaperones Ssb1, Ssb2, and Ssz1. In addition, there are three mitochondrial isoforms (Ssc1, Ssq1, and Ecm10) and one specific to endoplasmic reticulum (Kar2) (23). Ssa1 and Ssa2 are constitutively expressed, whereas Ssa3 and Ssa4 are not present during normal growth but up-regulated in response to stress and in the stationary phase (24-27). Yeast mutants lacking all four canonical Hsp70 chaperones are not viable (28). Ssa1–4 are partially functionally redundant, with overexpression of any single Ssa isoform enough to provide cell viability in an *ssa1–4*Δ strain (22).

Human Hsp70s are encoded by a multigene family, which constitutes 17 genes and 30 pseudogenes (29). This multigene family gives rise to 13 gene products, which vary in their location, amino acid composition, and expression levels in the cell. Hsp70-1 (HSPA1A, Hsp70) and Hsp70-2 (HSPA1B, Hsp70) are the two major stress-inducible isoforms, which

only differ from each other by two amino acids. The noninducible Ssz-like chaperone Hsp70-1t (HspA1L) is constitutively expressed and exhibits 90% identity to Hsp70-1. Hsp70-5 (HSPA5/BiP/GRP78) is localized to the endoplasmic reticulum and facilitates transport and folding of nascent polypeptides into the ER lumen. Hsp70-6 (HspA6) is an additional stress-inducible Hsp70 family member that has 85% homology to Hsp70-1 and is expressed in moderate levels in dendritic cells, monocytes, and natural killer cells but has no detectable basal expression level in other cells. HSPA7 has been considered a pseudogene transcribed in response to stress. Hsp70-8 (HSPA8, Hsc70, Hsp73, Hsc72) is the cognate Hsp70 family member that exhibits essential housekeeping functions such as folding of nascent polypeptides and misfolded proteins. Hsp70-9 (HSPA9, mortalin, GRP75, mtHsp70) is a mitochondrial Hsp70 isoform that bears a 46-amino acid target signal responsible for localization to the mitochondrial lumen (30, 31). Global knockouts of constitutively expressed Hsp70 isoform HSPA5, HSPA8, or HSPA9 are lethal, highlighting the central role of these chaperones in cellular physiology (32, 33).

Structural features of Hsp70 proteins

Structurally, Hsp70s consists of a 45-kDa N-terminal nucleotide-binding domain (NBD) and a 28-kDa substrate-binding domain (SBD) that are connected by a flexible linker (Figure 1, Figure 2) (34, 35). The NBD consists of four subdomains (IA, I, IIA, and IIB), which are required for the binding and hydrolysis of ATP to ADP. The SBD is further subdivided into a 15-kDa substrate-binding domain (SBDβ) and a 10-kDa helical lid domain (SBDα) acting as a flexible lid. The hydrolysis of ATP promotes NBD-conformational changes, which are transduced through the linker domain and trigger the clamping down of the lid domain onto unfolded protein clients, preventing substrate

dissociation and providing an opportunity for the protein to obtain its native fold (1). The release of ADP and subsequent binding of fresh ATP promotes the release of the folded substrate, setting Hsp70 up for the next round of folding.

Regulation of Hsp70 function

The activity of Hsp70 family chaperones is tightly regulated. A first layer of regulation is provided by the rapid expression of stress-inducible Hsp70 isoforms in the presence of protein-unfolding stress. The up-regulation of Hsp70-1 and Hsp70-2 in the cytoplasm and BiP in the ER are key events during the induction of cellular stress responses, such as the heat shock response or the unfolded protein response in the ER (UPR^{ER}). These compartment-specific Hsp70 enrichments provide cells with enhanced protein (re)folding capacities to prevent or resolve stress-induced damage. Historically, Hsp70 was thought to exist primarily in a monomeric state, but recent evidence suggests that Hsp70 can form monomers, dimers, trimers, and higher-order oligomers (36). Although the functions of these high-order forms have not been fully delineated, they are clearly required for at least a subset of chaperone functions (36-38). The Hsp70 folding cycle is accelerated and regulated by a suite of co-chaperone proteins, including Hsp40s and nucleotide exchange factors (NEFs). Hsp40s are a heterogenous family of co-chaperones bearing a conserved J-domain required for binding to Hsp70 (39). These co-chaperones can bind to unfolded proteins via their C terminus to prevent aggregation and transport them to Hsp70 for folding/refolding. Hsp40s also play a more direct role in regulating Hsp70 by directly stimulating the ATP hydrolysis activity of Hsp70, locking the client into the closed SBD (39, 40). Once a client protein is folded, NEFs facilitate ADP release and mediate the exchange of ADP with ATP, which is required for the opening of the lid and the release of

the folded client from the SBD (34, 35, 41-45). Another class of co-chaperones that regulate Hsp70 activity includes the tetratricopeptide repeat proteins Hip, Hop, and CHIP. Hip prevents the dissociation of ADP from Hsp70 binding to its NBD (46, 47). Hop coordinates with both Hsp70 and Hsp90 and targets Hsp90 to the Hsp70-client protein complex (48-50). CHIP acts as an E3 ubiquitin ligase, ubiquitinating Hsp70 substrates, which results in their degradation by the proteasome (51). The number of highly related co-chaperones (*e.g.* 13 NEFs and 41 J-domain–containing proteins in humans) substantially exceeds the number of Hsp70 isoforms, consistent with the idea that they are critically involved in regulating the functional diversity of Hsp70s (3).

History of the Hsp70 chaperone code

Early studies that identified modification of Hsp70 were generally descriptive in nature. PTMs, such as phosphorylation, were detected on chaperones, yet the sites of modification, their regulation, and their function remained elusive (52-54). A decrease in cost and increase in the resolution of proteomic experiments led to an abundance of PTMs being discovered on Hsp70s. In 2012, bioinformatic attempts to characterize regions of functionally important PTMs on proteins ("hotspots") identified two such hotspots on Hsp70 (55). The first region was located in the NBD (Thr-36 and Thr-38), whereas the second is present on the SBD (Thr-492, Ser-495, and Thr-499). Mutation of these sites led to viable cells that exhibited compromised chaperone function, including an inability to refold denatured proteins and increased global protein aggregation (55). The first mechanistic study of an Hsp70 PTM was published later in 2012, when it was demonstrated that a conserved site on Hsp70 was phosphorylated by cell cycle kinases, leading to altered cyclin stability (56). Follow-up studies demonstrating that both C-terminal

phosphorylation and methylation of Hsp70 can impact chaperone function led to the proposal of the "chaperone code" (14, 57, 58). In this model, multiple cellular signals converge on Hsp70 (and indeed other chaperones such as Hsp90), leading to the fine-tuning of chaperone interactions and altered flow of information through cellular pathways.

More recently, bioinformatics-based approaches, molecular weight shift analysis, isoelectric properties of protein, isotope labeling, and high-resolution MS have been used to uncover many more PTMs on the Hsp70 family of proteins, including acetylation, methylation, ubiquitination, SUMOylation, AMPylation, and ADP-ribosylation. Thankfully, several online resources facilitate tracking and interpreting the potential impact of Hsp70 PTMs. PhosphositePlus® (RRID:SCR_001837) is a comprehensive and curated online resource that collects information regarding the target proteins/residues and functional implications of abundant PTMs, such as phosphorylation, acetylation, methylation, ubiquitination, and *O*-glycosylation (59). The Global Proteome Machine Database (RRID:SCR_006617) is another excellent resource and is updated on a daily basis (60). Analysis of the available data from sites such as these reveals an astonishing number of PTMs on Hsp70s (Fig. 1). Below, we summarize the current state of knowledge of Hsp70 PTMs, including phosphorylation, acetylation, ubiquitination, AMPylation, ADP-ribosylation, and methylation, and their conservation and potential interplay.

Hsp70 phosphorylation

Over 100,000 phosphorylation events occur in mammalian cells, and improper protein phosphorylation is the cause of many human pathologies (61). Hsp70 family proteins are highly phosphorylated; a total of 88, 87, and 70 phosphorylated sites have been identified so far on Hsc70, BiP, and yeast Ssa1, respectively (Figure 1, Figure 2). Nevertheless, a

mechanistic understanding of how individual phosphorylation events impact distinct Hsp70 functions remains elusive, with exceptions discussed below.

Hsp70 phosphorylation in cell cycle progression and cell proliferation

Cells must tightly coordinate growth and division in response to a variety of internal and external cues that include nutrient availability and genome integrity. These signals are sensed and propagated throughout cells via complex interlinked signal transduction pathways. Early studies on the cell cycle had demonstrated a role for the yeast co-chaperone Ydj1 in regulating the entry of the Cln3 G_1 cyclin into the nucleus (62). Cln3 possesses a J-domain–like region and competes with Ydj1 for binding to Ssa1. In 2012, Truman *et al.* (56) established that the molecular trigger for displacement of Ydj1 and recruitment of Cln3 was phosphorylation of Ssa1 on Thr-36 mediated by two related CDKs (Pho85 and Cdk1). These two kinases activate Thr-36 under different cellular conditions. During periods of nutrient scarcity, Pho85 phosphorylates Ssa1, promoting Cln3 recruitment to Ssa1 and its eventual destruction, leading to G_1 cell cycle arrest. In cycling cells, transient Thr-36 phosphorylation of Ssa1 by Cdk1 promotes Cln3 destruction at the end of G_2/M, resetting G_1 cyclin levels in preparation for the beginning of the next cell cycle. Suggesting an evolutionarily conserved mechanism, phosphorylation of the equivalent Thr-38 residue on mammalian Hsc70 promotes Hsc70-cyclin D1 interaction and cyclin D1 destruction.

Although clearly important for G_1/S progression, Hsp70 phosphorylation can also impact later stages of the cell cycle. Polo-like kinase 1 (Plk1) is another serine/threonine kinase that regulates mitotic entry to cytokinesis and cell cycle progression (63). In arsenic trioxide–treated mitotically arrested HeLa S3 cells, Plk1 phosphorylates Hsp70 at five

sites: Thr-13, Thr-226, Ser-326, Ser-631, and Ser-633. The phosphomimetic mutants of Ser-631 and Ser-633 increase the proportion of cells arrested at mitosis. Thus, Plk1-mediated phosphorylation of Hsp70 plays a protective role against cell death by apoptosis. However, the significance of the other three phosphorylation sites by Plk1 remains obscure, and mechanisms by which Hsp70 provides protection remain to be explored. Hsp70 phosphorylated at Ser-631 and Ser-633 co-localizes with Plk1 at the centrosome. This association leads to an increase in microtubule stability, elongation of mitotic spindles, and mitotic arrest. Furthermore, when the interaction of Hsp70 and Plk1 is inhibited by 2-phenylethynesulfonamide or by inhibiting Plk1 activity by using BI2536, the apoptotic inhibition is released and leads to cell death. Hence, the phosphorylation of Hsp70 at Ser-631 and Ser-633 promotes Hsp70's role as a centrosomal chaperone (64). Although the mechanism of this apoptotic release still remains unclear, the inhibition of Hsp70 phosphorylation or Plk1 inhibition might serve as a key to increase efficiency of arsenic trioxide as a chemotherapeutic drug. In addition to Plk1, the mitotic Nek6 kinase phosphorylates Hsp72 in the NBD at Thr-66, promoting recruitment of Hsp72 to the mitotic spindles (65). This phosphorylation event activates the alignment of chromosomes to the spindle equator by stabilizing kinetochore fibers. This is achieved via recruitment of two proteins, ch-TOG and TACC3, to kinetochore fibers. Phosphoinhibitory mutants of Hsp72 fail to localize at spindle poles, resulting in the destabilization of kinetochore fibers, leading to abnormal mitotic progression (65).

Whereas it has been known for several years that chaperones can bind and regulate MAP kinase function (66), a recent study suggests that mitogen-activated protein kinase pathway activity can in turn regulate chaperone function (67). Treatment of cells with epidermal

growth factor triggers Hsp70 phosphorylation on Ser-385 and Ser-400. These sites are particularly interesting as they reside on and adjacent to the flexible linker that connects the NBD and SBD of Hsp70. Phosphorylation of Hsp70 at these two sites leads to an extended conformation of the protein, which in turn increases the binding affinity of the clients (67). Mutation of these two sites results in cells that have a reduced viability and growth rate. Although clearly dependent on the activity of extracellular signal–regulated kinase (ERK), these two phosphorylation sites do not fulfill the minimum requirements for ERK phosphorylation (proline in the +1 position to the site of phosphorylation) and thus are highly unlikely to be direct ERK substrates (68-70). Interestingly, Ser-400 lies next to a putative NLS on the Hsp70 sequence, and the S400A mutation prevents its nuclear export (71). Going forward, it will be interesting to identify the specific kinase for these sites, the impact these sites have on co-chaperone binding, and the specific clients impacted that result in the increased cellular proliferation. Taken together, it is clear that several sites on Hsp70 and Hsc70 are regulated by multiple kinases throughout the cell cycle, in turn leading to the targeted stabilization/destabilization of key effectors of the cell cycle.

Hsp70 phosphorylation in cancer

Many of the driver mutations involved in cancer alter writer and eraser enzymes in signal transduction pathways (72). It is a likely conclusion that chaperone PTMs will be altered to varying degrees in different cancers. These changes may impact the stability of oncoproteins, activity of key pathways required for tumorigenesis, and anticancer drug resistance. A known example of this is alteration of methotrexate resistance in leukemia cells upon Hsc70 tyrosine phosphorylation. The interaction between Hsc70 and reduced folate carrier protein (RFC), the primary transporter of folate and antifolate drugs, regulates

cellular methotrexate uptake (73). Tyr-288 phosphorylation is required for the binding of Hsc70 to methotrexate. A phosphoinhibitory mutant of Tyr-288 disrupted the interaction between Hsc70-RFC and methotrexate, which affects its transport into the cells, rendering the cells resistant to this drug (35). Decreases in tyrosine phosphorylation of Hsc70 further lead to increased methotrexate resistance in these cells (74).

Hsp70 phosphorylation exerts anti-apoptotic properties upon serum starvation in hepatocellular carcinoma. Retinoic acid–induced 16 (RAI16) is a protein kinase A–anchoring protein, which gets activated in response to serum starvation and drives protein kinase A–mediated phosphorylation of Ser-486 on Hsp70, thus preventing caspase-3 cleavage and apoptosis (75). Further studies are required to identify the key players that mediate this phosphorylation and dephosphorylation events so that the properties of PTM-based Hsp70 and Hsc70 regulation in cancer can be utilized as a novel chemotherapeutic option.

Hsp70 phosphorylation as regulator of Hsp70 client triaging

Although Hsp70 is required for the folding of both new synthesized and misfolded proteins, it is also able to target damaged proteins for degradation via the ubiquitin-mediated proteasomal system (76). The strategy that Hsp70 uses to decide whether to fold or degrade a client still remains unclear. The protein-folding and degradation activities of Hsp70 are mediated by its co-chaperones Hop and CHIP, respectively. The co-chaperone binding to C-terminal of Hsp70 is facilitated by the interaction between the tetratricopeptide repeat region of both Hop and CHIP with the C-terminal domain of Hsp70 (77). Phosphorylation of Hsp70 at Thr-636 leads to an increase in Hsp70-HOP binding and a corresponding decrease in Hsp70-CHIP binding, leading to increased client stability. Loss of this

phosphorylation has the converse effect, triggering enhanced client degradation resulting from Hsp70-CHIP interaction (58). Similarly, another study demonstrated that the SBD of Hsp70 is phosphorylated by Akt1 at Ser-631, which decreases Hsp70-CHIP interaction (78). In this report, the downstream effect observed was to prevent degradation of superoxide dismutase-2 (SOD2) and promote the import of SOD2 into the mitochondria. In this way, Hsp70 regulates SOD2 activity and is a dynamic regulator of mitochondrial redox homeostasis.

Hsp70 phosphorylation in host-pathogen interactions

Hsp70 folds a large proportion of cellular proteins and thus supports the activity of a wide range of signaling pathways. It is thus unsurprising that Hsp70 phosphorylation appears to be altered in both hosts and pathogens in response to infection. *Legionella pneumophila* secretes over 300 bacterial effector proteins into target host cells, several of which are eukaryotic-like Ser/Thr protein kinases (79). One of these kinases, LegK4, phosphorylates the host cytosolic Hsp70 and Hsc70 at Thr-495 in the SBD. Phosphorylation of this well-conserved site reduces the ability of the HDJ1 co-chaperone to stimulate the ATPase activity of Hsc70. At a cellular level, the knock-on effect of this phosphorylation is a reduction in the unfolded protein response and protein synthesis. Overall, this study reveals a fascinating mechanism by which *Legionella* is able to directly manipulate chaperone function to increase its probability of survival in host cells.

Hsp70 phosphorylation in pathogens themselves may also be important for infectivity. In the opportunistic pathogenic yeast *Candida albicans*, Ser-361, Tyr-370, and Thr-576 are constitutively phosphorylated. Upon transition to the pathogenic hyphal form, an additional eight sites (Thr-11, Thr-136, Thr-161, Thr-175, Ser-328, Thr-387, Thr-494, and Ser-578)

become activated (80). Mutation of these sites produces cells with growth defects, including loss of the ability to form hyphae.

In a similar manner, the malarial parasite *Plasmodium berghei* displays increased phosphorylation of Hsp70 at the gametocyte stage. This phosphorylation occurs on Ser-106, Ser-585, Thr-587, and Ser-588 (81). Although more mechanistic studies are required, these phosphorylation sites may have a possible role in conferring protection to the parasite in its host. It is interesting to note that some of the activated sites seen in host-pathogen interactions are conserved in other organisms under differing conditions. The functional changes brought about by these phosphorylations may have evolved to be utilized in organism-specific manners.

BiP phosphorylation

Early studies identified BiP as being serine/threonine-phosphorylated and that this may represent an inactive, noncomplexed form of BiP (82). Follow-up studies revealed that BiP phosphorylation is associated with a dimeric form and that its phosphorylation decreases upon cellular exposure to ER stressors such as tunicamycin (83, 84). Taken together, the current model suggests that phosphorylation may promote a dimeric, inactive form of BiP. Upon ER stress, BiP phosphorylation decreases, allowing dimer dissociation and formation of BiP-client complexes. Whereas many sites of phosphorylation have been detected on BiP (Figure 1, Figure 2, Figure 3), their individual functions remain unclear.

Hsp70 AMPylation (adenylylation, adenylation)

AMPylation (also known as adenylylation and adenylation) involves the covalent addition of AMP to serine, tyrosine, or threonine residues (85). Enzymes responsible for AMPylation (AMPylases) have been identified in all three domains of life (86).

Characterized AMPylases belong to four groups: Fic (filamentation induced by cAMP) domain-containing proteins (87), GS-ATase (glutamine synthetase adenylyltransferase), SelO (88), and DrrA (*Legionella pneumophila* effector protein) (89). Fic-domain–containing proteins are found in Archaea, Bacteria, and Eukarya, whereas SelO is found in Bacteria and Eukarya. GS-ATase is only present in Bacteria, and DrrA is restricted to strains of *Legionella pneumophila* (86, 90). Most metazoans express a single fic type AMPylase, all of which share a highly conserved catalytic site architecture characterized by the fic motif H*X*F*X*(D/E)GNGR*XX*R (16, 91). Metazoan AMPylases and their functions, particularly their roles in the regulation of Hsp70 family chaperones, have gathered increasing attention in recent years. AMPylation is considered to inhibit the activity of Hsp70 family chaperones, conserving a pool of chaperones in a "stand-by," or "primed," state, which can rapidly respond to stress when de-AMPylated (92, 93). The AMPylase FICD functions as a bidirectional enzyme, catalyzing both AMPylation and de-AMPylation involving a single active site (93, 94). This bidirectionality is regulated by the oligomeric state of FICD, with monomeric FICD acting as an AMPylator and the dimeric form de-AMPylating (92, 95).

AMPylation of Hsp70s has been investigated in *Homo sapiens* (humans), *Cricetulus griseus* (Chinese hamsters), *Drosophila melanogaster* (fruit flies), and *Caenorhabditis elegans* (worms). In each of these species, at least one member of the Hsp70 family is regulated by AMPylation. In Chinese hamster ovary (CHO-K1) cells, FICD AMPylates the ER-resident Hsp70 BiP on Thr-518 (96). AMPylation levels increase and decrease inversely to unfolded protein burden (96). When AMPylated, BiP's substrate "on" and "off" rate is elevated, basal ATPase activity is decreased, and J-protein co-chaperone–

stimulated ATP hydrolysis activity is attenuated, demonstrating that AMPylation is an inactivating modification in CHO-K1 cells (96). However, BiP AMPylation does not prevent the binding of ATP to BiP's active site nor the recruitment of J-type co-chaperones. AMPylated BiP is thus proposed to be trapped in an ATP- and J-domain co-chaperone–bound conformation that will engage in protein-refolding activities immediately following its de-AMPylation (96). Even when BiP is AMPylated in its ADP-bound state, it adopts an ATP-like state, with impaired oligomerization (97). Increasing BiP AMPylation by the expression of FICD (E234G), the constitutively AMPylating mutant of FICD, induces the UPR^{ER} in CHO-K1 cells, whereas FICD-inactivated cells show a delayed UPR^{ER} in rat pancreatic acinar AR42j cells, suggesting a regulatory role for BiP AMPylation in UPR^{ER} induction (96). WT FICD, but not the E234G or the non-AMPylating H363A FICD mutants, is able to reverse AMPylation *in vitro*. In fact, when WT FICD is co-expressed with FICD (E234G) in CHO-K1 cells, the AMPylation levels and UPR effects of FICD (E234G) are mitigated (93, 94).

The *Drosophila* ortholog of BiP is AMPylated and deAMPylated by dFic at Thr-366 and Thr-518 (92). AMPylation occurs in a Ca^{2+}-dependent manner, and preferentially on the inactive conformation of BiP (98). During homeostasis, BiP is highly AMPylated, whereas AMPylated BiP levels decrease when unfolded proteins accumulate in the ER, suggesting that AMPylation also plays an inactivating role in *Drosophila*. Further, transcription of both BiP and dFic is increased in response to ER stress (98). dFic can also be secreted and locate to the surface of capitate projections (glial projections that insert into the axons of photoreceptors in the eye of flies), and loss of dFic leads to blindness in flies, due to loss of postsynaptic neuron activation (98). BiP(T366A) is resistant to AMPylation, and BiP

(T366A) flies also exhibit loss of synaptic function, indicating that the effects of dFic loss are caused by deregulation of BiP (99). Expression of a constitutively active dFic mutant (FicE247G) in a dFic knockout background is lethal but tolerated in the presence of WT dFic or BiP (T366A), further demonstrating the importance of residue Thr-366 in AMPylation-mediated BiP regulation in *Drosophila* (98) (100).

In *C. elegans*, the BiP/GRP78 orthologs HSP3 and HSP4 and the cytosolic Hsc70 ortholog HSP1 are AMPylated (101, 102). Illustrating the role of AMPylation in regulation of Hsp70s, in strains expressing aggregating amyloid β or α-synuclein, hyper-AMPylation increases the formation of large protein aggregates while decreasing their cytotoxicity (103-106). RNAi-mediated knockdown of Hsp70 family chaperones HSP1 as well as HSP3 and HSP4 phenocopies this reduction in aggregate toxicity observed in strains with increased AMPylation levels, suggesting that the effects of hyper-AMPylation are caused by AMPylation-mediated inactivation of Hsp70s in these worms (105). The site of AMPylation on HSP3 is Thr-176, but the AMPylation site(s) of HSP-1 and HSP-4 remain to be mapped (105). Expression of the constitutively active *C. elegans* AMPylase Fic-1(E274G) in *S. cerevisiae* induces up-regulation of the heat shock response and HSPs expression, as well as growth arrest and increased protein aggregation (101). These phenotypes are partially rescued by increasing the expression of the cytosolic Hsp70 family member Ssa2, suggesting that Fic-1(E274G) targets Hsp70 family proteins in budding yeast as well (101).

Human BiP is AMPylated at Thr-366 and Thr-518 (94, 107). These sites play slightly different roles in regulation of the Hsp70 ATPase cycle. Whereas AMPylation of Thr-366 increases basal ATPase activity with no effect on J-protein–stimulated ATPase activity,

AMPylation of Thr-518 decreases J-protein–stimulated ATPase activity with no effect on basal ATPase activity (94, 107). In addition to BiP, human FICD also AMPylates other major chaperones, including Hsp70, Hsp40, and Hsp90 (101). *In vitro*, Hsp70 is AMPylated on five threonine residues in the ATPase domain (101). In HEK293T cells, expression of FICD (E234G) induces higher expression of BiP, presumably to compensate for the BiP inactivated by AMPylation (96). Transfection of HeLa cells with the constitutively AMPylating FICD (E234G) leads to up-regulation of the heat shock response and activation of heat shock factor 1 (HSF1), a key transcription factor negatively regulated by Hsp70 that promotes the transcription of chaperones and thereby regulates the heat shock response (101) (108). FICD (E234G) also inhibits translocation of Hsp70 to the nucleus (101).

A recent screen for AMPylated proteins in eight different human cell lines using a novel N6pA probe further revealed that HSPA2, HSPA4, BiP, Hsc70, and mortalin are AMPylated by endogenous FICD in a cell type–specific pattern (109): whereas BiP was modified in all cell lines, HSPA2 (fibroblasts), HSPA4 (fibroblasts), Hsc70 (fibroblasts, SH-SY5Ys), and HSPA9 (fibroblasts, IPSCs) were AMPylated in a subset of the tested cell types. This supports the claim that AMPylation elicits regulatory functions on distinct Hsp70 family members.

Taken as a whole, these studies show that AMPylation occurs on threonine and serine residues of several Hsp70 family proteins and is particularly important in regulating BiP function. Whether BiP is simultaneously AMPylated on multiple residues or Thr-365 and Thr-518 are uniquely modified in response to distinct cues remains to be defined. The majority of studies have shown that this modification inactivates or inhibits the activity of

Hsp70 proteins, at least with regard to its chaperone activities. This suggests a model in which AMPylation acts as a "holding" mechanism, in which a steady level of Hsp70s can be maintained in the cell inactive during times of low stress, but ready to rapidly respond to stress events without the need to wait for transcription and translation. The homeostasis/stress AMPylation cycle has not yet been worked out for all Hsp70 family members. In the case of BiP, however, under basal nonstressed conditions, BiP appears to be largely AMPylated, and when stress is induced, BiP is de-AMPylated in response. AMPylation can have both advantageous and deleterious effects on cells, depending on context. Whereas constitutive AMPylation leads to activation of the UPR in cell models, no AMPylation leads to delayed UPR activation (93, 96). In flies, constitutive AMPylation is lethal, but lack of AMPylation leads to blindness (99, 100). In *C. elegans* protein aggregation models, increased AMPylation leads to increased protein aggregates but reduces the toxicity of those aggregates (105). This balance reflects the tight balance needed to maintain homeostasis and illustrates the crucial role of AMPylation.

Hsp70 ADP-ribosylation

Another post translational modification observed on Hsp70s is ADP-ribosylation (82, 110-115). ADP-ribosylation, a process catalyzed by ADP-ribosyltransferases (ARTs), involves the transfer of an ADP-ribose from NADH (NAD^+) onto a target protein with a nucleophilic oxygen, nitrogen, or sulfur (110, 111). ARTs fall into three families of proteins: arginine-specific ADP-ribosyltransferases (ART/ARTC), poly(ADP-ribose) polymerases (PARP/ARTD), and sirtuins. Proteins can be either mono- or poly-ADP-ribosylated (110, 111). ADP-ribosylation can be removed by hydrolysis by ADP-ribosyl hydrolases or

hydrolases of the macrodomain family (116). In CHO and human HEK293T and HeLa cells, BiP is ADP-ribosylated by hamster ARTC2.1 and by human ART1, respectively. Early studies identified several conditions that induced BiP ADP-ribosylation, including suspension of protein translation and ER stress (114, 117-119). In mice, BiP is less ADP-ribosylated in B cells making γ1-heavy chains than in those making neither heavy nor light chains (82). In quiescent Swiss 3T3, Rat-1 cells, and mouse embryonic fibroblasts, BiP is ADP-ribosylated; however, when proliferation is induced, ADP-ribosylation is reduced (120). When mice are fasted overnight or administered cycloheximide to halt protein production, their pancreases have increased levels of ADP-ribosylated BiP, which is reversed by feeding (119).

The specific sites and exact function of ADP-ribosylation have not been well-validated. MS-based studies have identified ADP-ribosylation at residues Asp-78 and Lys-81 of BiP, as well as Asp-53 of Hsc70 in HeLa cells, and residue Arg-50 of BiP and Arg-346 of HSPA13 in murine skeletal muscle (121). Additionally, mutation of either Arg-470 or Arg-492 to lysine in hamster BiP substantially decreases ADP-ribosylation, and whereas ribosylation-mimicking mutations decrease client binding, they do not appear to alter intrinsic ATPase activity. It should be noted that the authors did not definitively identify Arg-470 or Arg-492 as a site of ribosylation (by MS or other related technologies), and advances in the field suggest that these sites may also be modified by AMPylation (see below). On size-exclusion chromatography columns, ADP-ribosylated BiP is present in lower-molecular weight fractions, indicating that ADP-ribosylation prevents BiP participating in multichaperone complexes (119).

Additionally, ADP-ribosylation is only found on the oligomeric form of BiP, which is the predominant form under low protein-folding burden (83). Combined, these studies indicate that higher levels of ADP-ribosylated BiP are found during low protein production/low unprocessed protein burden (82) (114, 117-119) . On the other hand, BiP ADP-ribosylation is decreased when the unprocessed protein burden is higher, as when more proteins are being produced and when protein glycosylation is hindered (82) (120) (122). Taken together, this suggests that ADP-ribosylation may play a role in regulation of BiP's chaperoning activities.

Overall, studies on BiP ADP-ribosylation describe a modification that is most present under conditions in which BiP's folding activities are not needed and which may be inhibitory to BiP's chaperoning functions. Inversely, when unfolded protein burden is high, or when BiP is actively bound to a client protein, ADP-ribosylation levels are low. This suggests that ADP-ribosylation may act as a temporary “off” switch for BiP.

Studies on ADP-ribosylation and AMPylation have been complicated by the fact that early studies on ADP-ribosylation used radiolabeled adenosine, which can also label AMPylated sites. Cleavage by an ADP-ribosyl hydrolase was not used to confirm ADP-ribosylation in the above studies. Chambers *et al.* (119), investigating BiP arginine modification, point out that the identified mammalian arginine hydrolase, ARH1 (116), is a cytoplasmic protein and unlikely to act on BiP. In some of these studies, ADP-ribosylation was confirmed by digestion with snake venom phosphodiesterase, which cleaves phosphodiester bonds (123), and by blocking ADP-ribosylation using nicotinamide, which inhibits ARTs as well as PARPs (124). Importantly, snake venom phosphodiesterase is also able to cleave the phosphodiester bond of an AMPylation modification. Furthermore, nicotinamide treatment

has many effects on the cell other than blockage of ADP-ribosylation, including stimulation of DNA damage repair and blocking hexose uptake, which could in turn have effects on cellular metabolism leading to decreases in AMPylation, not ADP-ribosylation (125, 126). In fact, Preissler *et al.* (96), the same group that published Chambers *et al*. (119), themselves postulate that previous studies of BiP ADP-ribosylation may have been mistakenly characterizing BiP AMPylation (96).

Hsp70 acetylation

Acetylation involves the transfer of an acetyl group onto a lysine residue, the source of which is the metabolite acetyl-CoA (127). Acetylation is catalyzed by three related families of lysine acetyltransferases, GCN5, p300, and MYST, whereas removal of acetyl groups is processed by Sirtuin NAD-dependent lysine deacetylases (127). The Hsp70 family of proteins are heavily modified by acetylation; a total of 50, 58, and 40 acetylated sites have been identified so far on Hsc70, BiP, and yeast Ssa1, respectively (Figure 1, Figure 2, Figure 3). As with phosphorylation, acetylation fine-tunes Hsp70 function in a wide range of cellular processes.

Hsp70 acetylation control of the heat shock response

The historical paradigm for the heat shock response is that during heat shock, Hsp70 levels are induced through increased expression to compensate for the increase in unfolded proteins (62, 128). A recent study in yeast has revealed that in addition, Ssa1 is rapidly deacetylated at four lysine residues, Lys-86, Lys-185, Lys-354, and Lys-562, in response to heat shock (129). These deacetylation events are required for interaction with key co-chaperones such as Ydj1, Zuo1, Sgt2, and Hsp26 during heat shock. Fascinatingly, the inducible Hsp70s (Ssa3 and Ssa4) have an alanine at position 562 and thus cannot undergo

acetylation at this site. It is interesting to speculate that this naturally occurring mutation in Ssa3 and Ssa4 makes them immediately prepared for action when expressed during heat shock (for more on isoform differences in the code, please see below).

Hsp70 acetylation in client triaging and cell survival

In response to oxidative stress, the ARD1 acetyltransferase acetylates Hsp70 at Lys-77, allowing Hsp70 to bind to Hop and allowing refolding of denatured clients. After longer periods of stress, Hsp70 becomes deacetylated, promoting interaction with CHIP to degrade damaged proteins. This switch from protein refolding to degradation is required for the maintenance of protein homoeostasis and protects the cells from stress-induced cell death. Thus, in a similar manner to phosphorylation-mediated triaging reported by Muller *et al*. (58), ARD1-mediated Hsp70 acetylation is a regulatory mechanism that balances protein refolding/degradation in response to stress (130). In addition to altered co-chaperone binding, Hsp70 acetylation on Lys-77 facilitates its binding with pro-apoptotic proteins Apaf-1 and AIF and inhibits Apaf-1– and AIF–dependent apoptosis. Hsp70 acetylation also attenuates autophagy by Atg12-Atg5 complex formation, Beclin-1 expression, and perinuclear LC3 puncta formation, resulting in the inhibition of autophagic cell death. It is worth noting that only the inducible Hsp70 has Lys-77; the corresponding site in the constitutive Hsc70 is a nonacetylatable arginine, suggesting isoform-specific functionality.

Aside from Lys-77, other Hsp70 acetylation sites can impact autophagy. Post-amino acid starvation, Hsp70 Lys-159 acetylation is up-regulated. Acetylated Hsp70 displays enhanced binding affinity to KAP1 (SUMO E3 ligase), which in turn increases the SUMOylation of autophagy protein Vps34. This newly formed Hsp70-KAP1-Vps34

complex binds to Beclin 1 (complexed to autophagy proteins ATG14L, Ambra1, Bif1, or UVRAG) and promotes phagophore formation. Subsequently, the ULK kinase complex (ULK1/2, ATG13, FIP200) proteins are recruited to the phagophore. Finally, the membrane encloses the cytosolic cargos, resulting in the formation of an autophagosome. Thus, under nutrient starvation, acetylation of Hsp70 is a key step for activating autophagy (131). Interestingly, in contrast to Hsp70 Lys-77 acetylation, Lys-126 acetylation weakens its binding to Hop and Hip yet strengthens the interaction between CHIP and Bag1. Lys-126 acetylation also inhibits Hsp70-mediated tumor cell invasion and migration and the binding of Hsp70 to AIF1 and Apaf1 for promoting mitochondria-mediated apoptosis (132). Going forward, it will be interesting to underpin how activation and function of Lys-77, Lys-126, and Lys-159 acetylation relate to one another.

Hsp70 methylation

Methylation represents a highly abundant PTM found on all Hsp70 isoforms (133-135). This modification is conferred by three enzyme families: methyltransferase-like proteins (METTL) (136, 137), protein arginine methyltransferases (PRMTs) (133, 135), and SET domain–containing histone methyltransferases (SETD) (138). Modifications occur on surface-exposed lysine residues, which can be mono- (me1), di- (me2), or trimethylated (me3) (139), and arginine residues, which are monomethylated, asymmetrically dimethylated, or symmetrically dimethylated (139) (140). Most sites of methylation were found in proteome-wide MS studies (134, 135, 137, 141). The functional consequences of Hsp70 methylation, with a few exceptions discussed below, remain poorly understood.

Hsp70 methylation in the regulation of gene expression

Histone and DNA methylation are well-known regulatory traits that control gene transcription. Recent advances in our understanding of histone methylases and demethylases highlight that some of these enzymes are also capable of modifying nonhistone substrates, including Hsp70 family chaperones. Upon methylation of the conserved Arg-469 residue, Hsp70s associate with chromatin and regulate retinoid acid–dependent retinoid acid receptor β2 (RARβ2) gene expression (133). Whereas both the methylation-incompetent R469A mutant and WT Hsp70 bind to the promoter region of RARβ2, only methylated Hsp70 recruits TFIIH to the preinitiation complex during RARβ2 transcription initiation (133). Arg-469 methylation is conferred by PRMT4, which monomethylates the conserved Arg-469 residue across Hsp70 isoforms (133). This methylation is at least partly removed from Hsp70s by the JmjC-domain–containing demethylase JMJD6 (133). Together, PRMT4 and JMJD6 constitute a classic "writer-eraser" pair that regulates transcriptional events through Hsp70, rather than histone methylation.

Hsp70 methylation in direct regulation of chaperoning function

The protein-folding and -refolding activities of Hsp70 chaperones are in part regulated by lysine methylation events. Hsc70 Lys-561 and the orthogonal residues in BiP, Hsp70, HSPA2/Hsp70-2, and HSPA6/Hsp70B are trimethylated by the nonhistone methylase METTL21A (134, 136, 137, 142). In the presence of ER stress, BiP K586me3 is degraded by the lysosome and replaced with methyl-free *de novo* translated BiP, implicating a role for K586me3 in the regulation of BiP's chaperoning function (143). Hsc70 Lys-561 trimethylation affects its ability to bind to substrates, such as α-synuclein (136). Conversely to BiP, methylation mimetic Hsc70 K561R is more stable than a K561A non methylatable

protein, suggesting that Hsc70 K561me3 regulates Hsc70 turnover and degradation (144). There are several possible explanations for the apparent opposite effects of trimethylation on BiP and Hsc70. One is that they are separate proteins in separate subcellular compartments, and so this same modification may play different roles in specific contexts. Additionally, BiP K586me3 is degraded following ER stress, as are several other ER-resident chaperones (143). Finally, the stabilizing effects of Hsc70 K561me3 were studied using a lysine-to-arginine mutation to mimic lysine methylation (144). However, another group used a Hsp70 K561R mutant as non-methylatable mutant (138), illustrating the complications of interpreting mutants. In addition, as others have pointed out, this is a conserved residue, and so mutants may investigate the importance of an important residue rather than methylation (142). A possible mechanism was proposed by Zhang *et al.* (145), showing that Hsc70 Lys-561 trimethylation interferes with CHIP-mediated Hsc70 ubiquitination (144). Interestingly, Lys-561 methylation is not required for Hsc70-dependent chaperone-mediated autophagy; nor is Lys-561 trimethylation inhibitory to Hsc70's chaperoning function (144). Knockout of METTL21C, a close paralogue of METTL21A, leads to increased Hsc70 Lys-561 dimethylation, indicating possible competing roles of di- and trimethylators (144). *In vitro*, METTL21A predominantly catalyzes mono- and dimethylation of Hsp70, BiP and Hsc70, with trimethylation only occurring at high METTL21A concentrations (136). METTL21A knock-out cells are deficient in Hsp70 methylation, suggesting that this enzyme is strictly required for Hsp70 Lys-561 methylation (142). Localization studies are conflicting. Cho *et al.* (138) found Hsp70 K561me2 predominantly located in the nucleus of cancer cells, whereas all other HSP70 predominantly localized to the cytosol. In contrast, Jakobsson *et al.* (142) found

me0, 1, 2, and 3 HSP70 Lys-561 in both the cytosol and nuclei in HeLa and HEK293 cells and found HSP70 K561me3 to be the most prevalent form in either compartment, with the relative amounts of each methylation status the same between both compartments. Gao *et al.* (133) also found Hsp70 R469me1 in both cytosolic and nuclear compartments. Cloutier *et al.* (137) found that most METTL21A and HSC70 in cells overexpressing METTL21A localizes to the cytosol. Further studies are needed to clarify how methylation of different Hsp70s affects localization, and which additional methylases might be critically involved in Hsp70 Lys-561 modification remains to be defined in detail (134) (136) (137) (142).

Given that methylated Hsp70-R469me1 promotes RARβ2 transcription (133) and is more stable (144), whereas Hsc70 K561me3 has impaired substrate-binding abilities (136), it is likely that methylated and nonmethylated Hsp70s play different physiologic roles. Just as Hsc70 K561me3 has reduced substrate affinity (136), this may be true for other trimethylated Hsp70s. As such, trimethylated forms of these chaperones would be expected to be lower in the case of high unfolded protein burden. Meanwhile, other functions of Hsp70s, such as induction of target protein degradation (144) and transcript initiation (136), appear to rely on trimethylation of Hsp70s. These diverse roles might occur in different cell compartments, which would explain why some methylated Hsp70 forms and methylators are restricted to or enriched in specific cellular compartments.

Hsp70 family methylation has been identified in other organisms, yet at a lower frequency. In yeast, Hsp70 isoforms Ssa2 and Ssa4 are monomethylated on Lys-421/422 or Glu-423/424, respectively, the consequence of which remains unknown (146).

Ubiquitination

In contrast to small chemical modifications on amino acids, ubiquitination refers to the covalent addition of an 8-kDa ubiquitin (Ub) protein to substrate proteins. Ubiquitination is an ATP-dependent process and is catalyzed by the sequential activity of three enzymes. First, ubiquitin-activating enzymes (E1) adenylate Ub and load this primed Ub unit to one of ∼40 ubiquitin-conjugating enzymes (E2). The Ub-containing E2 enzyme forms a complex with one of ∼600 ubiquitin ligases (E3) (147, 148). Directed by the E3 ligase, the E2-E3 complex finally interacts with its substrate and promotes the formation of an isopeptide bond connecting the carboxyl-terminal glycine residue of Ub with an accessible lysine residue. The presence of seven lysines in Ub itself (Lys-6, -11, -27, -29, -33, -48, and -63) enables the assembly of branched poly-Ub chains, which have different implications for substrate fates (149)(149). Whereas Lys-48–linked Ub chains label substrates for degradation by the 26S proteasome, Lys-63–linked ubiquitin chains contribute to signaling (150-152).

Hsp70s are modified by several undisclosed E3 Ub ligases at multiple residues (Figure 1, Figure 2, Figure 3). Most of these sites were identified in high-throughput Ub-proteomics studies, and the functional implications of these modifications remain largely unclear (153-156). The best-understood Ub ligase-Hsp70 interactions are CHIP-Hsp70/Hsc70 and Parkin-Hsp70/Hsc70. CHIP binds to Hsp70 and Hsc70 and modifies their client proteins as well as Hsp70/Hsc70 itself. Whereas most studies suggest that polyubiquitination of Hsp70 and Hsc70 promotes their proteasomal degradation, other work did not find supporting evidence for this process (157-161). CHIP-conferred Ub arrays on Hsp70 and Hsc70, while substantially overlapping, differ in the modification of specific sites (*e.g.* Lys-159 in Hsc70 and its orthologous residue in Hsp70) and the length

and branching of the added Ub chains (161), indicating that a single E3 ligase can imprint different Ub patterns on distinct substrates. Parkin is a Parkinson's disease–associated E3 Ub ligase that monoubiquitinylates Hsp70 and Hsc70 on multiple sites (162). Interestingly, monoubiquitination of Hsp70 and Hsc70 by Parkin does not alter their turnover, steady-state levels, or proteasomal degradation, suggesting a role for ubiquitination in signaling transduction or chaperone regulation beyond degradation.

The ubiquitin-mediated degradation of several important proteins is regulated by other nearby PTMs. For example, phosphorylation of Thr-286 on cyclin D1 promotes its degradation and correct cell cycle progression (163). It is interesting to note that several PTMs exist in close proximity to identified sites of Hsp70 ubiquitination (see Figure 1, Figure 2, Figure 3). Given the number of PTMs on Hsp70, it is also possible that ubiquitination acts as a reset button for the chaperone code. While currently just speculation by the authors, it is feasible that once a certain number/combination of modifications has been reached, ubiquitination may promote chaperone destruction, with newly synthesized unmodified Hsp70 taking its place.

Hsp70 thiol oxidation

Thiol oxidation occurs on cysteines that are modified under conditions of oxidative stress or under exposure to thiol chelators or oxidizers, perhaps as an oxidative stress signal (164-166). This can lead to new disulfide linkages on the same protein or between proteins, formation of new moieties (including sulfenic acid and glutathionylation), and electrophilic adduction (164, 167, 168). In yeast cells, Ssa1 and Ssa2 are subject to thiol oxidation on Cys-15, Cys-264, and Cys-303 when treated with thiol-reactive compounds (169). Mutation of these sites prevents Hsf1 activation in response to oxidative agents. Several of

these sites are conserved in mammalian cells and are also oxidized. Human Hsp70 (but not Hsc70) is also oxidized on Cys-267 and Cys-306, which inhibits its ATPase activity (71). This appears to be a primary mechanism of action for the anti-Tau drug methylene blue and suggests that going forward, compounds that manipulate Hsp70 oxidation status may be clinically relevant.

The above studies suggest a fascinating mechanism by which Hsp70 is a direct sensor in the cellular response to oxidative stress (164). It appears that other Hsp70 isoforms can also perform this function. The yeast BiP ortholog Kar2 is oxidized on Cys-63 under ER oxidative stress, which is reversed via one of Kar2's nucleotide exchange factors, Sil1, apparently via thiol-disulfide exchange between the oxidized Cys-63 of Kar2 and the Cys-52 and/or Cys-57 of Sil1 (165, 167, 170). Sulfenylation and glutathionylation diminish Kar2's ATPase activities while leaving its peptide binding activities intact, converting Kar2 from an ATP-dependent foldase into an ATP-independent holdase (167, 170). This modification is cytoprotective during oxidative stress, but not during nonstress conditions (167, 170). Recent work suggests that Cys-574 and Cys-603 of HSP70 can also undergo a novel type of modification (glutathionylation) that promotes *in vitro* an increase in ATPase activity but decreased interaction with HSF1 in HeLa cells (166). Although further studies are needed, this suggests that glutathionylation in response to oxidative stress may also contribute to the cellular response to oxidative stress though HSF1 activation. In human U2OS bone cells, the peroxidase GPx7/NPGPx interacts with BiP under oxidative stress, and *in vitro* mediates the formation of a disulfide bond between BiP Cys-41 and Cys-420 (169). The formation of this bond promotes increased BiP activity, ER protein folding, and ER oxidative stress resistance (134). Although this disulfide bond formation was not

shown *in vivo*, other proteins, including the peroxide-detoxifying enzyme PRDX-2, have been shown to form disulfide bonds in *C. elegans* in response to H_2O_2 (171-173), demonstrating oxidized disulfide bond formation *in vivo* and suggesting the possibility that Hsp70 family members that form disulfide bonds in yeast cells during stress response may also do so in other eukaryotic organisms (169). In *C. elegans*, Cys-307 of the cytosolic Hsc70 ortholog HSP1 is oxidized when H_2O_2 detoxification is impaired, during induced H_2O_2 stress, and during development (172, 173).

Other PTMs on Hsp70 family proteins

High-throughput proteomics studies continuously expand our understanding of which PTMs contribute to the chaperone code (155, 174). Succinylation is an emerging PTM in which a succinyl group is reversibly linked to available lysine residues. The mapping of succinylation sites in *S. cerevisiae*, human (HeLa) cells and mouse liver tissue demonstrated the presence of this modification on HSPA1A, HSPA5, HSPA8, and Ssa1, yet the functional implications of these modifications remain unknown (155, 175). SUMOylation refers to the covalent linkage of a small ubiquitin-like protein (SUMO) to exposed lysine residues. HSPA1A, HSPA5, and HSPA8 are all SUMOylated, but, similar to succinylation, the functional consequences of Hsp70 succinylation are elusive (174, 176, 177). NEDDylation, a modification in which the ubiquitin-like protein, NEDD8, is reversibly attached either singly or in a NEDD8-chain to a Lys residue on a target protein has also been shown to occur on Hsp70s (178, 179). NEDD8 attaches to the ATPase domain of Hsp70 between amino acids 190 and 394 (178). In human U2-OS cells, de-NEDDylation is required for Hsp70 to be released from APAF1 and allow APAF1 to

participate in the initiation of apoptosis (178). Interestingly, the presence of mono-NEDD8 stimulates, whereas NEDD8 chains inhibit, Hsp70 ATPase activity (178).

Conservation of PTM sites between Hsp70 isoforms

An unanswered question in chaperone research is why cells express so many highly related and apparently functionally redundant Hsp70s. The historical model is that cells express the Hsc70 isoform constitutively to maintain homeostasis and express inducible Hsp70 variants under stressful conditions to assist in the additional proteotoxic burden. Recent studies clearly demonstrate that human Hsp70 variants display differential preferences for clients and co-chaperones (180, 181). These studies are corroborated by functional studies in yeast that reveal phenotypic differences in yeast expressing single Ssa isoforms (23, 182-185). Taken together, the data suggest that cytoplasmic Hsp70 variants have overlapping but distinct client-binding specificities driving unique roles in the cell.

PTMs on Hsp70 isoforms fall into distinct categories: those that are highly conserved and maintained throughout different organisms and those where the site is not conserved. It is probable that sites that are conserved throughout evolution are involved in important and fundamental cellular processes. Examples can be found in three phosphorylation sites discussed in this review, Thr-38, Thr-504, and Thr-636 (Hsc70 numbering). Thr-38 regulates the cell cycle, Thr-504 regulates the Hsp70 monomer-dimer balance, and Thr-636 determines whether a client is refolded or targeted for degradation (57, 58, 186). The conservation of Thr-504 (and surrounding amino acids) is particularly fascinating as it suggests that dimerization of all Hsp70 isoforms (as either homodimers or heterodimers of two different isoforms) is possible.

As discussed throughout this review, several sites of PTM are not conserved between isoforms (Fig. 3). For example, Lys-562 is only present in constitutively expressed Ssa1 and Ssa2 and not in Ssa3 and Ssa4. In times of heat shock, Ssa3 and Ssa4 are induced to respond to the additional proteotoxic burden on the cell. However, this response relies on the relatively slow pace of transcription and would not be fast enough for a cell to deal with acute heat stress. It is our belief that in the initial stages of heat shock, the deacetylation seen on Ssa1 and Ssa2 temporarily switches their function to be closer to that of Ssa3 and Ssa4 to maintain cell viability until enough Ssa3 and Ssa4 has been translated. Whereas the idea that Hsp70 PTMs can switch the functions of isoforms from one to another may seem far-fetched, it is important to note that chaperone isoforms differ by a few amino acids. Previous work on yeast established that a single amino acid change can switch prion-related functions of Ssa1 to that of Ssa2 (184). The position of this amino acid, Ala-83, is interesting because the equivalent residues in Hsp70 and Hsc70 are both serines previously detected as phosphorylated residues (Fig. 3). Ssa3 possesses a threonine at this site and may also be modified. Whereas phosphorylation of Hsp70 and Hsc70 at this site may alter functionality in mammalian cells, perhaps the Ssas have diverged in sequence to produce isoforms with distinct cellular functions. Other less well-examined examples of site diversification exist. Early studies identified that Hsp70 was phosphorylated upon heat shock at Tyr-525 (187). Tyr-525 is a “hinge” residue that may alter C-terminal lid closure. Similar to the previous example, this tyrosine is present in Hsp70, Hsc70, and Ssa3 but is nonphosphorylatable phenylalanine in Ssa1, Ssa2, and Ssa4 (Fig. 3). Although further studies are needed, the authors speculate that variation in sites like this may also be a way of controlling stoichiometry of a modification. If a PTM site is totally conserved, then all

Hsp70s present will be modified on this site at one time. In contrast, if only certain isoforms have a particular PTM site, then smaller pools of chaperones will be altered by this modification.

Primary mechanisms of action of the chaperone code

There are clearly a large number of different PTMs present on Hsp70 proteins. A major question remains: What are the majority of these modifications doing? Hsp70 function is regulated through several different processes including co-chaperone binding, transcription, expression of related isoforms, cellular localization, client specificity and self-interaction (2) and Fig. 4). It is clear that many of these regulatory mechanisms are tied to one another. J-proteins bind and stimulate the ATPase activity of Hsp70; different Hsp70 isoforms have different expression patterns, ATPase activities and client specificities. It remains challenging to tease out the primary roles of Hsp70 PTMs from existing studies. For example, the monomer-dimer ratio of both Hsp70 and the ER-resident BiP proteins appears to be regulated by phosphorylation and acetylation (82, 186), but the roles for co-chaperones and effect on client specificity and whether this process allows heterodimerization of Hsp70 isoforms remains unclear (36). Likewise, the dynamic shuttling of Hsp70 to the nucleus post-heat stress is at least in part regulated by phosphorylation and AMPylation events: phosphorylation or phosphomimetic mutations of Tyr-525 increase their nuclear accumulation, whereas phosphoinhibitory mutations retain Hsp70-1 in the cytoplasm (187). Similarly, increased Hsp70 AMPylation prevents its nuclear shuttling following heat stress (101). The NBD is the site of ATP hydrolysis and the interacting region for several co-chaperone proteins. We believe that the majority of Hsp70 PTMs on the N terminus are directly impacting Hsp70 structure to alter ATPase

activity (either directly through ATPase site rearrangement or indirectly through co-chaperone binding). On the other hand, PTMs on the C terminus are much more likely to direct Hsp70-client specificity, folding, and release.

Conclusions and future perspectives

Hsp70s have been heavily researched for decades, resulting in several thousand publications on their mechanisms of action and their roles in the cell. Improvements in -omics technologies have resulted in the detection of a large number of Hsp70 PTMs, the majority of which have no known function. Linking these PTMs to chaperone function and determining the stresses/enzymes that regulate these specific sites remains a major challenge for understanding the chaperone code. Many of the existing studies have taken a "bottom-up" approach, mutating individual modified residues on Hsp70s to prevent PTM addition and analyzing the effect on both *in vitro* activity (refolding capability, structural changes, and ATP hydrolysis) and physiological relevance (client specificity, cellular localization, co-chaperone interaction). While these approaches have been effective, it is important to remember that it is common for multiple PTMs on proteins to be simultaneously activated in response to cellular stresses. It is thus also useful to take a "top-down approach," where global PTMs on Hsp70 are examined under stress conditions.

The number of currently identified PTMs on Hsp70 family proteins appears at first glance to be shockingly high. For Hsc70, 60% of the total Ser, Thr, and Tyr residues have been identified as phosphorylated (from the GPM database). However, to put this into perspective, this value is comparable with that for another major chaperone, Hsp90 (56%) and the metabolic enzyme GAPDH (62%). There are other proteins in the cell that have a much higher proportion of modified residues (*e.g.* the DNA damage response protein

53BP1 (93%)). At this time, it is hard to know how many of these sites are functionally relevant. Some of these sites may be false positives arising from the misinterpretation of low quality MS spectra by commonly used analysis software. Nevertheless, many of the modified amino acids are well-conserved throughout evolution, suggesting regulatory importance. Some sites may become important only in the context of other site modifications, making standard single-site mutagenesis ineffective.

Where will the future of chaperone code research take us? In the coming years, we might expect further studies to focus on determining how individual sites on Hsp70s are regulated and their impact on Hsp70 function, particularly in the context of cancer and neurodegeneration. Although phosphorylation, methylation, acetylation, AMPylation, NEDDylation, and ubiquitination have been detected on Hsp70, over 100 different PTMs have been identified on other proteins. As the resolution of proteomic technologies improves, we may thus find that Hsp70s are modified with many more PTMs than currently known. Studies of individual sites are still nontrivial, especially given the complex reciprocal relationship between chaperones and those clients that are able to modify chaperones and that choice of expression host dictates PTMs added to Hsp70 when made recombinantly (57, 188, 189).

A greater challenge will be understanding how multiple PTMs on Hsp70 interact and cross-talk. Several identified PTMs on Hsp70 family proteins modify the *same* amino acid and are thus mutually exclusive. For example, BiP Thr-518 can be modified by either phosphorylation or AMPylation. It is likely in this case that AMPylation prevents Thr-518 phosphorylation, holding BiP in an inactive state until needed by the cell. Lysine residues can also be modified by a wide range of PTMs, including ubiquitination, acetylation, and

methylation. Similarly, several lysines on Hsp70 family proteins have been identified as modified in multiple ways. For example, Lys-246 and Lys-601 on Hsp70 and Lys-268 and Lys-585 on BiP are modified by acetylation, methylation, and ubiquitination (Fig. 1). These mutually exclusive modifications may be activated by opposing signaling pathways in response to distinct cellular cues. The presence of multiple PTMs on single sites makes analysis more complex; for example, site-directed mutation of an amino acid would prevent *all modifications* occurring. It is interesting to note that there are several areas on Hsp70 where clustering of PTMs occur (*e.g.* amino acids 245–255, 275–285, 420–440, and 490–500) (see Figure 2, Figure 3). It is highly possible that some PTMs act in synergy and are required for others to be added, as in the case seen for the FNIP1 co-chaperone (190). In contrast, some PTMs may be antagonistic, particularly if they exist in close proximity. Many writer enzymes, such as kinases and acetyltransferases, have very specific substrate sequence requirements, and modification of the surrounding residues may prevent other PTMs from occurring.

If we think of the total sum of the modifications on a single Hsp70 "proteoform" as a complex code in response to internal and external cues, then the overall population of these proteoforms will reflect the overall health and status of a cell. The temporal and spatial resolution of Hsp70 proteoforms will be a major undertaking. Current proteomic technologies require the digestion of proteins to peptides, which destroys information about the combinations of PTMs present on a Hsp70 proteoform. Newer methodologies, however, such as top-down proteomics, should mitigate these issues, although the large size of Hsp70 makes this kind of analysis currently challenging (191).

Even when this level of complexity is resolved, we will have to contend with the multiple isoforms of Hsp70 in the cell. It is highly likely that different Hsp70 isoforms possess unique PTMs suited for their individual function. More intriguing is the possibility that PTMs are present on Hsp70s that allow instantaneous conversion of one isoform's function to another under particular stresses. This situation is further complicated by evidence that Hsp70 can form dimers, trimers, and higher-order oligomers, the formation of which is also linked to Hsp70 PTMs (36).

Finally, even when all of the mechanisms and physiological relevance of Hsp70 PTMs have been understood, these models will have to be incorporated into the understanding of the entirety of the chaperone code. Many other important chaperones, including Hsp90, Hsp104, and Hsp60, and co-chaperones, such as Hsp40 and CHIP, are highly modified, many of which influence their interaction with Hsp70. The understanding of this bewildering array of chaperone PTMs will take a concerted effort among researchers and should cement chaperones as the cross-roads for major signaling events in the cell.

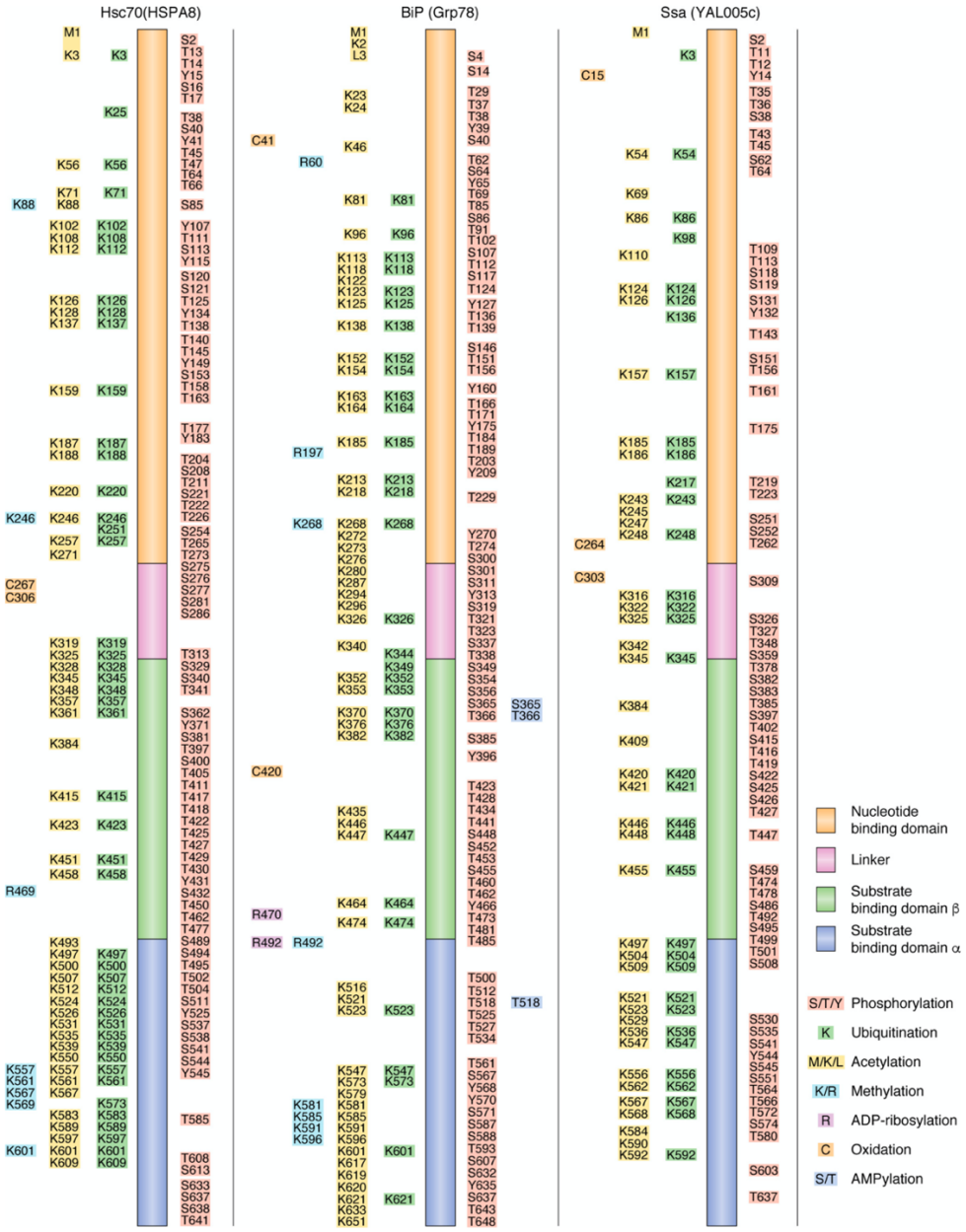

Figure 1. The post-translational modifications of mammalian Hsp70, Hsc70, and BiP and yeast Ssa1–4. Shown is a domain representation of the Hsp70 family members, with detected PTMs marked with appropriate residue numbers. PTMs are labeled as follows: phosphorylation in red, ubiquitination in green, acetylation in yellow, methylation in cyan, ADP-ribosylation in purple, and AMPylation in dark blue.

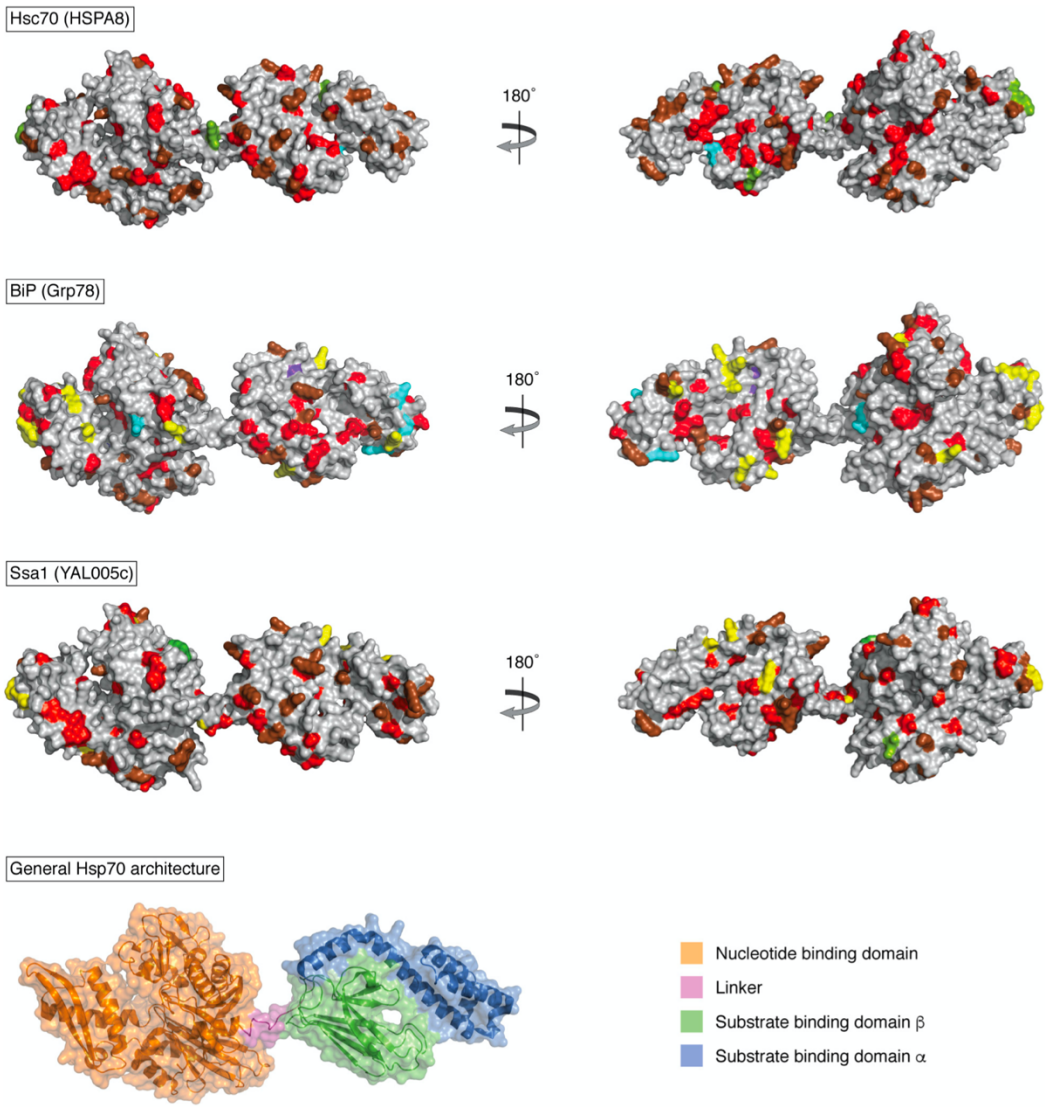

Figure 2. **Locations of PTMs on the Hsp70 structure.** PTMs were mapped onto predicted structural models created by SWISS-MODEL based on Protein Data Bank entry 2KHO for each Hsp70 isoform (192). PTMs are *colored* as in Fig. 1, except sites of multiple modification are *labeled brown*.

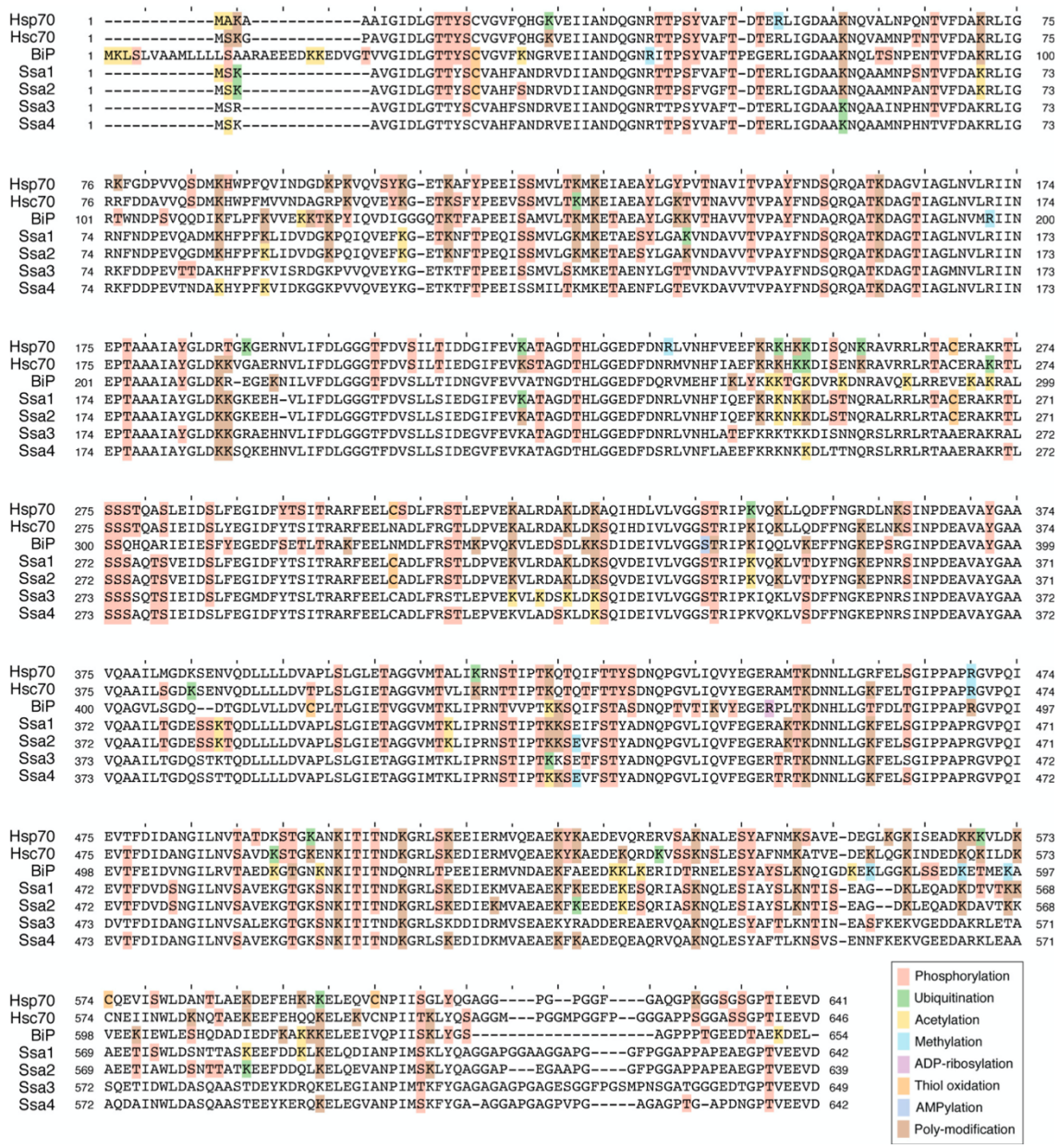

Figure 3. Conservation of Hsp70 PTMs and surrounding sequence between Hsp70 isoforms. Alignment was build using human Hsp70, Hsc70, and BiP as well as *S. cerevisiae* Ssa1, Ssa2, Ssa3, and Ssa4 sequences. Sequences were aligned using ClustalX (193), and sites of PTM were labeled as in Fig. 2.

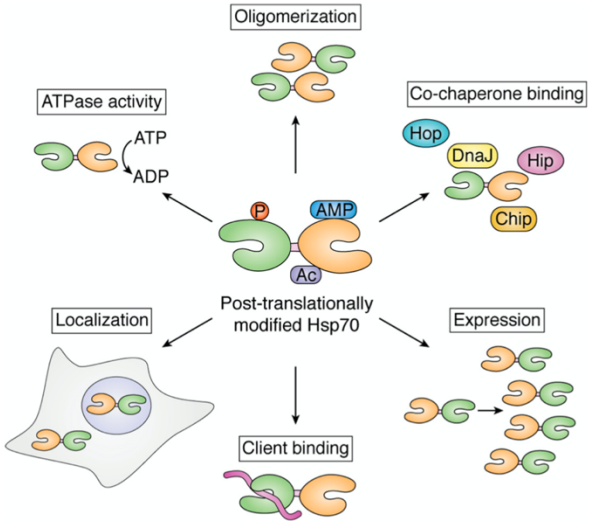

Figure 4. The hallmarks of Hsp70 regulation. This illustration encompasses six regulatory processes (*outside wheel*) that are affected by the post-translational modification of Hsp70: co-chaperone binding, expression, client binding, localization, ATPase activity, and oligomerization. Most of these processes are interdependent (*e.g.* ATPase activity and client binding).

CHAPTER 2: ENDOGENOUS EPITOPE TAGGING OF HEAT SHOCK PROTEIN ISOFROM HSC70 USING CRISPR/CAS9

This chapter has been published:

Nitika, Truman, A.W. Endogenous epitope tagging of heat shock protein 70 isoform Hsc70 using CRISPR/Cas9. Cell Stress and Chaperones 23, 347–355 (2018).

2.1 Introduction

The highly conserved molecular chaperone 70 kDa heat shock protein family (Hsp70s) are key players in protein homeostasis not only during stress, but also in optimal growth conditions. Members of the Hsp70 family are involved in folding of newly synthesized and misfolded proteins, solubilization of protein aggregates, degradation via the proteasome and autophagy pathways, transport of proteins through membranes, and assembly and disassembly of protein complexes(1). The structure of Hsp70 is comprised of highly conserved amino acid sequences and domains among the different family groups. These domains include: N–terminal ATPase domain, which is a 44-KDa structure that is involved in the binding of Hsp70 to client proteins and in the hydrolysis of ATP, mid region containing protease sensitive sites, substrate binding domain, weighing about 28-KDa and known to bind to substrates such as polypeptides, and a C-terminal region containing leucine rich EEVD motif, essential for co-chaperone binding and is missing in ER-specific/Grp78 (2). There are 17 different isoforms of Hsp70 family that have been identified but their functions are still unclear. These isoforms can be classified into two broad categories. The two most common isoforms are Hsp70, a stress-inducible form and

the constitutively expressed Hsc70 that provides major housekeeping functions and essential cell viability (3-5).

Co-chaperones of Hsp70 associate with the N-terminus and mediate both client protein binding activities often via stimulation of ATP binding and hydrolysis. There are suites of co-chaperones present at any one time in chaperone-client complexes that include J-domain, BCL2-associated athanogene (Bag), Hsp70 interacting proteins (Hip), Hsp70/Hsp90 organizing proteins (Hop), CHIP (Carboxyl-terminus of Hsp70 Interacting Protein) and Nucleotide Exchange Factors (NEFs). J-domain proteins assist in the targeting of the client protein to their substrate binding cavity (5) whereas Bag proteins promote substrate release by binding to Hsp70 chaperone, thus having an inhibitory role (6) .

Characterizing the interactome of a target protein by AP-MS offers a powerful approach to understanding its role in the cell (7-10). This holds especially true for chaperones whose interactomes are typically very large yet specific (11, 12). In addition, chaperone interactions are dynamic, changing upon stress and post-translational modification (13-15). The study of Hsp70 complexes has been greatly aided by the generation of isoform specific monoclonal antibodies for Hsc70 and Hsp72 (16, 17). These antibodies have been used to immunoprecipitate and analyze chaperone complexes via high-resolution mass spectrometry. This methodology has been particularly effective in detecting low abundance interactors of Hsp70 in a variety of conditions, allowing purification of complexes at native stoichiometry (18, 19). Alternative strategies for chaperone interactome analysis have employed the use of an epitope-tagged bait protein in cell lines from a transient, CMV-driven expression plasmid. Given that the HIS epitope and associated affinity reagents often used for such experiments are unaffected by denaturing

reagents such as urea or guanidine HCl, purification of chaperone complexes can be achieved under more stringent conditions. This has been employed with substantial success in a number of Hsp70 and Hsp90 interactome studies (13-15, 20).

Programmable sequence specific nucleases such as CRISPR/Cas9 facilitate precise editing of endogenous genomic loci. CRISPR/Cas9 is used to generate cell lines with tailored modifications such as gene knockouts, point mutation and knock-in of exogenous DNA (21). A particularly useful application of CRISPR/Cas9 is the endogenous epitope tagging of genes at their genomic loci. Several DNA repair and chromatin-modifying proteins have been tagged and purified using this methodology (22).

In this study, we have optimized the CRISPR/Cas9 system to epitope tag *HSC70* at its N-terminus with a tandem affinity tag (HIS_6-FLAG) using a single stranded oligonucleotide template (ssODN) with substantially smaller homology arms than is traditionally used. The resulting cell line ($HEK293T^{HIS\text{-}FLAG\text{-}Hsc70}$) expresses tagged Hsc70 from its native promoter offering several benefits for researchers interested in the systematic and unbiased mapping of Hsc70 interactions.

2.2 Materials and Methods

Design of *HSC70* sgRNA and generation of the *HSC70*-sgRNA-Cas9 plasmid

An *HSC70*-targeting sgRNA for was generated using the CRISPOR algorithm (http://crispor.tefor.net/). We identified a suitable sgRNA sequence (TTTTCAGCAACCATGTCCAA) based on two criteria-minimal off-targeting and proximity to 5' end of *HSC70*. The *HSC70*-targeting sgRNA was cloned via BbsI into pX458 plasmid (21) that allows simultaneous expression of chosen sgRNA, Cas9 and a GFP marker.

Cell Culture and Transfection

HEK293T cells were obtained from the ATCC and maintained at 37°C under 5% CO_2 in DMEM medium (Gibco) supplemented with 10% fetal bovine serum (Gibco), penicillin-streptomycin (Gibco), and GlutaMAX (Gibco). Cells were transfected in six-well plates at 70% confluency using 5 μg of *HSC70* gRNA-pX458 or pX458 control using Lipofectamine 3000 (Life Technologies). Twenty-four hours after DNA transfection, cells were washed one time with PBS (Gibco) and media was changed. After 72 hours, the cells were prepared for FACS Cell Sorting.

FACS Cell Sorting

Cells were washed with PBS, trypsinized then resuspended in PBS and 1 % BSA solution and kept in ice prior to sorting. Cells positive for GFP (and therefore Cas9) expression were sorted by flow cytometry. 2×10^4 cells were sorted in 1 well of a 6 well plate in DMEM using a BD FACS ARIA II flow cytometer and accompanying software (BD Biosciences).

Limiting Dilution

Cells were allowed to reach 70% confluency after sorting and harvested by trypsinizing. Cells were resuspended in 10 ml media and counted using Cell Counter. The cells were diluted to 10^3 cells /ml and were diluted to 1 cell/well. The diluted cells were allowed to expand in 12-well plate. The wells containing single cell colonies were selected. When the colonies reached 70% confluency, the cells were harvested for further analysis.

SURVEYOR Assay

The SURVEYOR assay was performed according to the manufacturer's instructions (Integrated DNA Technologies). Genomic DNA was isolated using QuickExtract DNA

Extraction Solution (Epicentre) according to manufacturer's protocol. Briefly, pelleted cells were resuspended in QuickExtract solution and incubated at 65 °C for 15 min, 68 °C for 15 min, and 98 °C for 10 min. The genomic region flanking the CRISPR target site for each gene was PCR amplified using Forward primer (5'-GTGCAGCCTCCACACAGGCCTGTTG-3') and Reverse primer (5'-GGTTCGGTTTCCCTGATCATTGGC-3'). PCR product was purified using PCR Purification kit. PCR products were then mixed with 2 µl 10X Dream TaqDNA Polymerase PCR buffer (Thermo) to a final volume of 20 µl, and subjected to a re-annealing process to enable heteroduplex formation: 95 °C for 10 min, 95 °C to 85 °C ramping at −2 °C/s, 85 °C to 25 °C at −0.25 °C/s, and 25 °C hold for 1 min. After re-annealing, products were treated with SURVEYOR nuclease and SURVEYOR enhancer S following the manufacturer's recommended protocol, and analyzed on 10%TBE Gel (Invitrogen) and imaged using Gel Doc imaging system (Bio-rad).

In–out PCR of HIS$_6$-FLAG-*HSC70* genomic region

Genomic DNA from the clones was purified using QuickExtract DNA Extraction Solution (Epicentre). PCR amplification for SURVEYOR assay was performed by an initial amplification using Forward primer 5'-GTGCAGCCTCCACACAGGCCTGTTG-3' and Reverse primer 5'-CTCCTCACGTTTCATAAACTTTTGTGC-3' was done with a denaturation step at 98°C for 10 min, followed by 34 cycles of denaturation at 98°C for 1 min, primer annealing at 64°C for 30 s, and primer extension at 72°C for 45s. Upon completion of the cycling steps, a final extension at 72°C for 5 min was done and then the reaction was stored at 4°C. PCR was carried out using a Bio-Rad PCR machine. The In-out PCR was done on genomic DNA isolated from the clones using Forward primer 5'-

GACTACAAGGACGACGATGACAAAGGTTC-3' and Reverse primer 5'-CTTAACCCTGAGCTGAGCCCCATCTGTTC-3' using the same PCR program as above.

Sequencing of CRISPR-edited region

A 1kb region of DNA containing 5' sequence of *HSC70* gene along with gRNA binding site and HIS-FLAG epitope tag was amplified via PCR and cloned into pGEX-6P-1 for sequencing. To allow for multiple integration events, multiple clones were sequenced via multiple primers in forward and reverse orientation.

Immunoprecipitation of Hsc70 complexes

Total cell extract was prepared from the individual clones using M-PER (Thermo) containing EDTA-free protease and phosphatase inhibitor cocktail (Thermo) according to the manufacturer's recommended protocol. Protein was quantitated using the Bradford Assay. His-tagged proteins were purified as follows: 200µg of cell lysate was incubated with 30 µl of His-Tag Dynabeads (Invitrogen) with gentle agitation for 20 minutes at 4° C. Dynabeads were collected by magnet then washed 5 times with 500 µl Binding/Wash buffer. After final wash, buffer was aspirated and beads were incubated with 100 µl Elution buffer (300 mM imidazole, 50 mM Na-phosphate pH 8.0, 300 mM NaCl, 0.01% Tween-20) for 20 min, then beads were collected via magnet. The supernatant containing purified Hsc70 complex was transferred to a fresh tube, 25 µl of 5x SDS-PAGE sample buffer was added and the sample was denatured for 5 min at 95° C. 20 µl of sample was analyzed by SDS-PAGE and processed for conventional Western blot analysis. FLAG-tag proteins were purified as follows: 200µg of cell lysate was incubated with 30 µl Anti-FLAG® M2 Magnetic Beads (Sigma) overnight on a rotator at 4° C. FLAG beads were collected by

magnet then washed 5 times with 500 µl 1x TBS. After the final wash, buffer was aspirated and beads were incubated with 100 µl Elution buffer (TBS supplemented with 10 µg/ml FLAG peptide) for 20 mins. The supernatant containing purified FLAG-Hsc70 complex was transferred to a fresh tube, 25 µl of 5x SDS-PAGE sample buffer was added and the sample was denatured for 5 min at 95° C. 20 µl of sample was analyzed by SDS-PAGE and processed for conventional Western blot analysis with HSP110 (StressMarq, SPC-195), HDJ2 (Thermo, MA512748), HSP27 (Thermo, MA3015), FLAG (Sigma, F3165) and HIS (Qiagen, 34670) antibodies.

Immunoblotting

Total cell extracts were prepared from the single cell clones using Mammalian Protein Extract Reagent (Thermo). Samples were loaded on 8-12% Bis-Tris Gel(Invitrogen) and ran at 200V for approximately 60 minutes. Gels were transferred onto Nitrocellulose membrane by transfer at 500 mA for 60 minutes. Membranes were blocked for 1 hour with TBS-Tween and 1% BSA and probed with HIS, FLAG and α-Tubulin primary antibodies overnight in blocking solution overnight at 4°C. Membranes were incubated with α-mouse and α-rabbit secondary antibodies (GE Healthcare) for 1 hour at room temperature in blocking buffer. The blots were imaged using MP Gel Doc imaging system (Bio-rad).

Luminespib treatment of cells

Wildtype and CRISPR Clones were seeded in a 6-well plate and treated with 50 nM Luminespib/AUY922 (LC Laboratories N-5300) for 24 hours. Protein was extracted, run on SDS-PAGE gels and Western blotted with antibodies to either HSP72 (Enzo, C92F3A-5), HIS or α-tubulin.

2.3 Results

Designing a tandem affinity tag for endogenous tagging of Hsc70

An ideal Tandem Affinity Purification (TAP) tag aids in the recovery of a fusion protein and associated complexes with minimal background contaminants. We chose a TAP tag that comprised of two highly utilized epitope tags, hexahistidine (HIS_6) FLAG (DYKDDDK). Both of these tags are relatively small in size, having minimal impact on protein function. Tagging of Hsp70s in model organisms such as budding yeast with HIS_6 and FLAG does not impair essential chaperone function (13). Both of these tags can be utilized to isolate highly purified native protein complexes (23). Given that epitope tagging of Hsp70s on the C-terminus impairs client binding, we chose to epitope tag Hsc70 on its N-terminus (24). CRISPR-mediated epitope tagging requires expression of 3 components in the cell: 1) the Cas9 enzyme which creates a DNA double strand break 2) a gRNA that binds Cas9 and targets it to the desired location and 3) a repair template containing both the epitope tag and regions of homology to the location of insertion. The majority of CRISPR knock-in studies have utilized repair templates between 250-1000bp (22, 25), amplifying expense and technical difficulties. For this study, we decided to examine the feasibility of endogenously tagging Hsc70 using a repair template with exceptionally small overhangs-less than 100bp each side. Using the maximum size of IDT's ultramers (200bp), we designed an ssODN repair template that contained the sequence for the Start codon, HHHHHH (His_6 tag), DYKDDDDK (Flag tag) and GG linker. In addition, the ssODN contained a 5' homology arm of 78bp and a 3' homology arm of 71bp (Fig. 5). To prevent continued Cas9 digestion of the 5' of the HSC70 gene post-CRISPR-mediated epitope tagging, a silent mutation was incorporated into Serine 2 of the Hsc70 gene (TCC to TCA).

Generation of *HSC70*-sgRNA-pX458

CRISPR-mediated genome requires expression of the Cas9 nuclease and a guide RNA (gRNA) that targets Cas9 to a required region. A suite of vectors have been created for targeted gene deletion and knock-in, but pX458 (pSpCas9(BB)-2A-GFP, (21)) was chosen for our study based on its ability to co-express Cas9, a GFP marker and specific gRNA from the U6 promoter. Using the CRISPOR algorithm (http://crispor.tefor.net/), we designed a gRNA (TTTTTCAGCAACCATGTCCA) that had a specificity score of 67/100 and produces no off-targets even with a single base mismatches present next to the genomic PAM sequence.

***HSC70*-sgRNA-pX458 induces DSBs at the 5' region of the *HSC70* gene**

HEK293T cells were chosen to express our CRISPR construct given their high average transfection efficiency, ease of culturing and their tolerance for limiting dilution and genome editing experiments (26, 27). Moreover, the HEK cell line is designated as a tier 3 cell line by the Encyclopedia of DNA Elements (ENCODE) project meaning a multitude of genomic data is available for this cell line (28). We transfected the HEK293T cell line with *HSC70*-sgRNA-pX458 and checked expression of Cas9 by monitoring of GFP expression in the cells using microscopy. Approximately 70% of cells expressed GFP, expected given the standard rate of transfection of the HEK293T cell line (Fig. 6). To isolate cells that had been edited by Cas9, we sorted the GFP positive cells using FACS in a petri dish 72 hours post-transfection. To examine the ability of *HSC70*-sgRNA-pX458 to promote cleavage at the *HSC70* gene, we isolated the pooled DNA from sorted cells and subjected them to the SURVEYOR nuclease assay. Genome editing was observed in cells

transfected with *HSC70*-sgRNA-pX458 but not with untransfected cells or cells transfected pX458 plasmid lacking a targeting gRNA (Fig. 7).

***HSC70*-sgRNA-pX458 allows creation of cell lines expressing epitope tagged Hsc70 at native levels**

Based on the success of *HSC70*-sgRNA-pX458 to create DSBs at the specified genomic region, we decided to attempt creation of cells that would express HIS_6-FLAG Hsc70 at native promoter levels. As before, we transfected HEK293T cells with *HSC70*-sgRNA-pX458, but added our tailored ssODN expressing the tandem HIS-FLAG tag along with homology arms to the *HSC70* gene. GFP+ cells were sorted via FACS and were cloned by limiting dilution. Single cell clones were picked after 10 days and expanded. We checked the integration of a single HIS_6-FLAG tag at the N-terminus of *HSC70* in each of the isolated clones via PCR amplification of the genome using the primers flanking the epitope tag *HSC70*. Presence of the HIS_6-FLAG tag was observed in 11/14 (79%) clones (Fig. 8). After limited dilution, single cells were identified in 12-well plate format and expanded.

Expression of HIS_6-FLAG-Hsc70 protein from native promoter in HEK293T cells

Given the myriad of factors that controls protein expression, correct integration of the HIS_6-FLAG tag at the genomic level by no means guaranteed correct expression of the fusion protein. To confirm the expression of HIS_6-FLAG-Hsc70 we analyzed our individual clones via Western blotting of total lysate using HIS and FLAG (α-Tubulin was used as a loading control). 7 out of 14 clones (50%, clones 1-4, 8, 9 and 14) correct expression of HIS_6-FLAG-tagged Hsc70 protein while one clone (clone 12) lacked a detectable HIS tag despite showing cross-reaction with the FLAG antibody.

Standard mammalian plasmids drive constitutive protein expression via promoters such as CMV. To examine how our native promoter controlled HIS_6-FLAG Hsc70 compared with traditional methods, we also ran a control of cell lysate from cells transiently expressing a CMV-driven HIS_6-FLAG-Hsc70 (Fig. 9). CMV-driven Hsc70 proteins levels were substantially higher than those detected for the CRISPR clones (Fig. 5, 7). The DNA region containing HSC70 and HIS-FLAG tag was amplified from multiple clones and sequenced. The sequence contained the HIS-FLAG tag in frame with HSC70. No mutations were detected, except the silent mutation engineered to prevent repeat gRNA binding (Sequence attached as supplemental File S1).

CRISPR-mediated tagging is isoform specific

Several different isoforms of Hsp70 exist in cells, the most common being Hsc70 and Hsp72. To assess the probability of unwanted tagging of Hsp72 with our methodology, we compared the amino acid and genomic sequences of *HSC70* and *HSP72* genes. Interestingly, we identified low homology between the 2 genes, suggesting minimal probability that either the *HSC70* gRNA or *HSC70* ssODN could bind to the equivalent region of the *HSP72* gene (Fig. 10A). To confirm this, we relied on 1) specific antibodies that selectively detect Hsp72 protein and 2) that Hsp72 can be induced by several stresses/small molecules that leave Hsc70 protein unaffected. We grew WT and 3 CRISPR clones in untreated media or media containing 50mM AUY922/Luminespib. Luminespib is a well-characterized small molecule inhibitor of Hsp90 and due to indirect effects on the HSF1 transcription factor triggers increased expression of Hsp72(29). While Hsp72 levels were induced upon Luminespib treatment, levels of HIS protein remained constant. In addition, the molecular weight of Hsp72 protein observed in the CRISPR clones

corresponded to that seen in WT cells. These data suggest that as expected the epitope tagging seen was only present on the Hsc70 protein and not on the Hsc72 isoform (Fig. 10B).

Recapitulation of well-characterized Hsc70 interactions in HEK293T$^{HIS\text{-}FLAG\text{-}Hsc70}$

Hsc70 interacts with a suite of co-chaperone proteins that activate Hsc70 through stimulation of the N-terminal ATPase domain (30). Given that a primary use of this cell line is analyze Hsc70 complexes at native stoichiometry, we examined whether known interactions of Hsc70 were maintained in HEK293T$^{HIS\text{-}FLAG\text{-}Hsc70}$ cells. We purified Hsc70 complexes from control cells that had been transiently transfected with CMV-HIS_6-FLAG-Hsc70 and from 3 independent CRISPR clones expressing HIS_6-FLAG-Hsc70 from the native *HSC70* promoter using either FLAG affinity beads or IMAC. Confirming that the CRISPR-driven Hsc70 epitope tag functioned as intended, Hsc70 interactions with Hsp110, Hdj2 and Hsp27 were detected in HEK293T$^{HIS\text{-}FLAG\text{-}Hsc70}$ cells but not in cells lacking epitope-tagged Hsc70 (Fig. 11).

2.4 Discussion

Although Hsp70 has been studied for several decades, much of this work has focused on the biochemical and biophysical properties of the molecule (31, 32). Several studies have attempted to obtain a true "systems view" of the Hsp70 interaction network using yeast two-hybrid and affinity-purification followed by mass spectrometry (AP-MS) (13, 33) . These attempts have been made more challenging by the fact that that the Hsp70 interactome is highly dynamic, changing in response to cellular stress, post-translational modifications and disease state of the cell (13, 14). Recent work has suggested that the "chaperome" of a cell may be an important trigger and/or response to disease (34).

Although drug-based affinity reagents for purifying and identifying Hsp70 complexes have been developed, these suffer from several drawbacks. Cost of generating the affinity reagent is high, and the specificity of the drug may result in purification of unwanted Hsp70 isoform complexes. It has yet to be determined whether post-translational modification on Hsp70 alter drug binding in the same way they do for the related chaperone Hsp90 (35, 36). Conventional approaches to expressing epitope tagged proteins in mammalian cells for affinity purification-mass spectrometry typically fall into two categories; transient transfection with a plasmid expression the fusion protein of interest (typically from a constitutive promoter such as CMV) or stable transfection where cells are transfected with an expression plasmid and then maintained for several weeks to months on selectable media to induce integration into the cell's genome. Endogenous epitope tagging of proteins offers significant advantages over conventional approaches used to study protein complexes in the mammalian cells. Tagging of genes at their natural chromosomal locations retains native promoter control of the target protein. This is important because overexpressing (or underexpressing) a target gene may change the stoichiometry of its protein-protein or protein-DNA interactions, creating artifacts in interactomic data. Many genes are finely regulated at the transcriptional level, changing based on factors such as cell cycle stage and stress. Native promoter control allows observation of native protein expression under any cellular condition.

In this study, we set out to create a mammalian cell line expressing tap-tagged Hsc70 from its endogenous promoter using CRISPR. We managed to achieve this, utilizing only a CAS9-Hsc70gRNA targeting plasmid and a small ssODN containing a tandem HIS-FLAG tag and overhangs homologous to the genome. A relatively high success rate was achieved,

with 50% of clones expressing HIS_6-FLAG-Hsc70. This is encouraging given the homology arms of the ssODN were only 71bp and 78bp respectively.

The HEK293T$^{HIS\text{-}FLAG\text{-}Hsc70}$ cells produced in this study are stable and thus are suitable for experiments lasting longer than 72 hours after which expression from transient transfection would decline. Although traditional stable transfection methodologies mitigate this issue, this technology suffers from lack of control over copy number of and location of integration events, with causing varied expression between cells in a growing population. Our CRISPR cells were expanded from a single clone producing homogeneity of expression. In addition, given that the CRISPR integration method does not use any selectable resistance markers, cells can be grown in drug-free media conditions. A common concern of epitope tagging is potential disruption of protein function and interactions. While HIS and FLAG-tagged Hsc70 constructs have been utilized in many previous studies, it was hard to assess functionality given that the native Hsc70 was still expressed alongside the exogenous protein. All interactions of well-established Hsc70 binding proteins tested in this study were maintained in HEK293T$^{HIS\text{-}FLAG\text{-}Hsc70}$ cells. In addition, no growth defects were observed for these cells compared to standard HEK293T cells, attesting to the functionality of these constructs when expressed as the sole Hsc70 in the cell. Advantages of the tandem HIS_6-FLAG tag include flexibility in choice of affinity reagents that can be used and ability to significantly reduce non-specific complex binding through tandem purification protocols (typically IMAC purification followed by FLAG purification).

In conclusion, we have developed a protocol for generating epitope tagged chaperones from their native promoter using only minimal reagents. The cell line generated in this study (HEK293T$^{HIS\text{-}FLAG\text{-}Hsc70}$ cells) will be a freely available and useful reagent for

chaperone researchers, especially in the quest to understand the complexities of the Hsc70 interactome.

2.5 Figures

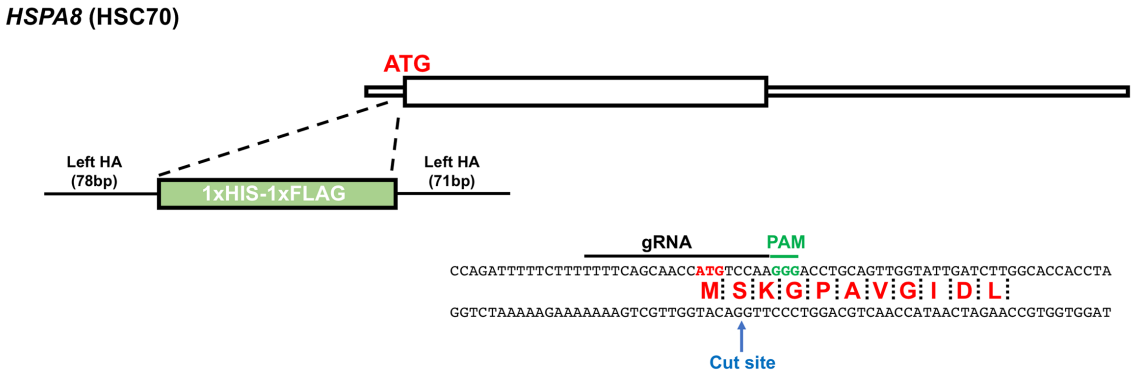

Figure 5. Design of a tandem HIS-FLAG epitope suitable for endogenous tagging of Hsc70. Schematic of the *HSC70* locus, Cas9 targeting site, and donor construct used to insert the HIS-FLAG tag. Annotated are the positions of the stop codon (TAG), the Protospacer Adjacent Motif (PAM) that specifies the cleavage site, and homology arms left and right (Left-HA, Right-HA).

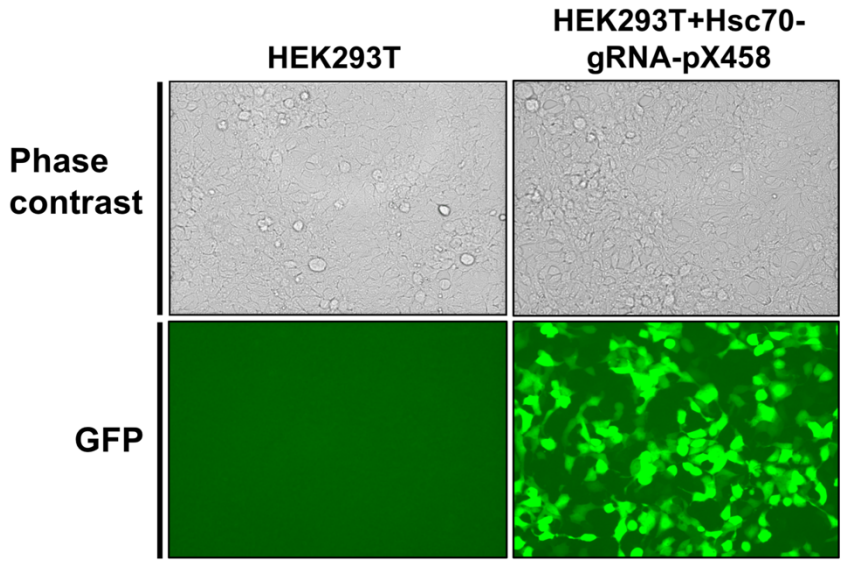

Figure 6. Expression of Cas9-2A-GFP in HEK293T cells transfected Hsc70-gRNA-pX458. Phase contrast and GFP fluorescence images of HEK293T cell line and HEK 293T cell line transfected with Hsc70-gRNA-pX458.

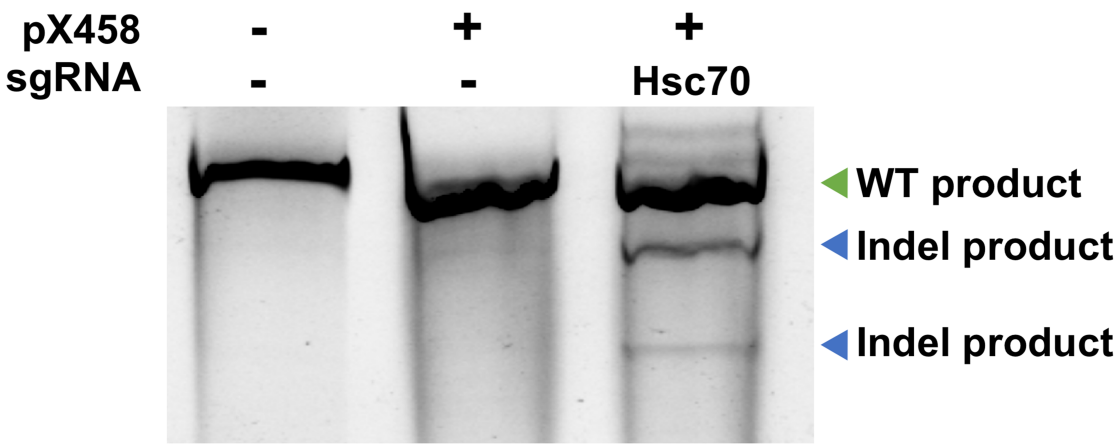

Figure 7. Determining CRISPR-mediated cleavage using SURVEYOR assay. DNA was extracted from unsorted untransfected HEK293T cells (control), transfected with either Cas9 expressing plasmid with no guide RNA or a plasmid expressing both Cas9 and *HSC70*-targeting gRNA. CRISPR-mediated genome editing was assessed by SURVEYOR assay. Correctly sized Indel products obtained from the SURVEYOR assay are annotated (Blue arrow).

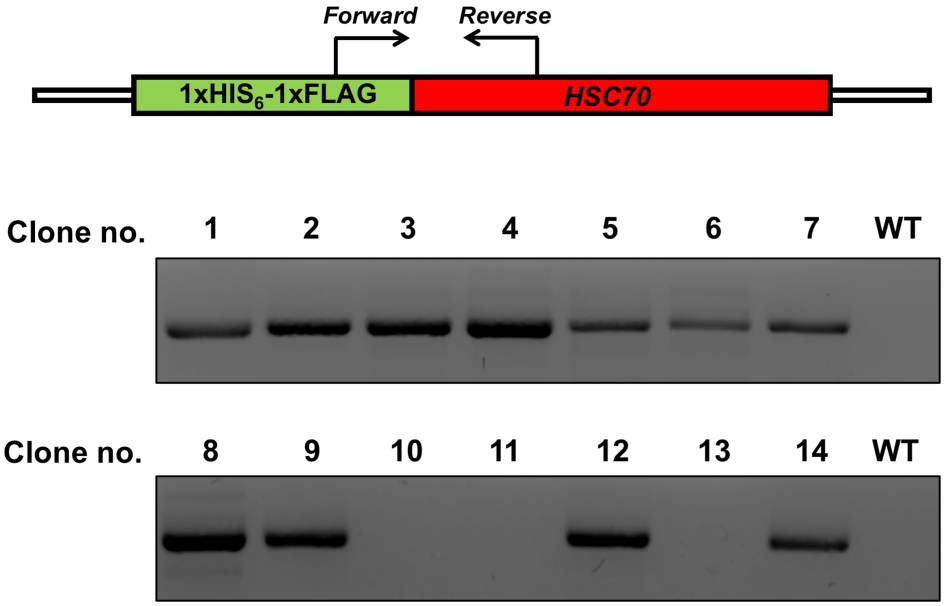

Figure 8. Schematic and results of a PCR-based assay (in-out PCR). PCR based assay used to detect targeted integration of the tag sequence in single-cell-derived HEK293T clones obtained by limiting dilution following CRISPR/Cas9-driven gene targeting. Primers are located outside of the homology arms and are designed to yield a PCR product if the tag is inserted. WT indicates untagged cells and 1-14 are single cell derived clones.

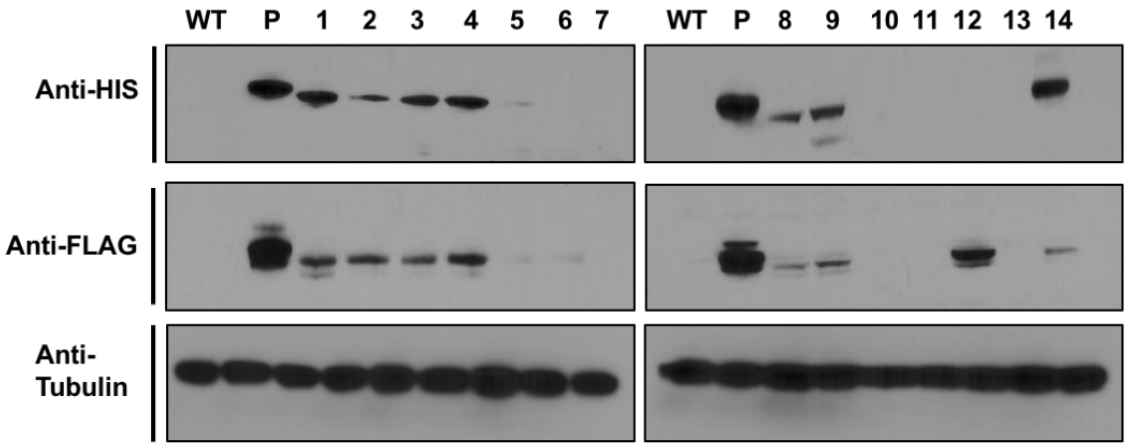

Figure 9. Western Blot analysis of single-cell-derived HEK293T clones. Western Blots showing HIS-tag (Upper panel) and FLAG-tag protein expression in single cell-derived HEK293T clones obtained by limited dilution following CRISPR/Cas9-driven gene targeting using HIS and FLAG antibody, α-tubulin is used as a loading control. WT indicates untagged cells, P indicates Hsc70 expressed on a plasmid and 1-14 are single cell derived clones.

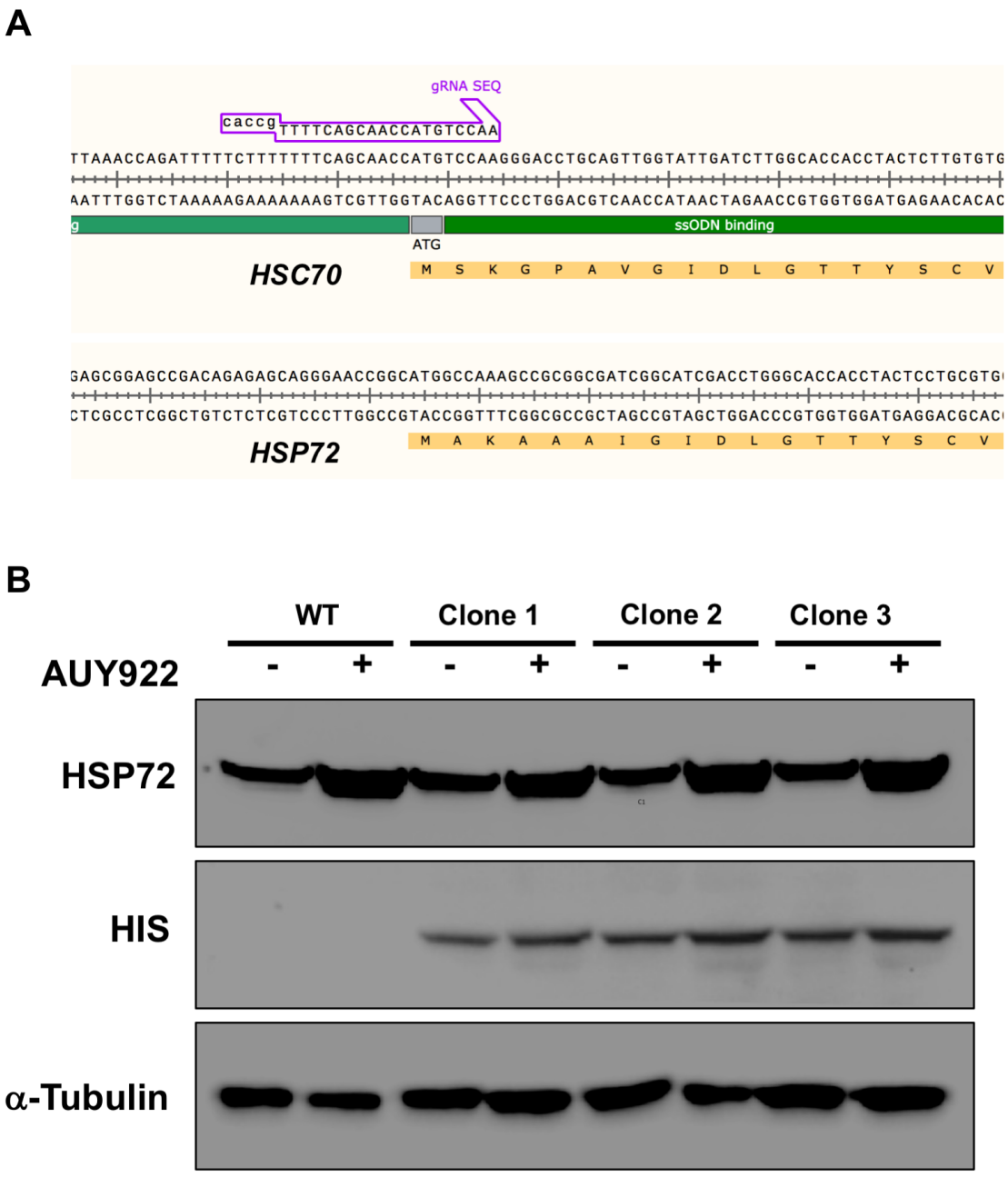

Figure 10. CRISPR-mediated tagging of Hsc70 is isoform specific. (A) Amino acid and genomic DNA sequences of *HSC70* and *HSP72*. The *HSC70* gRNA binding site is absent in the *HSP72* gene. (B) Luminespib induces Hsp72 levels but not HIS-Hsc70 levels. WT indicates untagged cells, clones 1-3 are three separate HEK293T$^{\text{HIS-FLAG-Hsc70}}$ clones. α-tubulin is used as a loading control in this instance.

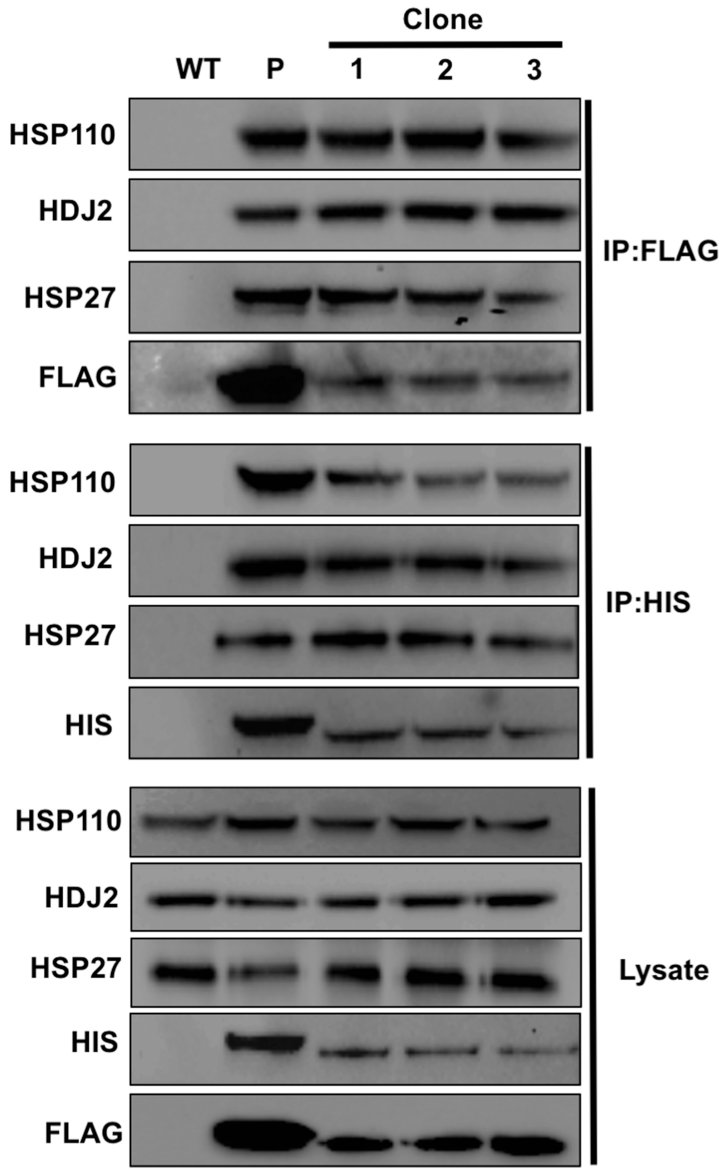

Figure 11. Validation of known Hsc70 interactions in HEK293T$^{HIS\text{-}FLAG\text{-}Hsc70}$ cells. Protein extracts were obtained from WT and three separate HEK293T$^{HIS\text{-}FLAG\text{-}Hsc70}$ clones. Hsc70 complexes were purified using either HIS or FLAG magnetic beads. Hsc70 complexes were resolved by SDS-PAGE and analyzed by Western Blot using antibodies to co-chaperone proteins HSP27, HDJ2 and HSP110.

2.6 References

1. Hartl FU, Bracher A, Hayer-Hartl M. Molecular chaperones in protein folding and proteostasis. Nature. 2011;475(7356):324-32.
2. Mayer MP, Bukau B. Hsp70 chaperones: cellular functions and molecular mechanism. Cell Mol Life Sci. 2005;62(6):670-84.
3. Rohde M, Daugaard M, Jensen MH, Helin K, Nylandsted J, Jaattela M. Members of the heat-shock protein 70 family promote cancer cell growth by distinct mechanisms. Genes Dev. 2005;19(5):570-82.
4. Boorstein WR, Ziegelhoffer T, Craig EA. Molecular evolution of the HSP70 multigene family. J Mol Evol. 1994;38(1):1-17.
5. Kelley WL. Molecular chaperones: How J domains turn on Hsp70s. Curr Biol. 1999;9(8):R305-8.
6. Takayama S, Reed JC. Molecular chaperone targeting and regulation by BAG family proteins. Nat Cell Biol. 2001;3(10):E237-41.
7. Aebersold R, Mann M. Mass spectrometry-based proteomics. Nature. 2003;422(6928):198-207.
8. Gavin AC, Bosche M, Krause R, Grandi P, Marzioch M, Bauer A, et al. Functional organization of the yeast proteome by systematic analysis of protein complexes. Nature. 2002;415(6868):141-7.
9. Ho Y, Gruhler A, Heilbut A, Bader GD, Moore L, Adams SL, et al. Systematic identification of protein complexes in Saccharomyces cerevisiae by mass spectrometry. Nature. 2002;415(6868):180-3.
10. Kocher T, Superti-Furga G. Mass spectrometry-based functional proteomics: from molecular machines to protein networks. Nat Methods. 2007;4(10):807-15.
11. Taipale M, Krykbaeva I, Koeva M, Kayatekin C, Westover KD, Karras GI, et al. Quantitative analysis of HSP90-client interactions reveals principles of substrate recognition. Cell. 2012;150(5):987-1001.
12. Zhao R, Davey M, Hsu YC, Kaplanek P, Tong A, Parsons AB, et al. Navigating the chaperone network: an integrative map of physical and genetic interactions mediated by the hsp90 chaperone. Cell. 2005;120(5):715-27.
13. Truman AW, Kristjansdottir K, Wolfgeher D, Hasin N, Polier S, Zhang H, et al. CDK-dependent Hsp70 Phosphorylation controls G1 cyclin abundance and cell-cycle progression. Cell. 2012;151(6):1308-18.
14. Truman AW, Kristjansdottir K, Wolfgeher D, Ricco N, Mayampurath A, Volchenboum SL, et al. Quantitative proteomics of the yeast Hsp70/Hsp90 interactomes during DNA damage reveal chaperone-dependent regulation of ribonucleotide reductase. J Proteomics. 2015;112:285-300.
15. Woodford MR, Truman AW, Dunn DM, Jensen SM, Cotran R, Bullard R, et al. Mps1 Mediated Phosphorylation of Hsp90 Confers Renal Cell Carcinoma Sensitivity and Selectivity to Hsp90 Inhibitors. Cell Rep. 2016;14(4):872-84.
16. Tanaka M, Shiota M, Okada S, Harada A, Odawara J, Mun S, et al. Generation of a rat monoclonal antibody specific for hsp72. Hybridoma (Larchmt). 2011;30(4):397-400.

17. Shiota M, Saiwai H, Mun S, Harada A, Okada S, Odawara J, et al. Generation of a rat monoclonal antibody specific for heat shock cognate protein 70. Hybridoma (Larchmt). 2010;29(5):453-6.
18. Tanaka M, Mun S, Harada A, Ohkawa Y, Inagaki A, Sano S, et al. Hsc70 contributes to cancer cell survival by preventing Rab1A degradation under stress conditions. PLoS One. 2014;9(5):e96785.
19. Tanaka M, Shiota M, Nakao T, Uemura R, Nishi S, Ohkawa Y, et al. Identification of low-abundance proteins in serum via the isolation of HSP72 complexes. J Proteomics. 2016;136:214-21.
20. Dunn DM, Woodford MR, Truman AW, Jensen SM, Schulman J, Caza T, et al. c-Abl Mediated Tyrosine Phosphorylation of Aha1 Activates Its Co-chaperone Function in Cancer Cells. Cell Rep. 2015;12(6):1006-18.
21. Ran FA, Hsu PD, Wright J, Agarwala V, Scott DA, Zhang F. Genome engineering using the CRISPR-Cas9 system. Nat Protoc. 2013;8(11):2281-308.
22. Dalvai M, Loehr J, Jacquet K, Huard CC, Roques C, Herst P, et al. A Scalable Genome-Editing-Based Approach for Mapping Multiprotein Complexes in Human Cells. Cell Rep. 2015;13(3):621-33.
23. Rigaut G, Shevchenko A, Rutz B, Wilm M, Mann M, Seraphin B. A generic protein purification method for protein complex characterization and proteome exploration. Nat Biotechnol. 1999;17(10):1030-2.
24. Shaner L, Wegele H, Buchner J, Morano KA. The yeast Hsp110 Sse1 functionally interacts with the Hsp70 chaperones Ssa and Ssb. J Biol Chem. 2005;280(50):41262-9.
25. He X, Tan C, Wang F, Wang Y, Zhou R, Cui D, et al. Knock-in of large reporter genes in human cells via CRISPR/Cas9-induced homology-dependent and independent DNA repair. Nucleic Acids Res. 2016;44(9):e85.
26. de Los Milagros Bassani Molinas M, Beer C, Hesse F, Wirth M, Wagner R. Optimizing the transient transfection process of HEK-293 suspension cells for protein production by nucleotide ratio monitoring. Cytotechnology. 2014;66(3):493-514.
27. Yang L, Yang JL, Byrne S, Pan J, Church GM. CRISPR/Cas9-Directed Genome Editing of Cultured Cells. Curr Protoc Mol Biol. 2014;107:31 1 1-17.
28. Consortium EP. An integrated encyclopedia of DNA elements in the human genome. Nature. 2012;489(7414):57-74.
29. Taniguchi H, Hasegawa H, Sasaki D, Ando K, Sawayama Y, Imanishi D, et al. Heat shock protein 90 inhibitor NVP-AUY922 exerts potent activity against adult T-cell leukemia-lymphoma cells. Cancer Sci. 2014;105(12):1601-8.
30. Radons J. The human HSP70 family of chaperones: where do we stand? Cell Stress Chaperones. 2016;21(3):379-404.
31. Mayer MP. Hsp70 chaperone dynamics and molecular mechanism. Trends Biochem Sci. 2013;38(10):507-14.
32. Liu Q, Li H, Yang Y, Tian X, Su J, Zhou L, et al. A disulfide-bonded DnaK dimer is maintained in an ATP-bound state. Cell Stress Chaperones. 2017;22(2):201-12.
33. Gong Y, Kakihara Y, Krogan N, Greenblatt J, Emili A, Zhang Z, et al. An atlas of chaperone-protein interactions in Saccharomyces cerevisiae: implications to protein folding pathways in the cell. Mol Syst Biol. 2009;5:275.

34. Rodina A, Wang T, Yan P, Gomes ED, Dunphy MP, Pillarsetty N, et al. The epichaperome is an integrated chaperome network that facilitates tumour survival. Nature. 2016;538(7625):397-401.
35. Walton-Diaz A, Khan S, Bourboulia D, Trepel JB, Neckers L, Mollapour M. Contributions of co-chaperones and post-translational modifications towards Hsp90 drug sensitivity. Future Med Chem. 2013;5(9):1059-71.
36. Woodford MR, Dunn D, Miller JB, Jamal S, Neckers L, Mollapour M. Impact of Posttranslational Modifications on the Anticancer Activity of Hsp90 Inhibitors. Adv Cancer Res. 2016;129:31-50.

CHAPTER 3: CHEMOGENOMIC SCREENING IDENTIFIES THE HSP70 CO-CHAPERONE DNAJA1 AS A HUB FOR ANTICANCER DRUG RESISTANCE

This chapter has been published:

Nitika, Jacob S Blackman, Laura E Knighton, Jade E Takakuwa, Stuart K Calderwood, Andrew W Truman. Chemogenomic screening identifies the Hsp70 co-chaperone DNAJA1 as a hub for anticancer drug resistance.

3.1 Introduction

Hsp70 is a molecular chaperone that plays important roles in protein quality control processes such as protein folding, transport, degradation, and the prevention of protein aggregation(1). Hsp70 levels are elevated in various cancers and overexpression correlates with poor prognosis for survival and response to cancer therapy (2). The elevated levels of Hsp90 and Hsp70 chaperones in cancer and their role in fostering multiple oncogenic pathways has made these proteins attractive drug targets with numerous anti-chaperone compounds having been developed so far (3). Problematically, Hsp70 is required for cell survival and protein homeostasis, and thus its inhibition is detrimental to the viability of both normal and cancer cells, with dubious selectivity for tumor cells (4).

Hsp70 performs all its functions in association with a large spectrum of helper proteins known as co-chaperones that include J-proteins, tetratricopeptide repeat (TPR) domain-containing proteins and nucleotide exchange factors (NEFs) which fine-tune Hsp70 specificity and activity in the cell. The J-proteins recruit the protein substrates or clients and interact with such clients at the interface of NBD and SBDβ of Hsp70. This interaction leads to increased Hsp70-mediated ATP turnover and activation of protein folding. J-proteins have a highly conserved 70 amino acid motif containing Histidine, Proline and

Aspartic acid amino acid residues known as HPD motif which is essential for stimulating ATPase activity of Hsp70 (5). In humans, the J-protein family has about 50 members which are further divided into three groups based on the localization of J-domain within a protein (6). The Hsp40 DNAJA1 (more commonly referred to as DNAJA1) associates with unfolded polypeptide chains, preventing their aggregation (6). Several Hsp70 inhibitors have failed in clinical trials due to their toxicity. More recently, alternative strategies have focused on sensitizing cells to anticancer agents by either manipulating post-translational modification of chaperones or their interaction with specific co-chaperones (4, 7-11). DNAJA1 (mammalian homolog of yeast Ydj1) is an interesting possible anticancer target as a key mediator of Hsp70 function that appears to regulate specific features of tumorigenesis (8, 12). A recent study demonstrated that CRPCs expressing ARv7 are insensitive to Hsp90 inhibitors but are sensitive to Hsp40 inhibition (13). In addition, we have shown that targeting specific oncoprotein complexes (ribonucleotide reductase) with a combination of traditional as well as a DNAJA1 inhibitor produces highly synergistic effects (8). We propose that targeting DNAJA1 in cancer may offer an attractive alternative to the toxicity induced by full Hsp90/Hsp70 inhibition.

Anticancer monotherapies using broadly active cytotoxic or molecularly targeted drugs are limited in their ability to demonstrate a reliable clinical response. This is due to redundant signaling pathways, feedback loops and resistance mechanisms in cancer cells (14). Thus, combination anticancer therapies have been used clinically for over 50 years to improve the responses achieved by monotherapies alone. Cancer cell line-based models for these combination therapies are easy and inexpensive to perform using high-throughput drug screening protocols (HTS) to identify the most effective drug combination (15, 16).

HTS helps to explore the relationship between the cell line characteristics and drug specific dose responses (15). Chemogenomics is one such HTS-based approach where a large collection of anticancer chemical drugs are screened to identify biological targets. These screening sets often contain small molecules that are well annotated and have defined molecular targets. Such an approach is particularly beneficial for cancer research because malignant cells often contain multiple aberrations that require targeted therapy to inactivate cancer driver activities and mitigate deleterious effects of the drugs to normal cells (14).

Here, we performed an unbiased screen of the NIH Approved Oncology Drug set containing 131 anti-cancer drugs in combination with HAP1 cancer cell lines depleted of J-protein DNAJA1. We identified 41 compounds showing strong synergy with the loss of DNAJA1, and in contrast 18 molecules that displayed reduced potency in the knockout cell line. We validated three drugs (cabozantinib, clofarabine and vinblastine) in combination with a unique DNAJA1 inhibitor (116-9e) for synergy in the LNCaP cancer cell lines and confirmed omacetaxine mepesuccinate, idarubicin and sorafenib for antagonism (i.e. with reduced potency after DNAJA1 inhibition). This study demonstrates the validity of developing Hsp70 co-chaperone inhibitors to sensitize cells to current anticancer therapies and suggests that determining DNAJA1 status of a tumor may be beneficial in selecting the most appropriate course of treatment.

3.2 Materials and Methods

Cell culture. The HAP1 Chronic Myelogenous Leukemia cancer cell line and DNAJA1 knockout cell line was purchased from Horizon Discovery and were cultured in Iscove's Modified Eagle Medium (Invitrogen) with 10% fetal bovine serum (Gibco), 100 units/ml penicillin, and 100 μg/ml streptomycin at 5% CO_2 and 37° C. The LNCaP cancer cell line

was purchased from ATCC and were cultured in RPMI-1640 medium (Invitrogen) with 10% fetal bovine serum (FBS, Clontech), 100 units/ml penicillin, and 100 µg/ml streptomycin at 5% CO_2 and 37° C.

Drug Screening. Approved Oncology Drug plates consisting of the most current FDA approved anticancer drugs were obtained from the National Cancer Institute (NCI). For experiments delineating the synergy between the loss of DNAJA1 and approved anticancer drug, HAP1 cells and HAP1 (DNAJA1 KO) cells were plated in growth media at 20% confluency 1 day prior to drug treatment. On Day 1 of treatment, cells were treated with DMSO (control), Approved oncology anticancer drugs at 50 µM for 72 hours. Following drug treatments, Cell Titer-Glo reagent was added directly to the wells according to the manufacturer's instructions. The luminescence was measured on Bio-Tek Plate reader. Luminescence reading was normalized to and expressed as a relative percentage of the plate averaged DMSO control. The data shown are the mean and SEM of three independent biological replicates.

Combination index (CI) calculations. For IC_{50} calculations, LNCaP cells were seeded in triplicates in 96-well white bottom Nunc plates in growth media at 20% confluency 1 day prior to initiation of drug treatment. On Day 1 of treatment, cells were treated with DMSO (control) and ten folds serial dilution of anti-cancer drugs cabozantinib, clofarabine, vinblastine, sorafenib, idarubicin and omacetaxine mepesuccinate and 116-9e. After 72 h, cell viability was measured using Promega Cell Titer-Glo cell viability assay on Bio-Tek plate reader. The combination index was calculated using the Chou-Talalay method using CompuSyn software(17).

Spheroid Generation. Single-cell suspensions (5000/well) were plated in one well of 24-well plates in a 1:1 mixture of RPMI medium and Matrigel (BD Bioscience CB-40324). Cells in Matrigel were kept cold at all times and under continuous agitation. Warm PBS was added to all empty wells, if any. Plates were incubated at 37 °C with 5% CO_2 for 15 min to solidify the gel before addition of 100 µl of pre-warmed RPMI to each well. Two days after seeding, the media was fully aspirated and replaced with fresh RPMI containing the indicated drugs. The same procedure was repeated daily on two consecutive days. Twenty-four hours after the last treatments, the media was aspirated and the wells were washed with 100 µl of pre-warmed PBS. To prepare for downstream assays, spheroids were released from the Matrigel by incubating at 37 °C for 40 min in 100 µl of 10 mg/mL Dispase I (Sigma).

Apoptosis assay. Apoptosis of LNCaP spheroids was detected by the Annexin V–FITC/propidium iodide–binding assay. Cells were treated with either 0.1% DMSO (dimethyl sulfoxide),116-9e, cabozantinib, clofarabine, vinblastine, sorafenib, idarubicin, omacetaxine mepesuccinate and sorafenib alone or in combination with 116-9e for 48 hours at the IC_{50} concentrations, and then stained with Annexin V–FITC and propidium iodide. The rate of apoptosis was determined using a BD Fortessa flow cytometer, and the collected data were analyzed using FlowJo software. Apoptosis was reported as the mean ± SD. The results are representative of three independent experiments.

Bioinformatics. Cancer genome data and Cancer Cell Line Encyclopedia data were accessed from the cBioPortal (www.cbioportal.org) for Cancer Genomics (18). Total patient numbers and detailed information regarding published datasets and associated publications are indicated in Fig 1A and 1B.

Statistical analysis. Data were analyzed using GraphPad Prism built-in statistical tests indicated in relevant figure legends. The following asterisk system for P-value was used: P <0.05; P <0.01; 0.001; and P <0.0001.

Western Blotting. Protein extracts were made as described (8). 30 μg of protein was separated by 4%–12% NuPAGE SDS-PAGE (Thermo). Proteins were detected using the following antibodies; anti-DNAJA1/HDJ2 (Thermo # MA5-12748), anti-Actin (CST # 9774), Anti-Hsc70 (Santa Cruz, # sc-7298), anti-Hsp70 (Enzo # C92F3A-5), anti-Hsp90 α/$\mathscr{B}$ (Santa Cruz # sc-13119), anti-Bag3 (Santa Cruz # sc-136467), anti-Hsp110 (Stress Marq, # SPC-195),) at 1:4000 dilution in TBST+1% BSA. The secondary antibody (StarBright Blue 700 Fluorescent Secondary Mouse) was used at 1:3000 dilution in TBST+1% BSA. Blots were imaged on a Chemi Doc MP imaging system (Bio-Rad).

3.3 Results

DNAJA1 is mutated and overexpressed in a variety of cancers.

While the roles of Hsp90 and Hsp70 in cancer have been thoroughly studied, much less is known of the role that regulatory co-chaperone proteins such as DNAJA1 play in tumorigenesis. As a first step, we queried the cBioPortal cancer genomic database (cbioportal.org) to determine the incidence of *DNAJA1* alterations in cancer. Analysis of data from 176 non-redundant studies representing 44,347 patient samples revealed that *DNAJA1* was altered at a frequency of greater than 1% in 35 cancer types (Fig. 12A). Although the majority of alterations in *DNAJA1* occur at a relatively low frequency (<5% of cancers) *DNAJA1* is significantly amplified in prostate neuroendocrine cancer (PNC) and castration-resistant prostate cancer at a frequency of 17.31% and 17.14% respectively (Fig. 1A). Hsp70 and Hsp90 are often overexpressed in tumors (2). To determine whether

the *DNAJA1* expression is also overexpressed in cancer, we analyzed *DNAJA1* mRNA expression in samples from the TGCA PAN-CAN Atlas. Interestingly, *DNAJA1* mRNA was expressed at significantly higher levels in these samples, with a median expression in cancer over 3000x relative to WT reference samples (Fig. 12B). To determine if this dramatic overexpression of DNAJA1 was a result of amplification, we plotted DNAJA1 expression vs amplification (Fig. 12C). Interestingly, there was minimal correlation between amount of amplification and DNAJA1 expression (r=0.45) suggesting that while DNAJA1 may be an important marker in cancer it is not caused by gene amplification.

Characterizing the role of DNAJA1 in anticancer drug resistance.

The existing literature is contradictory as to whether DNAJA1 may possess tumor suppressor or driver properties (12, 19). To clarify whether silencing of DNAJA1 could be beneficial in the treatment of cancer, we screened wildtype HAP1 cells and HAP1 cells lacking DNAJA1 ($HAP1^{DNAJA1\ KO}$) for comparative resistance against the NIH NCI Approved Oncology Collection (Fig. 13A) (https://dtp.cancer.gov/organization/dscb/obtaining/available_plates.html). Prior to screening, we validated the status of the *DNAJA1* knockout cell line by Western blotting for DNAJA1 and other major chaperones and co-chaperones (Hsp70, Hsc70, Hsp90, Bag-3 and Hsp110). As expected, we confirmed loss of DNAJA1 and interestingly did not observe any compensatory effects on the levels of the other chaperones/co-chaperones studied (Fig. 16). According to pharmacologic action, the compounds in the library have been divided into seven categories: protein synthesis inhibitors, proteasome inhibitors, epigenetic modifiers, metabolic inhibitors, cytoskeletal inhibitors, signal transduction inhibitors and DNA synthesis/repair inhibitors. Further fold enrichment of each drug

category was calculated for the drugs whose potency increased or decreased with loss of DNAJA1. To monitor the screening quality, each screening plate contained control wells treated with vehicle (1% DMSO). The final concentration of the screening compounds was 50 μmol/L. Positive hits (synergistic) or negative hits (antagonistic) were determined by normalizing the $\log_2$ ratio of viability of DNAJA1 knockout cells over wildtype cells. A full list of the screening results is shown in Supplementary Table T1 and the sorted data are graphically plotted in Fig. 13B. The effectiveness of a large proportion of anticancer molecules in the collection were impacted, with 41 of (31%) showing increased potency and 18 (14%) showing reduced potency upon loss of *DNAJA1* (Fig. 13C). Drug target analysis was carried out by calculating fold enrichment of positive hits (synergistic) or negative hits (antagonistic) over the total number of drugs in that category. Drug target analysis of the synergistic drug hits revealed significant enrichment in DNA synthesis and repair inhibitors, signal transduction inhibitors as well as cytoskeletal inhibitors (Fig. 13D). In contrast, drug target analysis of antagonistic drug hits revealed a higher enrichment in categories such as epigenetic modifiers, protein synthesis inhibitors, cytoskeletal inhibitors and proteasome inhibitors (Fig. 13E). For a full list of drugs in each category and raw data from screen, please see supplemental Table T1.

Strikingly, a small number of compounds with supposedly related function showed dissimilar alteration of potency upon loss of DNAJA1 function, potentially caused by off-target drug effects (see discussion).

Validation of anticancer drugs significantly altered for potency upon loss of DNAJA1. Many anticancer compounds have low potency, poor therapeutic index or suffer from the development of resistance . Monotherapy is rarely efficient and instead drug cocktails are

widely used in the clinic(16). Establishing these combinations can enhance the scope of preclinical studies and inform the design of future clinical trials. Although knockout of *DNAJA1* substantially increased the potency of a number of anticancer molecules, it remained to be determined whether small-molecule inhibition of DNAJA1 could produce a similar result. Our previous bioinformatics analysis indicated that a large proportion of prostate cancer cells contain either amplification or mutation of *DNAJA1* (approximately 18%, see Fig. 12 A). To validate the results of our initial screen, we analyzed the effect of treating prostate cancer cells (LNCaP) with a combination of 116-9e, a small molecule inhibitor of DNAJA1(20) and selected hits from our screen. We decided to focus on three synergistic drugs discovered in the screen: cabozantinib (receptor tyrosine kinase inhibitor), clofarabine (an RNR inhibitor) (21) and vinblastine (microtubule inhibitor/G2 arresting agent) (22, 23). We also validated three drugs that demonstrated a significant loss of potency in cells lacking DNAJA1: sorafenib (a VEGFR-2 inhibitor) (24), omacetaxine mepesuccinate (more commonly known as homoharringtonine, a protein translation inhibitor) (25) and idarubicin (topoisomerase II inhibitor) (26). To determine synergy in a quantitative manner, we calculated drug synergy (Combination Index values, CI) between 116-9e and either synergistic or antagonistic drugs hits across a broad range of concentrations using the Chou-Talalay method (27) (for effects of individual drugs, please see Fig. 17). For three hits identified in our screen (cabozantinib, clofarabine and vinblastine) we confirmed significant synergy (CI<1) with 116-9e across a range of doses (Figure 14A, B, C). In contrast, idarubicin, omacetaxine and sorafenib displayed a significantly antagonistic interaction (CI>1) across a range of doses (Figs. 14D, E & F).

These data suggest that while DNAJA1 inhibition is a promising strategy to sensitize cells to some inhibitors, it might have inverse effects with other inhibitors.

Evaluating the effects of dual targeting of identified drugs with DNAJA1 inhibition on morphology and viability of prostate cancer spheroids.

Recent studies have suggested that precision therapy approaches involving the exposure of drugs directly to the primary tumor tissue have the potential to augment the personalized medicine efforts and influence clinical decisions(28). Establishing *ex vivo* three-dimensional (3D) tumor spheroids or organoids derived from primary cancers can be easily established and potentially scaled to screen drug combinations. These 3D cancer models appear to recapitulate features of the tumor of origin in terms of heterogeneity, cell differentiation, histoarchitecture, and clinical drug response and can be used for rapid drug screening (29). We therefore next examined the effect of drug combination (three antagonistic and synergistic hits) on LNCaP spheroids. Specifically, changes in spheroid size and shape induced by the 3 antagonistic and synergistic drugs were determined. Visual examination revealed that for the synergistic drugs combination with 116-9e resulted in physical disruption of LNCaP spheroids, resulting in decrease in spheroid size (Fig. 15A). The disruption started on the second day of the treatment. However, when the 3 antagonistic drugs were administered along with 116-9e, there were minimal changes in spheroid morphology indicating that the combination was ineffective.

Next, we measured the induction of apoptosis in the spheroids post drug treatments. We determined the kinetics of apoptosis induction using AnnexinV/PI staining. Drug-induced apoptosis was readily detected in the LNCaP spheroids treated with mono and dual drug combinations. In concurrence with the previous results, the combination of the three

synergistic drugs with 116-9e displayed enhanced apoptosis as compared to the single drug treatment whereas spheroids treated with the 3 antagonistic drugs showed little or no difference in the rate of apoptosis as compared to the dual drug combination with 116-9e (Figure 15B).

3.4 Discussion

Although inhibitors of Hsp70 and Hsp90 have been developed for research purposes, the conversion of these molecules for use in patient treatment have been hampered by toxicity issues (4). We undertook this study to resolve conflicting literature on whether inhibiting DNAJA1, a co-chaperone of Hsp70 may be useful as a novel anticancer strategy. Our bioinformatic analysis of DNAJA1 expression and mutation clearly identify DNAJA1 as being highly altered in a range of cancers, particularly in Prostate Cancer. Interestingly, DNAJA1 despite being substantially overexpressed in a range of cancers, there was minimal correlation between DNAJA1 copy number and level of expression. While beyond the scope of this study, it is possible that the high levels of DNAJA1 expression observed may be a result of increased transcription brought on hyperactive signaling pathways common in cancer cells. This data in conjunction with a recent finding that Hsp40 is involved in regulation of ARv (13) makes DNAJA1 inhibition an ideal choice as a novel therapeutic target in Prostate Cancer.

In this study, loss of DNAJA1 increased the potency of a substantial number (31%) of clinically used anticancer drugs. This increased potency may be related to the destabilization of clients that are the target of these small molecules. For example, Hsp70 activates many proteins involved in the DNA damage response and DNA repair pathways (DDR), including ATM, APE1, PARP1, XRCC1 (30). Recently, studies from our group

have established roles for both Hsp70 and DNAJA1 in stability of the RNR complex (8, 30, 31). It is unsurprising then that many of the anticancer agents displaying synergy with loss of DNAJA1 are connected to inhibition of the DNA damage response/repair. These include molecules such as 5-fluorouracil (5-FU), premetrexed, clofarabine, olaparib and niraparib etoposide, teniposide and valrubicin. Here we validated synergy with the RNR inhibitor clofarabine. Clofarabine is phosphorylated intracellularly to form cytotoxic active 5'-triphosphate metabolite, which inhibits the enzymatic activities of RNR and DNA polymerase, resulting in inhibition of DNA synthesis and repair (32). While most DDR inhibitors displayed increased potency with DNAJA1 depletion, four of them were antagonistic to loss of DNAJA1. These include topoisomerase inhibitors and nucleic acid synthesis inhibitors such as trifluridine, irinotecan, epirubicin (4'-epi-isomer of the antibiotic doxorubicin) and idarubicin (4-demethoxy analogue of daunorubicin) (33). While at first these results seem paradoxical, it is worth noting that inrinotecan is a type I topoisomerase inhibitor, whereas Etoposide (synergistic with loss of DNAJA1) a type II topoisomerase inhibitor. It may be that Hsp70 and DNAJA1 play opposing regulatory roles in the stabilization and activation of these related proteins.

In addition to DDR, DNAJA1 is also involved in signal transduction, with previous reports indicating that the yeast homolog of DNAJA1 (Ydj1) is critical for supporting the integrity of kinase signaling networks (34). DNAJA1 is mobilized to specific sites within the nucleus in response to inappropriate targeting or folding of specific mutant receptors. DNAJA1 overexpression ameliorates the defective transactivation and trans-repression activity of mutant Glucocorticoid receptors (35). In line with the previous studies, we found that a handful of Receptor Tyrosine kinase inhibitors were synergistic with DNAJA1

depletion. These included Vascular endothelial growth factor receptor (VEGFR) inhibitors such as sunitinib, cabozantinib, lenvatinib and pazopanib. Interestingly, randomized phase III clinical trials are being conducted to validate the efficacy of Cabozantinib in heavily pretreated prostate cancer patients (36). One implication from our study is that DNAJA1 inhibition might significantly enhance the effect of cabozantinib monotherapy.

Strikingly, some of the kinase inhibitors were antagonistic to DNAJA1 depletion. These include VEGFR inhibitors such as regorafenib and sorafenib. This disparity can be explained by the different target receptors and mechanisms of action of these drugs. Interestingly, recent studies indicated that these small molecule inhibitors exhibit off-target effects. Some of these drugs are misidentified and mischaracterized for their target specific inhibition, which has contributed to the high failure rate of these drugs in the treatment of cancer patients (37).

In addition to its role in signal transduction, DNAJA1 is also important for maintaining the cellular cytoskeleton. Previous studies have suggested that YDJ1 (the yeast homolog of DNAJA1) is important for the proper assembly of microtubules (38). Another report showed that DNAJA1 depletion causes relocation of N-cadherin and enhanced activity of metalloproteinases. This leads to changes in the actin cytoskeleton indicating that DNAJA1 is important for prevention of the amoeboid-like transition of tumor cells (39). These studies indicated the involvement of DNAJA1 in maintaining cytoskeletal organization. We found 3 anticancer drugs targeting the cytoskeleton to be synergistic with DNAJA1 depletion, including vinblastine sulfate (cytoskeletal inhibitor that disrupts microtubule formation during mitosis and interferes with glutamic acid metabolism), estramustine (binds to microtubule-associated proteins (MAPs) and inhibits microtubule dynamics) and

ixabepilone (promotes tubulin polymerization and microtubule stabilization, thereby arresting cells in the G2-M phase (40). Strikingly, two of the tubulin inhibitors were found to be *antagonistic* to DNAJA1 depletion. These include paclitaxel and ixabepilone. Paclitaxel inhibits the disassembly of microtubules resulting in the inhibition of cell division whereas Ixabepilone promotes tubulin polymerization and microtubule stabilization, arresting cells in the G2-M phase of the cell cycle (40). This apparent discrepancy may be explained by off-target effects of these molecules (see below).

Epigenetic modifying drugs display substantially modified potency depending on cellular DNAJA1 status. While previous studies have indicated the association between proteomic changes and histone PTMs in response to Hsp90 inhibitor treatment in bladder carcinoma cells, no such association has been shown for DNAJA1 and Histone PTMs (41). Interestingly, vorinostat was the only drug that was synergistic to DNAJA1 inhibition. It is a histone deacetylase inhibitor that binds to the catalytic domain of the histone deacetylases (HDACs). However, we also identified two histone deacetylase inhibitor drugs to be antagonistic to DNAJA1 depletion**,** panobinostat and romidepsin. These inhibit histone deacetylase (HDAC) which may impact cell cycle protein expression, cell cycle arrest in the G2/M phase and apoptosis (42). Excitingly, our data suggest a functional link between histones, their modifications and DNAJA1. While these findings require further investigation, it is possible that DNAJA1 may regulate the stability of histones themselves or histone chaperones. Interestingly, bortezomib (a proteasome inhibitor) lost potency when DNAJA1 was either inhibited with 116-9e or knocked out with CRISPR. Interestingly, a similar phenomenon has been observed in B16F10 melanoma cells. While treatment of these cells with 10nM bortezomib was cytotoxic, this effect was not observed

in cells treated with a combination of both quercetin (an Hsp70 inhibitor) and bortezomib (43). This apparent antagonism may be explained by their mechanism of action on the heat shock transcription factor, HSF1. While bortezomib acts to trigger the heat shock response in some cancers, the Hsp70/co-chaperone system maintains HSF1 in an less active immature form (44-47). It is interesting to note that while there are clear classes of drugs that are made more potent by loss of DNAJA1 function (DNA damage response, cytoskeletal function etc.), there are a small number of drugs in these classes that are not impacted at all or even made less potent. This apparent discrepancy implies that some of these inhibitors might have multiple cellular targets in addition to their proposed primary mechanism of action. This theory has been validated in fascinating studies comparing effects of small molecule therapies, gene knockout and knockdowns that theoretically target the same genes (37).

As in the case of any chemogenomic screen, care must be taken to validate screening results with other methods. In this study, we took the approach of following up our screen with small molecule validation in 2D and 3D cell culture models. Going forward, we intend to validate several of these hits *in vivo* (mouse) model systems. 116-9e is an interesting molecule. While 116-9e clearly impacts JDP binding (8, 20), the exact impact on all JDPs has not been characterized. The *DNAJA1* knockout cell line grows effectively the same as WT and suggests perhaps compensation by other unknown JDPs. In future studies, we hope to determine this using global RNA expression/proteomics analysis. Given the essential nature of Hsp70/Hsc70 in cancer cells, if 116-9e truly inhibited all JDP interactions it would be highly toxic to cells which we do not observe, suggesting there must be some selectivity in JDP inhibition.

Recent studies from our group and other have described the clear impact of Hsp70/JDP inhibition on individual oncoprotein client stability and prostate cancer cell survival (8, 13). Overall, this study demonstrates the larger feasibility of inhibiting Hsp70 co-chaperones such as DNAJA1 as a novel anticancer therapy, acting to fine-tune Hsp70 function rather than completely abolishing it. Nearly a third of the anticancer compounds screened demonstrated increased potency in DNAJA1 knockout cells. Rather than attempting to develop co-chaperone inhibitors as a monotherapy, we believe their strength lies as sensitizing agents to existing therapies. Moreover, our data imply that overexpression of *DNAJA1* in patient tumors may impact the effectiveness of a number of commonly used anticancer drugs. While further in vivo studies are required, our studies suggest perhaps a future precision medicine approach that uses tumor *DNAJA1* status to guide treatment strategy.

3.5 Figures

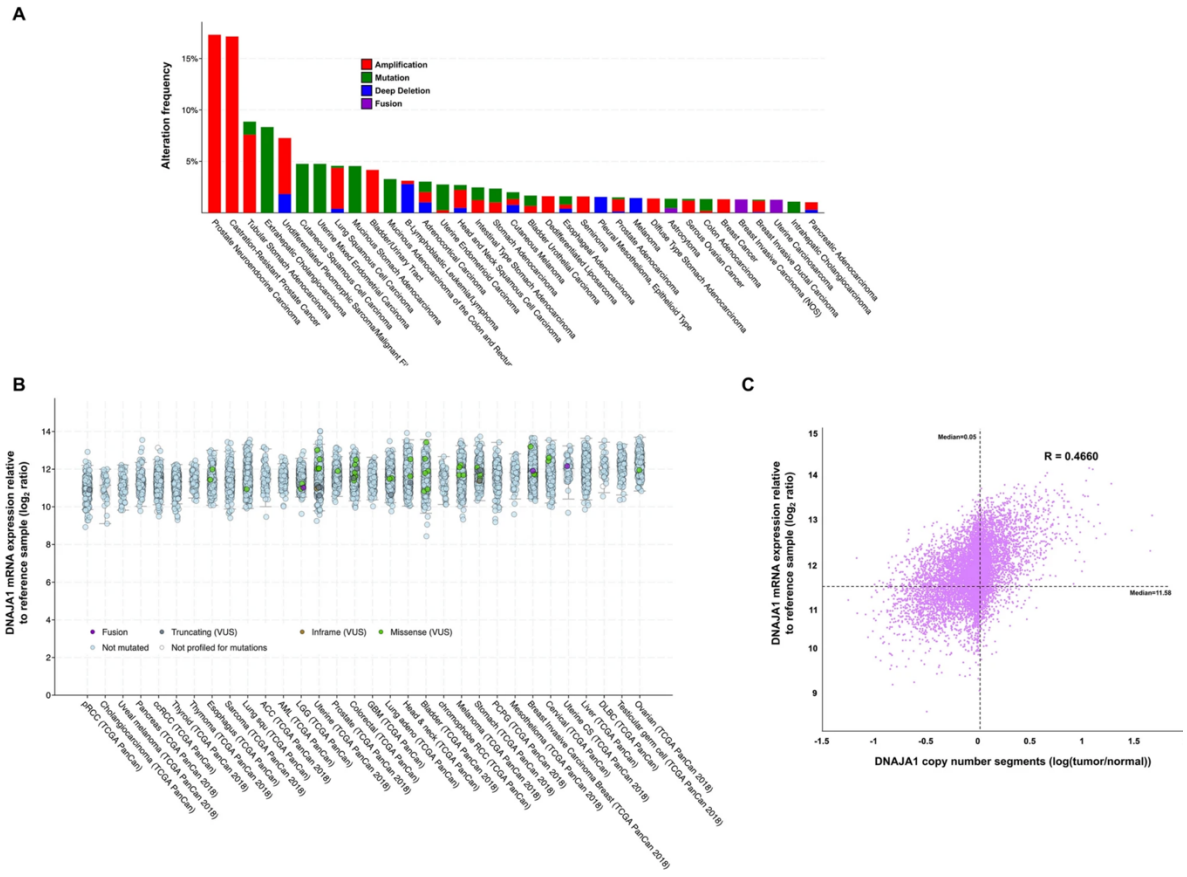

Figure 12. DNAJA1 is altered in cancer. (A) Prevalence of *DNAJA1* alterations in various cancer genomes analyzed via the cBioPortal. (B) *DNAJA1* mRNA expression in cancers (TGCA PanCan) obtained from cBioPortal. mRNA expression value is log2 ratio of expression seen in cancer vs reference cells (please see www.cbioportal.org/faq for more information). (C) increased DNAJA1 expression is not driven by copy number increase. DNAJA1 copy number vs DNAJA1 was plotted and Pearson's correlation coefficient (R-value) was calculated. Median of both variables is marked by dotted line on the graph.

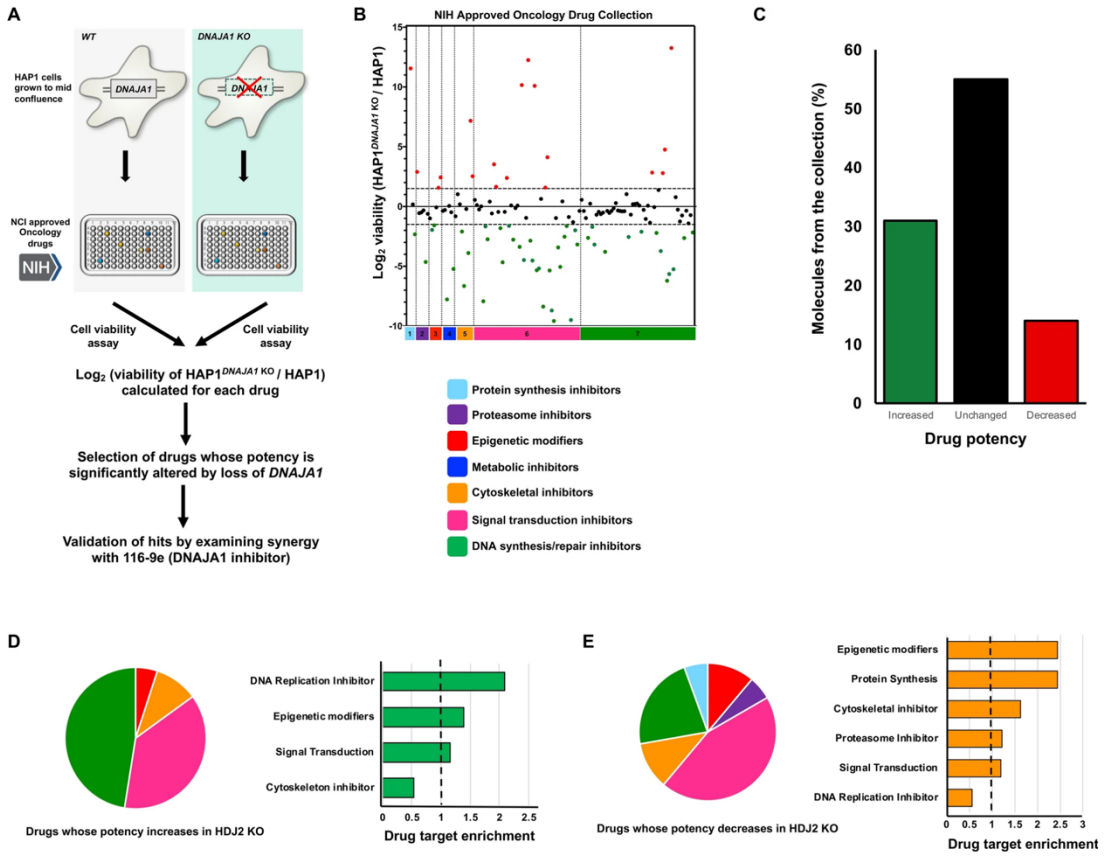

Figure 13. Sensitivity of WT and DNAJA1 knockout cells to the NIH Approved Oncology Collection. (A) Workflow of high-throughput cell-based screen. (B) A collection of 132 drugs were screened at 50μmol/L with Wild-type and DNAJA1 KO cells. Results are the average of at least triplicates and error is SEM. The dotted lines represent a potency change of $Log_2 > 1.5$ or $Log_2 < -1.5$. The effect of *DNAJA1* knockout on drug potency is colored as follows: red (decreased drug potency), green (increased drug potency) or black (no change in drug potency). (C) Summary of effect of *DNAJA1* knockout on the potency of the NIH approved oncology collection. (D&E) Drug ontology of synergistic and antagonistic hits based on the pathways affected by the approved oncology drugs in the screen.

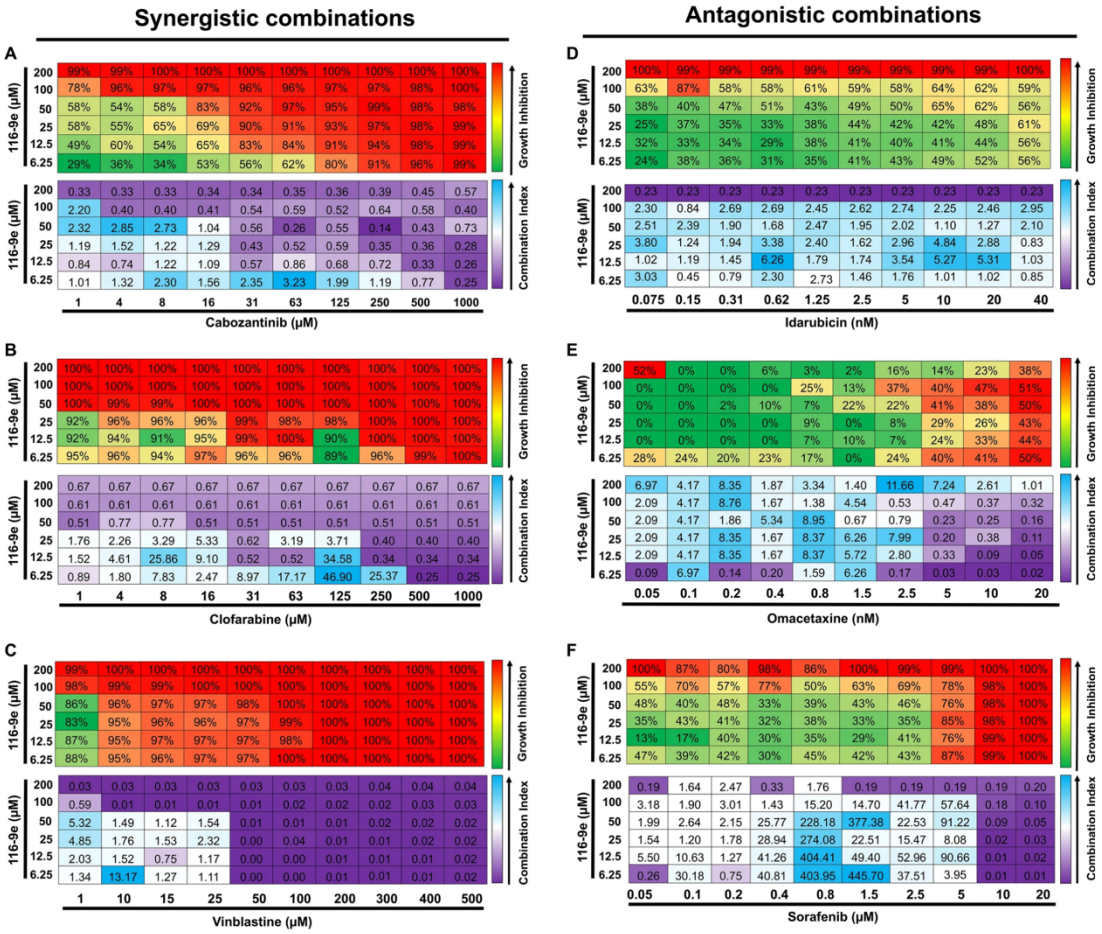

Figure 14. Drug interaction between 116-9e (DNAJA1 inhibitor) and selected hits. LNCaP cells were treated with different concentrations of cabozantinib, clofarabine, vinblastine, idarubicin, omacetaxine and sorafenib with or without 116-9e for 72 hours in RPMI-1640 medium containing 10% FBS. Each point is the mean ± SD for three independent experiments. Growth inhibition was determined using Cell Titer-Glo assay. Combination Index (CI, measure of drug synergy) was determined using Chou-Talalay method via Compusyn software. CI values are as follows: <0.1 (very strongly synergistic), 0.1-0.3 (strongly synergistic), <0.9 (synergistic), 0.9-1.1 (additive), 1.1-3.3 (antagonistic), 3.3-10 (strongly antagonistic), >10 (very strongly antagonistic).

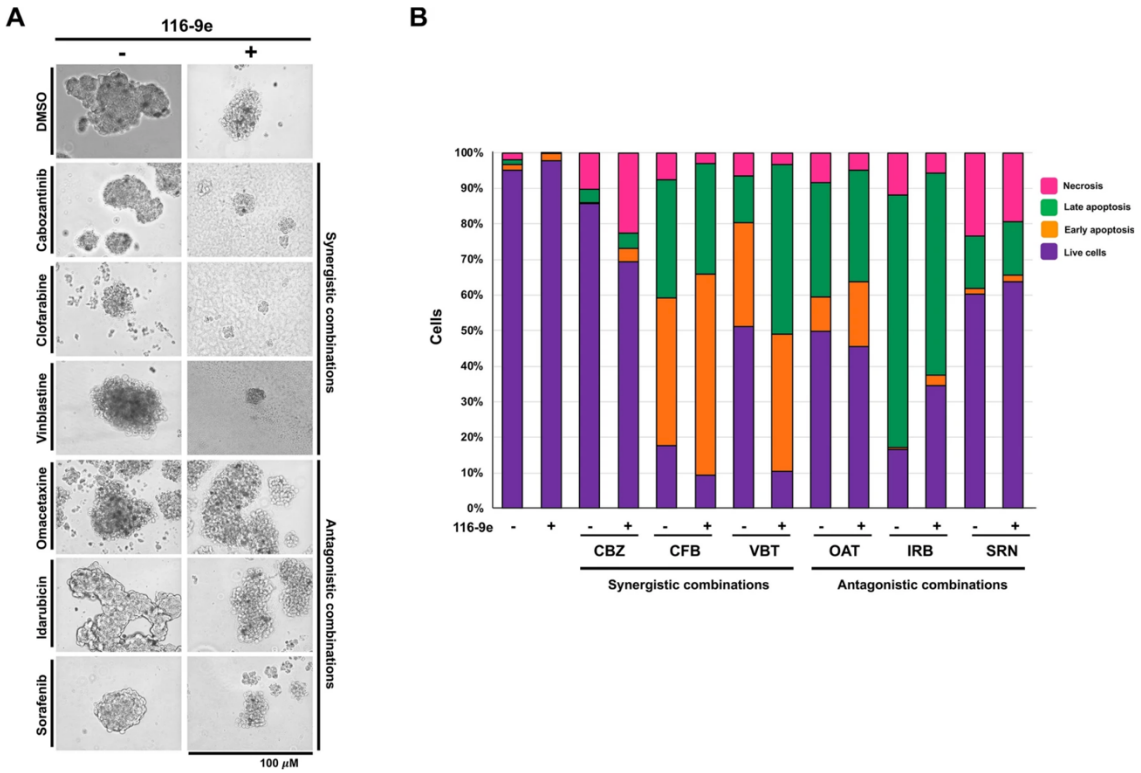

Figure 15. Effect of combination treatments on prostate cancer spheroids. A. Cells were plated on Matrigel-coated 24 well plates. Six drugs (cabozantinib, clofarabine, vinblastine, idarubicin, omacetaxine and sorafenib) were tested on prostate cancer spheroids. These experiments were performed in triplicate and are average of 3 replicates from 3 different wells of a cell culture plate. The pictures are representative images as acquired using an EVOS cell imager. B. Proliferation of spheroids treated with cabozantinib (CBZ), clofarabine (CFB), vinblastine (VBT), idarubicin (IRB), omacetaxine (OAT) and sorafenib (SRN) measured using AnnexinV/PI staining.

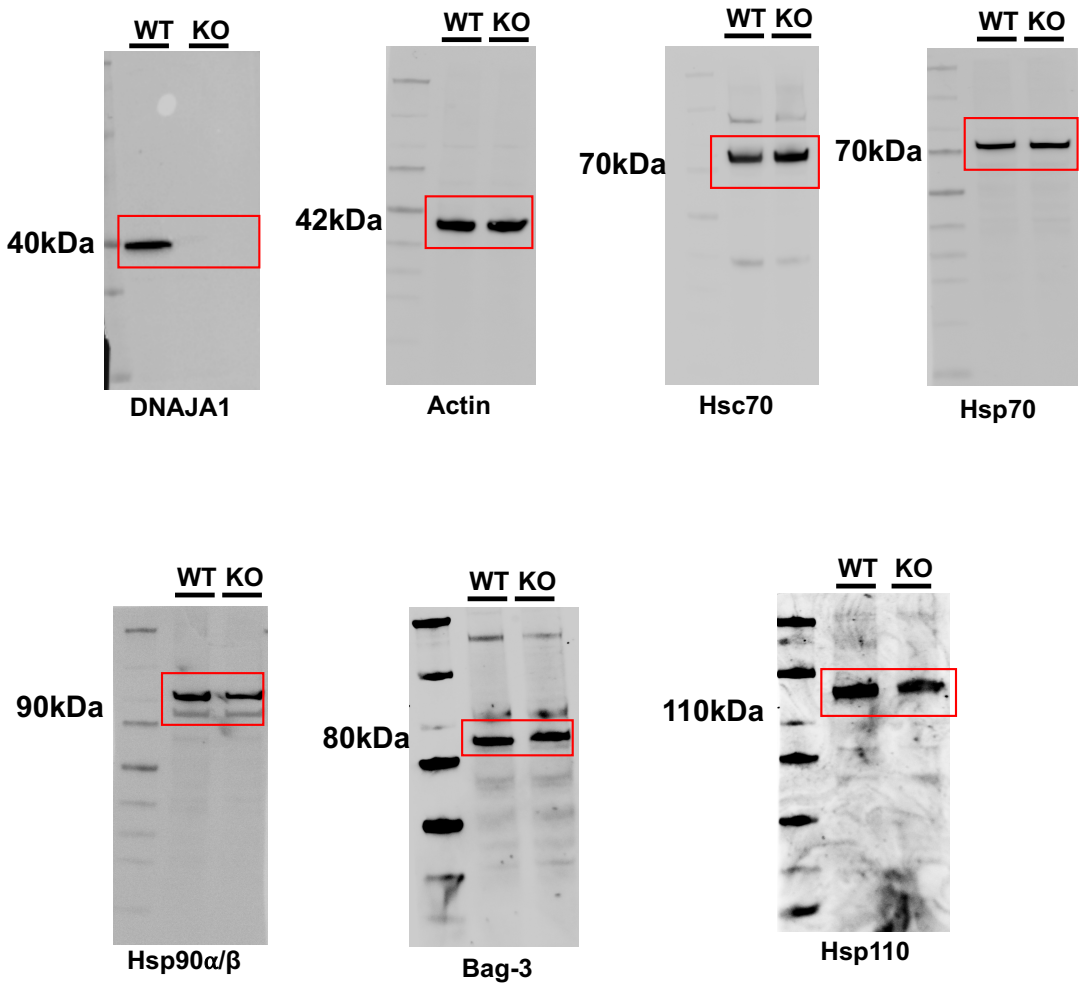

Figure 16. Expression of various chaperone/co-chaperone proteins in HAP1 WT/DNAJA1 knockout cells. Cell lysates extracted from HAP1 WT and DNAJA1 CRISPR KO cells were resolved on SDS-PAGE gels and further processed by immunoblotting with anti-DNAJA1, Actin, Hsc70, Hsp70, Hsp90, Bag-3, Hsp110 and Actin antibodies.

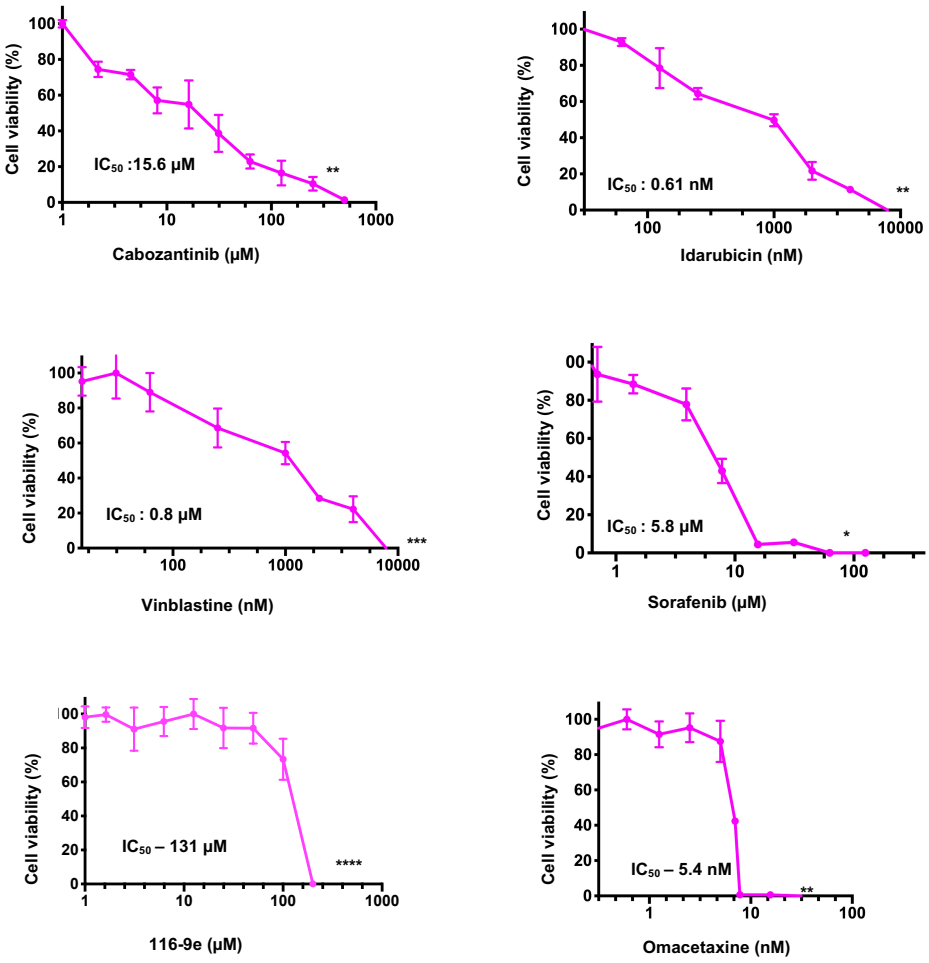

Figure 17. Effects of selected FDA-approved drugs on LnCaP cells. LNCaP cells were treated with serial dilutions of indicated drugs for 3 days. Cell viability was determined using Cell Titer Glo assay and results shown are average and SD from three replicates (***P<0.001 compared to DMSO control, t-test).

Drugs with increased potency upon loss of DNAJA1	Cellular Target	Function
Ixazomib citrate	Proteasome inhibitor	Proteasome inhibitor
Cabazitaxel	Microtubule Inhibitor	Cytoskeleton
Vinblastine sulfate	Disrupts microtubule formation	Cytoskeleton
Bosutinib	Abl and Src kinases inhibitor	Cytoskeleton
Docetaxel	Microtubule Inhibitor	Cytoskeleton
Estramustine phosphate sodium	Inhibits microtubules	Cytoskeleton
Ceritinib	Tyrosine Kinase Inhibitor	Cytoskeleton
Chlorambucil	DNA replication inhibitor	DNA synthesis and repair
Fluorouracil	DNA synthesis inhibitor	DNA synthesis and repair
Decitabine	DNA synthesis inhibitor	DNA synthesis and repair
Bendamustine hydrochloride	DNA synthesis inhibitor	DNA synthesis and repair
Mitomycin	DNA synthesis inhibitor	DNA synthesis and repair
Mercaptopurine	DNA synthesis inhibitor	DNA synthesis and repair
Fludarabine phosphate	DNA synthesis inhibitor	DNA synthesis and repair
Tretinoin	Inhibits telomerase	DNA synthesis and repair
Thiotepa	Interferes with DNA replication	DNA synthesis and repair
Pipobroman	DNA replication inhibitor	DNA synthesis and repair
Olaparib	PARP inhibitor	DNA synthesis and repair
Teniposide	DNA synthesis inhibitor	DNA synthesis and repair
Bleomycin	DNA synthesis inhibitor	DNA synthesis and repair
Triethylenemelamine	DNA synthesis inhibitor	DNA synthesis and repair
Vorinostat	Histone deacetylases	Epigenetic modifiers
Melphalan hydrochloride	Inhibition of RNA transcription	Protein synthesis
Lenvatinib	VEGFR inhibitor	Signal Transduction
Mitotane	Inhibiting adrenal cortical hormone production	Signal Transduction
Raloxifene	Estrogen Receptor Modulator	Signal Transduction
Gefitinib	RTK inhibitor	Signal Transduction
Erlotinib hydrochloride	Protein kinase inhibitor	Signal Transduction
Sunitinib	EGFR inhibitor	Signal Transduction
Pemetrexed	DNA synthesis inhibitor	Signal Transduction
Abiraterone	177-MAO inhibitor	Signal Transduction
Etoposide	DNA synthesis inhibitor	Signal Transduction
Dabrafenib mesylate	Protein Kinase Inhibitor	Signal Transduction
Amifostine	Free Radical Scavenging Activity	Signal Transduction
Tamoxifen citrate	Antineoplastic nonsteroidal selective estrogen receptor modulator	Signal Transduction
Ponatinib	RTK inhibitior	Signal Transduction
Temsirolimus	mTOR Inhibitor	Signal Transduction
Imiquimod	Interferon Inducer	Signal Transduction
Nilotinib	Bcr-Abl tyrosine kinase inhibitor	Signal Transduction
Cabozantinib	RTK inhibitor	Signal Transduction
Sirolimus	mTOR Inhibitor	Signal Transduction

Drugs with decreased potency upon loss of DNAJA1	Cellular Target	Function
Paclitaxel	Microtubule Inhibitor	Cytoskeleton
Ixabepilone	Microtubule Inhibitor	Cytoskeleton
Trifluridine	Nucleic Acid Synthesis Inhibitor	DNA synthesis and repair
Irinotecan	Topoisomerase Inhibitor	DNA synthesis and repair
Epirubicin	Topoisomerase Inhibitor	DNA synthesis and repair
Idarubicin	DNA Synthesis and Repair	DNA synthesis and repair
Panobinostat	Hyperacetylation of core histone proteins	Epigenetic modifiers
Romidepsin	Histone Deacetylase Inhibitor	Epigenetic modifiers
Bortezomib	Proteasome Inhibitor	Proteasome Inhibitor
Omacetaxine mepesuccinate	Protein Synthesis Inhibitor	Protein Synthesis Inhibitor
Crizotinib	ALK (anaplastic lymphoma kinase) and ROS1 inhibitor	Signal Transduction
Sorafenib	VEGFR-2/PDGFR-beta inhibitor	Signal Transduction
Afatinib	Epidermal growth factor receptor Inhibitor	Signal Transduction
Alectinib	Anaplastic lymphoma kinase (ALK) inhibitor	Signal Transduction
Osimertinib	Epidermal growth factor receptor (EGFR) inhibitor	Signal Transduction
Erismodegib	Hedgehog signaling pathway inhibitor	Signal Transduction
Regorafenib	VEGFR2-TIE2 tyrosine kinase inhibition	Signal Transduction
Vemurafenib	Braf kinase inhibitor	Signal Transduction

Supplemental Table T1 for Chemogenomic screening identifies the Hsp70 co-chaperone DNAJA1 as a hub for anticancer drug resistance.

3.6 References

1. Rosenzweig R, Nillegoda NB, Mayer MP, Bukau B. The Hsp70 chaperone network. Nat Rev Mol Cell Biol. 2019.
2. Ciocca DR, Calderwood SK. Heat shock proteins in cancer: diagnostic, prognostic, predictive, and treatment implications. Cell Stress Chaperones. 2005;10(2):86-103.
3. Gestwicki JE, Shao H. Inhibitors and chemical probes for molecular chaperone networks. J Biol Chem. 2019;294(6):2151-61.
4. Evans CG, Chang L, Gestwicki JE. Heat shock protein 70 (hsp70) as an emerging drug target. J Med Chem. 2010;53(12):4585-602.
5. Kampinga HH, Craig EA. The HSP70 chaperone machinery: J proteins as drivers of functional specificity. Nat Rev Mol Cell Biol. 2010;11(8):579-92.
6. Craig EA, Marszalek J. How Do J-Proteins Get Hsp70 to Do So Many Different Things? Trends Biochem Sci. 2017;42(5):355-68.
7. Nitika, Truman AW. Cracking the Chaperone Code: Cellular Roles for Hsp70 Phosphorylation. Trends Biochem Sci. 2017;42(12):932-5.
8. Sluder IT, Nitika, Knighton LE, Truman AW. The Hsp70 co-chaperone Ydj1/HDJ2 regulates ribonucleotide reductase activity. PLoS Genet. 2018;14(11):e1007462.
9. Truman AW, Kristjansdottir K, Wolfgeher D, Hasin N, Polier S, Zhang H, et al. CDK-dependent Hsp70 Phosphorylation controls G1 cyclin abundance and cell-cycle progression. Cell. 2012;151(6):1308-18.
10. Woodford MR, Dunn D, Miller JB, Jamal S, Neckers L, Mollapour M. Impact of Posttranslational Modifications on the Anticancer Activity of Hsp90 Inhibitors. Adv Cancer Res. 2016;129:31-50.
11. Dushukyan N, Dunn DM, Sager RA, Woodford MR, Loiselle DR, Daneshvar M, et al. Phosphorylation and Ubiquitination Regulate Protein Phosphatase 5 Activity and Its Prosurvival Role in Kidney Cancer. Cell Rep. 2017;21(7):1883-95.
12. Stark JL, Mehla K, Chaika N, Acton TB, Xiao R, Singh PK, et al. Structure and function of human DnaJ homologue subfamily a member 1 (DNAJA1) and its relationship to pancreatic cancer. Biochemistry. 2014;53(8):1360-72.
13. Moses MA, Kim YS, Rivera-Marquez GM, Oshima N, Watson MJ, Beebe KE, et al. Targeting the Hsp40/Hsp70 Chaperone Axis as a Novel Strategy to Treat Castration-Resistant Prostate Cancer. Cancer Res. 2018;78(14):4022-35.
14. Palmer AC, Sorger PK. Combination Cancer Therapy Can Confer Benefit via Patient-to-Patient Variability without Drug Additivity or Synergy. Cell. 2017;171(7):1678-91 e13.
15. Ding KF, Petricoin EF, Finlay D, Yin H, Hendricks WPD, Sereduk C, et al. Nonlinear mixed effects dose response modeling in high throughput drug screens: application to melanoma cell line analysis. Oncotarget. 2018;9(4):5044-57.
16. Koh SB, Wallez Y, Dunlop CR, Bernaldo de Quiros Fernandez S, Bapiro TE, Richards FM, et al. Mechanistic Distinctions between CHK1 and WEE1 Inhibition Guide the Scheduling of Triple Therapy with Gemcitabine. Cancer Res. 2018;78(11):3054-66.

17. Chou TC. Theoretical basis, experimental design, and computerized simulation of synergism and antagonism in drug combination studies. Pharmacol Rev. 2006;58(3):621-81.
18. Cerami E, Gao J, Dogrusoz U, Gross BE, Sumer SO, Aksoy BA, et al. The cBio cancer genomics portal: an open platform for exploring multidimensional cancer genomics data. Cancer Discov. 2012;2(5):401-4.
19. Wang CC, Liao YP, Mischel PS, Iwamoto KS, Cacalano NA, McBride WH. HDJ-2 as a target for radiosensitization of glioblastoma multiforme cells by the farnesyltransferase inhibitor R115777 and the role of the p53/p21 pathway. Cancer Res. 2006;66(13):6756-62.
20. Wisen S, Bertelsen EB, Thompson AD, Patury S, Ung P, Chang L, et al. Binding of a small molecule at a protein-protein interface regulates the chaperone activity of hsp70-hsp40. ACS Chem Biol. 2010;5(6):611-22.
21. Wisitpitthaya S, Zhao Y, Long MJ, Li M, Fletcher EA, Blessing WA, et al. Cladribine and Fludarabine Nucleotides Induce Distinct Hexamers Defining a Common Mode of Reversible RNR Inhibition. ACS Chem Biol. 2016;11(7):2021-32.
22. Wu CC, Li TK, Farh L, Lin LY, Lin TS, Yu YJ, et al. Structural basis of type II topoisomerase inhibition by the anticancer drug etoposide. Science. 2011;333(6041):459-62.
23. Senra JM, Telfer BA, Cherry KE, McCrudden CM, Hirst DG, O'Connor MJ, et al. Inhibition of PARP-1 by olaparib (AZD2281) increases the radiosensitivity of a lung tumor xenograft. Mol Cancer Ther. 2011;10(10):1949-58.
24. Dudgeon C, Peng R, Wang P, Sebastiani A, Yu J, Zhang L. Inhibiting oncogenic signaling by sorafenib activates PUMA via GSK3beta and NF-kappaB to suppress tumor cell growth. Oncogene. 2012;31(46):4848-58.
25. Gandhi V, Plunkett W, Cortes JE. Omacetaxine: a protein translation inhibitor for treatment of chronic myelogenous leukemia. Clin Cancer Res. 2014;20(7):1735-40.
26. Hevener K, Verstak TA, Lutat KE, Riggsbee DL, Mooney JW. Recent developments in topoisomerase-targeted cancer chemotherapy. Acta Pharm Sin B. 2018;8(6):844-61.
27. Chou TC. Drug combination studies and their synergy quantification using the Chou-Talalay method. Cancer Res. 2010;70(2):440-6.
28. Vlachogiannis G, Hedayat S, Vatsiou A, Jamin Y, Fernandez-Mateos J, Khan K, et al. Patient-derived organoids model treatment response of metastatic gastrointestinal cancers. Science. 2018;359(6378):920-6.
29. Pickl M, Ries CH. Comparison of 3D and 2D tumor models reveals enhanced HER2 activation in 3D associated with an increased response to trastuzumab. Oncogene. 2009;28(3):461-8.
30. Knighton LE, Delgado LE, Truman AW. Novel insights into molecular chaperone regulation of ribonucleotide reductase. Curr Genet. 2019;65(2):477-82.
31. Truman AW, Kristjansdottir K, Wolfgeher D, Ricco N, Mayampurath A, Volchenboum SL, et al. Quantitative proteomics of the yeast Hsp70/Hsp90 interactomes during DNA damage reveal chaperone-dependent regulation of ribonucleotide reductase. J Proteomics. 2015;112:285-300.
32. Huguet F, Leguay T, Raffoux E, Rousselot P, Vey N, Pigneux A, et al. Clofarabine for the treatment of adult acute lymphoid leukemia: the Group for Research

on Adult Acute Lymphoblastic Leukemia intergroup. Leuk Lymphoma. 2015;56(4):847-57.
33. Deng S, Yan T, Jendrny C, Nemecek A, Vincetic M, Godtel-Armbrust U, et al. Dexrazoxane may prevent doxorubicin-induced DNA damage via depleting both topoisomerase II isoforms. BMC Cancer. 2014;14:842.
34. Gillies AT, Taylor R, Gestwicki JE. Synthetic lethal interactions in yeast reveal functional roles of J protein co-chaperones. Mol Biosyst. 2012;8(11):2901-8.
35. Tang Y, Ramakrishnan C, Thomas J, DeFranco DB. A role for HDJ-2/HSDJ in correcting subnuclear trafficking, transactivation, and transrepression defects of a glucocorticoid receptor zinc finger mutant. Mol Biol Cell. 1997;8(5):795-809.
36. Grullich C. Cabozantinib: a MET, RET, and VEGFR2 tyrosine kinase inhibitor. Recent Results Cancer Res. 2014;201:207-14.
37. Lin A, Giuliano CJ, Palladino A, John KM, Abramowicz C, Yuan ML, et al. Off-target toxicity is a common mechanism of action of cancer drugs undergoing clinical trials. Sci Transl Med. 2019;11(509).
38. Oka M, Nakai M, Endo T, Lim CR, Kimata Y, Kohno K. Loss of Hsp70-Hsp40 chaperone activity causes abnormal nuclear distribution and aberrant microtubule formation in M-phase of Saccharomyces cerevisiae. J Biol Chem. 1998;273(45):29727-37.
39. Meshalkina DA, Shevtsov MA, Dobrodumov AV, Komarova EY, Voronkina IV, Lazarev VF, et al. Knock-down of Hdj2/DNAJA1 co-chaperone results in an unexpected burst of tumorigenicity of C6 glioblastoma cells. Oncotarget. 2016;7(16):22050-63.
40. Cobham MV, Donovan D. Ixabepilone: a new treatment option for the management of taxane-resistant metastatic breast cancer. Cancer Manag Res. 2009;1:69-77.
41. Li QQ, Hao JJ, Zhang Z, Krane LS, Hammerich KH, Sanford T, et al. Proteomic analysis of proteome and histone post-translational modifications in heat shock protein 90 inhibition-mediated bladder cancer therapeutics. Sci Rep. 2017;7(1):201.
42. Eckschlager T, Plch J, Stiborova M, Hrabeta J. Histone Deacetylase Inhibitors as Anticancer Drugs. Int J Mol Sci. 2017;18(7).
43. Yerlikaya A, Okur E, Eker S, Erin N. Combined effects of the proteasome inhibitor bortezomib and Hsp70 inhibitors on the B16F10 melanoma cell line. Mol Med Rep. 2010;3(2):333-9.
44. Mitsiades N, Mitsiades CS, Poulaki V, Chauhan D, Fanourakis G, Gu X, et al. Molecular sequelae of proteasome inhibition in human multiple myeloma cells. Proc Natl Acad Sci U S A. 2002;99(22):14374-9.
45. Shah SP, Nooka AK, Jaye DL, Bahlis NJ, Lonial S, Boise LH. Bortezomib-induced heat shock response protects multiple myeloma cells and is activated by heat shock factor 1 serine 326 phosphorylation. Oncotarget. 2016;7(37):59727-41.
46. Abravaya K, Myers MP, Murphy SP, Morimoto RI. The human heat shock protein hsp70 interacts with HSF, the transcription factor that regulates heat shock gene expression. Genes Dev. 1992;6(7):1153-64.
47. Baler R, Welch WJ, Voellmy R. Heat shock gene regulation by nascent polypeptides and denatured proteins: hsp70 as a potential autoregulatory factor. J Cell Biol. 1992;117(6):1151-9.

CHAPTER 4: BIOLOGICALLY IMPORTANT PTM-BASED INTERACTIONS VIA HSP70 PROTEOMICS.

4.1 Introduction

The maintenance of a correctly folded proteome (proteostasis) is critical for cell survival. Cells maintain proteostasis under basal and stress conditions through the expression of chaperones that include Hsp70 and its co-chaperone regulators (1, 2). Hsp70 comprises an N-terminal ATPase domain (NBD), a substrate-binding domain (SBD) and C-terminal ("lid") (3, 4). The binding and hydrolysis of ATP to ADP in the NBD promotes large-scale structural rearrangements that allow the closing of the C-terminal ("lid") over substrates bound in the SBD, promoting protein folding (5, 6). The established roles of Hsp70 include folding of new and denatured proteins; transport of mitochondrial proteins and disaggregation of protein complexes (7-9).

The importance of Hsp70 in a variety of human pathologies that include cancer as well as being a fundamental protein required for cell viability have prompted researchers to seek out the full Hsp70 "interactome. Although several strong efforts have been made towards this goal these have been hampered by limitations in the technologies used. These methods include affinity purification followed by mass spectrometry (AP-MS), yeast two-hybrid (Y2H) and proximity proteomics all of which lack the ability to discriminate between direct and bridged interactions (10-14). Chemical crosslinking with mass spectrometry (XL-MS) is a powerful interactomic technique that circumvents this issue, providing information on direct interactions in protein complexes by using chemical cross linkers (15, 16). Indeed, XL-MS studies are often complementary to the traditional

structural biology methods such as X-ray crystallography, nuclear magnetic resonance, and cryo-electron microscopy (16).

Importantly, a key role for the Hsp70 system is stabilization and activation of a wide range of signaling molecules including those involved in processes such as DNA damage response, cell cycle control, autophagy and nutrient sensing (17-20). These proteins tend to be either highly post translationally modified (PTMs) or regulate PTMs on other proteins. These PTMs tightly regulate a multitude of protein properties including subcellular localization, enzymatic activity and protein interactions (21). Advances in mass spectrometry-based methods have allowed identification of more than 200 different types of PTMs on proteins including phosphorylation, acetylation, and ubiquitination (22-24). Given the huge number of PTMs identified on proteins, researchers are now faced with difficult choices in how to select specific PTMs for further study. Computational methods for identifying important PTMs on proteins have been partially successful but rely on already obtained MS data (22, 25). Here, we have utilized XL-MS to understand fundamental properties of the Hsp70-client system. In doing so, we have uncovered not only a new set of Hsp70 clients, but have shown that these clients bind at multiple points throughout Hsp70, including the N-terminus. Importantly, many Hsp70 interactions with clients are in close proximity to biologically-important PTMs. Going forward our data suggest that this methodology may be used to identify whole sets of previously unknown PTMs with important biological functions.

4.2 Materials and Methods

Sample preparation and cross-linking

Yeast cells expressing His-tagged Ssa1 were grown to mid log phase in SD -leu media. Cells were harvested and protein was extracted via bead beating followed by sonication. His tagged Ssa1 was purified using an ÄKTA prime Plus fast protein liquid chromatography (FPLC) system (GE Healthcare) equipped with a 1-ml His-Trap HP column, followed by buffer exchange into dialysis buffer. Purified protein concentration was quantified by Coomassie assay (Thermo Fisher Scientific). 150ug of purified His-Ssa1 complex was cross-linked with 5mM DSSO and incubated at room temperature for 1 hour. The reaction was quenched using 20mM Tris-HCl pH 8.0.

In-solution sample digestion and SCX fractionation

150ug of cross-linked or uncross-linked samples were mixed with 6X volumetric excess of ice cold acetone and precipitated overnight at -80˚C. Precipitated proteins were pelleted at 21k RCF at 4 ˚C and re-solubilized in 150µL of 8M Urea/0.1MNH_4HCO_3 reduced with 10mM DTT for 30min. and alkylated with 50mM IAA for 30min. in the dark. Samples were diluted 4x with 100mM NH_4HCO_3 to reach 2M Urea concentration and digested with trypsin (trypsin/protein ratio of 1/50) overnight at 37˚C. Resulting mixture of tryptic peptides was concentrated using SpeedVac and re-suspended-in 10 mM KH_2PO_4, pH 2.8, 20% ACN and loaded on preconditioned polysulfoethyl A (12µm, 300Å) solid phase cartridges. Peptides were eluted with increasing concentration (0, 4, 8, 12, 25, 50, 125, 250 and 500mM) of KCl. Resulting fractions were desalted with Peptide Desalting Spin Columns (Thermo Fisher Scientific Pierce™- 89851) according to manufacturer's protocol, dried down on SpeedVac and resuspended in 0.1% Formic Acid.

Liquid chromatography – tandem mass spectrometry peptide analysis

Resuspended cross-linked peptides were separated by nanoflow reversed-phase liquid chromatography (LC). An Easy-nLC 1000 (Thermo Scientific, San Jose, CA) was used to load ~1 ug of peptides on the column and separate them at a flow rate of 300 nl/min. The column was a 50 cm long EASY-Spray C18 (packed with 2 µm PepMap C18 particles, 75 µm i.d., Thermo Scientific, Sunnyvale, CA). The analytical gradient was performed by increasing the relative concentration of mobile phase B in the following steps: from 2% to 28% in 65 min, from 28% to 36% in 10 min, and from 32 to 90% in 5 min (for washing the column). The wash at high organic concentration was followed by re-equilibration of the column at 2% B for 10 min, for a total run time of 90 min. A shorter version of the gradient (total run time of 60 min, obtained by shortening the first step) was used for blanks and for standard shotgun proteomics targeting all peptides (not only cross-linked ones) present in the sample. Mobile phase A was composed of an aqueous solution of 0.1% formic acid (FA), while mobile phase B consisted of 19.9% water, 80% acetonitrile and 0.1% FA. A 2 kV potential was applied to the column outlet using an EASY-Spray nanoESI source (Thermo Fisher Scientific, San Jose, CA) for generating nano-electrospray.

All mass spectrometry (MS) measurements were performed on a tribrid Orbitrap Fusion Lumos (Thermo Scientific, San Jose, CA). For the identification of cross-linked peptides, a specific data-dependent acquisition method described by Liu *et al* was applied (26). Briefly, broadband mass spectra (MS1) were recorded in the Orbitrap over a 375-1500 *m/z* window, using a resolving power of 60,000 (at 200 *m/z*) and an automatic gain control (AGC) target of 4e5 charges (maximum injection time: 50 ms). Precursor ions were quadrupole selected (isolation window: 1.6 *m/z*) based on a data-dependent logic, using a

maximum duty cycle time of 5 s. Monoisotopic precursor selection and dynamic exclusion (30 s) were applied. Peptides were filtered by intensity and charge state, allowing the fragmentation only of precursors from 4+ to 8+. Tandem mass spectrometry (MS2) was performed by fragmenting each precursor passing the selection criteria using both collision-induced dissociation (CID) with normalized collision energy (NCE) set at 25% and electron transfer dissociation – higher energy collisional dissociation (EThcD), with ETD reagent target set at 5e5, reaction time calculated on the basis of a calibration curve and supplemental collisional activation set at NCE=15%. The AGC target for both CID and EThcD MS2 was set at 5e4 (maximum injection time: 100 ms), and spectra were recorded at 30,000 resolving power. CID MS2 spectra where a diagnostic neutral loss characteristic of the DSSO crosslinker (Δm=31.9721 Da) was found between 2 pairs of product ions were used to trigger a data-dependent MS3 scan based on higher-energy collisional dissociation (HCD) with NCE=30%, using a multi-notched isolation (notch width = 2 *m/z*, 2 precursors selected), an AGC target of 2e4 and spectral detection in the linear ion trap (operating in rapid mode).

For the identification of all proteins included in the samples, the data-dependent acquisition method was simplified using uniquely HCD for tandem MS, recording MS2 spectra over a 110-2000 *m/z* window using 15,000 resolving power (at 200 *m/z*), and an AGC target of 2e4 (maximum injection time: 30 ms). Peptides with charge states from 2+ to 7+ were considered for fragmentation. MS1 scans were recorded at 120,000 resolving power (at 200 *m/z*).

MS Data analysis

All data analysis was carried out with Protein Discoverer 2.2. For identification of crosslinked peptides CID/EThcD RAW data were searched with a crosslink processing workflow. For XlinkX, Detect node parameters were as follows; Acquisition strategy: MS2_MS3 with Crosslink Modification : DSSO/+158.004Da(K). Both XlinkX search node and in the SequestHT nodes search a SGD orf FASTA database (SGD_orf_trans_2015-01-13 - because of high degree of identity we decided to keep only Ssa1 isoform of Ssa in searched database) and trypsin enzymatic specificity with 2 maximum missed cleavages. Precursor Mass Tolerance was 10ppm and Fragment Mass Tolerance was 0.6Da. Carbamidomethylation (C) was allowed as a static modification. Dynamic modifications were as follows: Oxidation(M), DSSO Hydrolyzed(K), DSSO Tris (K) Acetyl (protein N-term). Additionally, we searched data for phospho (S, T, Y), acetyl (K) and single, di, tri methylation (K) separately.

Crosslinks were validated using the Percolator strategy and the FDR threshold was set to 0.01. Finally, results were filtered for high confidence peptides using consensus step. Control peptide error rate strategy was used and 0.01 (strict) and 0.05 (relaxed) values were used for Target FDR for both PSM and Peptide levels. Only high confidence peptides were included and minimal peptide length was set to 5.

For general identification of all-proteins included in the samples, HCD fragmentation data were processed with Protein Discoverer 2.2 utilizing Sequest HT and MS Amanda search engines. For both Precursor Mass Tolerance was 10ppm and Fragment Mass Tolerance was 0.2Da. Carbamidomethylation (C) was allowed as a static modification and dynamic

modifications were as follows: Oxidation(M), Acetyl (protein N-term). Identified peptides were validated using Percolator and target FDR value was set to 0.01 (strict) and 0.05 (relaxed). Finally, results were filtered for high confidence peptides using consensus steps. Control peptide error rate strategy was used and 0.01 (strict) and 0.05 (relaxed) values were used for Target FDR for both PSM and Peptide levels. A full table of Ssa1-Ssa1cross links, Ssa1- client cross links and PTMs identified can be found in Table S2, S3 and S4.

Gene Ontology analysis was performed using GO Slim Mapper on the Saccharomyces Genome Database (http://www.yeastgenome.org/cgi-bin/GO/goSlimMapper.pl). Crosslink distances were measured using PyMOL software.

Yeast Strains and growth conditions

Yeast cultures were grown in either YPD (1% yeast extract, 2% glucose, 2% peptone) or grown in SD (0.67% yeast nitrogen base without amino acids and carbohydrates, 2% glucose) supplemented with the appropriate nutrients to select for plasmids and tagged genes. *Escherichia coli* DH5α was used to propagate all plasmids. *E. coli* cells were cultured in Luria broth medium (1% Bacto tryptone, 0.5% Bacto yeast extract, 1% NaCl) and transformed to ampicillin or kanamycin resistance by standard methods.

For serial dilutions, cells were grown to mid-log phase, 10-fold serially diluted and then plated onto appropriate media using a 48-pin replica-plating tool. Images of plates were taken after 3 days at 30℃.

For tagging genomic copies of *CCT8*, *PCL7*, *URA8* and *SSE1* with a HA epitope tag at the carboxy terminus, the pFA6a-HA-His3MX6 plasmid was used.

For tagging the genomic copies of SSA1 for BiFC, pFA6a-VN-His3MX6 and pFA6a-VC-kanMX6 plasmids were used. A full table of reagents, yeast strains and plasmids that were used can be found in Table S1, S5 and S6.

For growth curves, yeast cells were grown to mid log phase and optical density was measured at 600 nM for indicated times.

For halo assay, yeast cells were grown to mid log phase. The following day the culture was diluted 1:1000 and 150 µl of cells were spread onto a YPD plate. After the plate had been incubated for 2 hr at 30°C, 10 µl of 5 µg/ml of synthetic α factor peptide (WHWLQLKPGQPNleY) in DMSO was spotted onto circular filter paper and placed onto the aforementioned media. The plate was incubated for 2 days at 30°C and then photographed.

For the real-time luciferase activity assay, cells expressing the pHSE-lucCP+ plasmid were grown to mid-log phase at 30 °C. Activity of Hsf1 was determined by adding luciferin (final concentration 0.5 mm) and distributing 150µl aliquots of the cultures into a white 96-well plate. Cells were incubated in a Synergy MX Microplate reader (Biotek Instruments) at 37 °C for 200 min, and luminescence was read every 5 min. Graph was prepared using GraphPad Prism 7.

Immunoprecipitation of protein complexes

For FLAG IP, cells were harvested and FLAG-tagged proteins were isolated as follows: Protein was extracted via bead beating in 500 µl binding buffer (50 mM Na-phosphate pH 8.0, 300 mM NaCl, 0.01% Tween-20). 200 µg of protein extract was incubated with 30 µl

anti-Flag M2 magnetic beads (Sigma) at 4˚C overnight. Anti-FLAG M2 beads were collected by magnet then washed 5 times with 500 µl binding buffer. After the final wash, the buffer was aspirated and beads were incubated with 65 µl Elution buffer (binding buffer supplemented with 10 µg/ml 3X FLAG peptide (Apex Bio) for 1 hour at room temperature, then beads were collected via magnet. The supernatant containing purified FLAG-protein was transferred to a fresh tube, 25 µl of 4X SDS-PAGE sample buffer was added and the sample was denatured for 5 min at 95˚C. 20 µl of sample was analyzed by SDS-PAGE.

For HA IP, cells were harvested and HA-tagged proteins were isolated as follows: Protein was extracted via bead beating in 500 µl binding buffer (50 mM Na-phosphate pH 8.0, 300 mM NaCl, 0.01% Tween-20). 200 µg of protein extract was incubated with 30 µl anti-HA magnetic beads (Thermo Fisher Scientific) at 4˚C for 30 minutes. Anti-HA beads were collected by magnet then washed 5 times with 500 µl binding buffer. After the final wash, the buffer was aspirated and beads were incubated with 65 µl Elution buffer and 15 µl of 4X loading dye and boiled at 100˚C for 10 minutes, then beads were collected via magnet. The supernatant containing purified HA-protein was transferred to a fresh tube, 25 µl of 4X SDS-PAGE sample buffer was added and the sample was denatured for 5 min at 95˚C. 20 µl of sample was analyzed by SDS-PAGE.

For GFP IP, cells were harvested and GFP-tagged proteins were isolated as follows: Protein was extracted via bead beating in 500 µl binding buffer (50 mM Na-phosphate pH 8.0, 300 mM NaCl, 0.01% Tween-20). 200 µg of protein extract was incubated with 30 µl anti-GFP magnetic beads at 4˚C overnight. Anti-GFP beads were collected by magnet then washed 5 times with 500 µl binding buffer. After the final wash, the buffer was aspirated and beads were incubated with 65 µl Elution buffer and 15 ul of 4X loading dye and boiled at 100˚C

for 10 minutes, then beads were collected via magnet. The supernatant containing purified HA-protein was transferred to a fresh tube, 25 µl of 5x SDS-PAGE sample buffer was added and the sample was denatured for 5 min at 95˚C. 20 µl of sample was analyzed by SDS-PAGE.

Immunoblotting

For testing the inactivation of Ssa1 function (achieved via the temperature-labile mutant *ssa1-45*), cells were grown to mid log phase and heat shocked at 39°C for 4 hours.

Cell lysates obtained were probed for HA and FLAG antibodies for Hir1, 2 and Mtw1 respectively. Protein extracts were made as described in (27). 30 µg of protein was separated by 4%–12% NuPAGE SDS-PAGE (Thermo Fisher Scientific). Proteins were detected using the following antibodies mentioned in star methods. Blots were imaged on a ChemiDoc MP imaging system (Bio-Rad). After treatment with SuperSignal West Pico Chemiluminescent Substrate (Thermo Fisher Scientific). Blots were stripped and re-probed with the relevant antibodies using Restore Western Blot Stripping Buffer (Thermo Fisher Scientific).

β-Galactosidase assays

For *Fus1-lacZ* fusion expression experiments, cells were grown overnight in SD-ura media at 30℃ and then re-inoculated at OD600 of 0.2 - 0.4 and then grown for a further 4 hours. Cells were treated with 0.5µM and 5µM alpha factor for 30 minutes and then *Fus1-lacZ* fusion assays were carried out as described previously (28) . Briefly, protein was extracted through bead beating and protein was quantitated via Bradford assay. The ß-galactosidase reaction containing 100 µg of protein extract in 1 ml Z-Buffer (30) was initiated by addition

of 200 µl ONPG (4 mg/ml) and incubated at 28℃ until the appearance of a pale-yellow color was noted. The reaction was quenched via the addition of 500 µl Na_2CO_3 (1M) solution. The optical density of the reaction was measured at 420nm. β-Gal activity was calculated using ((OD420 x 1.7)/(0.0045 x protein x reaction time)), where protein is measured in mg, and time is in minutes. The mean and standard deviation from three independent transformants were calculated.

Microscopy

For BiFC experiments, yeast cells were grown to mid-logarithmic phase in SC drop-out media and were examined on a Leica DM6 inverted microscope with an oil immersion objective. Fluorescence images for BiFC were taken using a standard fluorescein isothiocyanate filter set (excitation band pass filter, 450 – 490 nm; beam splitter, 510 nm; emission band pass filter, 515 – 565 nm). For Pim1, cells were cultured in SC complete and YPD for imaging and growth assay, respectively. Gene deletion and fluorescent protein tagging were performed with PCR mediated homologous recombination and verified by PCR genotyping. Live-cell images were acquired using a Yokogawa CSU-10 spinning disc on the side port of a Carl Zeiss 200 m inverted microscope or a Carl Zeiss LSM-780 confocal system. Imaging quantification was described previously using imageJ (29). For Mtw1, a Zeiss Axioimager Z2 microscope (Carl Zeiss AG, Germany) was used to image cells using a 63x 1.4NA apochromatic oil immersion lens. Fluorescence was excited using a Zeiss Colibri LED illumination system (GFP=470 nm, YFP=505 nm, and RFP=590 nm) and differential interference contrast (DIC) prisms were used to enhance the contrast in bright field. The emitted light was captured using a Hamamatsu Flash 4.0 Lte CMOS camera with FL-400 (6.5 µm pixels, binned 2x2). The exposure time was set to 300ms to

ensure that signal intensities remained below saturation. Images were acquired using the Zen software (Zeiss) and analyzed and prepared using the Icy BioImage Analysis unit (version 2.0.3.0) (30) and FIJI/ImageJ.

Fluorescence intensities were quantified using the semi-automated FociQuant ImageJ script (31). Intensities were compared using the Student's t-Test (p-value=1.8E-12).

Mammalian cell culture

HEK293T cells were cultured in Dulbecco's modified Eagle's minimal essential medium (DMEM; Thermo Fisher Scientific) supplemented with 10% fetal bovine serum (Thermo Fisher Scientific), GlutaMAX (Thermo Fisher Scientific), 100 U/ml penicillin (Thermo Fisher Scientific) and 100 µg/ml streptomycin (Thermo Fisher Scientific). All cell lines were incubated at 37℃ in a 5% CO2 containing atmosphere. HEK293T cells were either un-transfected or transfected with plasmids for expression of Flag, HA or GFP- tagged proteins using Lipofectamine 3000 (Thermo Fisher Scientific). After 48 hours, the cells were washed with 1XPBS and total cell extract was prepared from the cells using M-PER (Thermo Fisher Scientific) containing EDTA-free protease and phosphatase inhibitor cocktail (Thermo Fisher Scientific) according to the manufacturer's recommended protocol. Protein was quantitated using the Coomassie protein assay.

For JG-98 and bortezomib treatments, HEK293T cells were treated with the drugs at indicated concentration and kept in incubator at 37℃ and 5% CO2 for the indicated time points. After each time point, cells were washed with 1X PBS and total cell extracts were prepared using Mammalian Protein Extract Reagent (Thermo Fisher Scientific).

4.3 Results

Cross-linking mass spectrometry analysis of yeast Hsp70

Previous studies have identified proteins in complex with yeast Hsp70 (Ssa1) using quantitative AP-MS (11). To identify direct clients of Ssa1 and surfaces of interaction, we took a novel cross-linking proteomics approach. HIS-tagged Ssa1 was expressed in *ssa1-4*Δ, a yeast strain in which all four SSA (Hsp70) genes have been deleted. After cross-linking with DSSO, Ssa1 complexes were characterized via mass spectrometry (Figure 18A). This approach facilitated the characterization of Ssa1 complexes without competition from other native Hsp70 isoforms. Quantitative proteomics identified 1,511 interactors associated with Ssa1 cross-linked complexes and 1,152 were identified in the control samples (Figure 18B). We obtained a total of 363 cross-linked peptides, out of which 177 were Ssa1-client/co-chaperone crosslinks, 106 were Ssa1-Ssa1 crosslinks and 80 were client-client cross-links (Figure 18C). Validating our methodology, no cross-linked peptides were observed in the control sample.

To determine whether the cross-linking process had enriched any particular class of protein, we performed Gene ontology (GO) analysis of unique candidate interactors of cross-linked and control samples revealed significant enrichment of multiple cellular functions (Fig. 18D). In the control samples, the GO term translation was the most enriched with *transcription and protein folding* present in the 2nd or 3rd most enriched term, correlating with the established role of Hsp70 in the folding of newly synthesized client proteins. In the crosslinked proteins, the GO term transcription was the most enriched while chromosome segregation and mitotic cell cycle were 2nd or 3rd most enriched term (Fig.

18E). Given the well characterized function of Hsp70, it was unsurprising that transcription, translation protein folding were highly enriched.

Ssa1 forms dimers *in vivo*

Nearly a third of the cross-linked peptides detected in our experiment were between two Ssa1 peptides. To determine whether these Ssa1-Ssa1 peptides were consistent with that expected though internal cross-linking of an Ssa1 monomer, we mapped these cross links on homology-modelled closed structure (ADP bound) and open structure (ATP bound) of Ssa1 (Figure 19A and B). Importantly, while a substantial number of monomer mapped Ssa1-Ssa1 peptides had cross-links lengths well within the spacer arm limit for DSSO (Figure 19B), many Ssa1-Ssa1 peptides were not compatible with the Ssa1 monomer structure. Given that both bacterial and mammalian Hsp70 can form dimers, we evaluated whether these cross-links were coming from two different Ssa1 molecules. After we mapped Ssa1-Ssa1 cross-linked peptides onto a possible Ssa1 dimer structure (Figure 19C), it seemed likely that at least a proportion of Ssa1 could form dimers in yeast (Figure 19C and 19D). To confirm the presence of Ssa1 dimers we expressed both FLAG- and HA-tagged versions of Ssa1 in yeast. After immunoprecipitation of FLAG-Ssa1, the interaction between both tagged forms was observed (Figure 19E). Although self-interaction of Hsp70 has been previously observed *in vitro (32)* , it has never been detected in a living cell. To visualize Ssa1-Ssa1 interaction in a live cell, we utilized bimolecular fluorescence complementation (BiFC). Yeast expressing VN and VC-tagged Ssa1 were examined via high-resolution fluorescence microscopy. Not only was the presence of an Ssa1 dimer clearly visible, but it localized primarily to the nucleus (Figure 19F). To demonstrate *in*

vivo functionality of the Ssa1 dimer, we mutated residues on the Ssa1 dimer interface E540 and N537 based on DnaK (32). Although yeast expressing dimer-deficient mutants E540A/N537K were viable and grew at approximately WT rates, they were impaired for growth at high temperature (Figure 19G). In an attempt to explain this phenotype, we assessed HSE-luciferase activity in WT and Ssa1 dimer-deficient cells. Although WT cells produced a robust HSE-luciferase signal after heat exposure, E540A/N537A cells did not (Figure 19H). Taken together, these data confirm that Ssa1 self-interacts in yeast and that this interaction is functionally important.

Ssa1 is a major hub for protein folding in yeast. We considered the possibility that the Ssa1-Ssa1 interaction we had observed might also be the result of active Ssa1 folding a newly synthesized Ssa1 polypeptide chain. To examine this possibility, we studied the interaction of FLAG-Ssa1 (WT and substrate-binding deficient mutant V435F) with a known client, Rnr2 (11), a co-chaperone, Ydj1 (27) and HA-Ssa1. Although Ssa1 co-purified with Rnr2, Ydj1 and Ssa1, the V435F Ssa1 only lost interaction with Rnr2, demonstrating that Ssa1 is not a client of other Ssa1 molecules (Figure 19I).

Hsp70 interacts with clients throughout its domains

Our Hsp70 cross-linking strategy identified 121 new direct interactors of Ssa1 (Figure 20A). Unique direct binding proteins identified using XL-MS were mapped on the domain structure of Hsp70. We detected interactions on 58% of the possible surface accessible lysines (Figure 3A). Interestingly, in contrast to the established paradigm that Hsp70 clients are bound and processed solely by the SBD, the majority (79%) of the direct interactions were observed at the NBD (Figure 20A). Given that DSSO cross-links lysines, we considered that an explanation for such a high number of interactions with the Ssa1 NBD

may be explained by the number and distribution of lysines present in each domain. Analysis showed that 54% of surface lysines on NBD were crosslinked. (Figure 24 B and 24C).

We then classified these direct interactors into various functional categories which include cell cycle, translation, protein folding, chromatin organization and DNA replication and repair etc. Interestingly, several of the direct interactors were of unknown biological functions (Figure 20 B).

To validate our XL-MS screen, we confirmed several of our hits using co-immunoprecipitation/western Blotting. Consistent with our MS data, Cct8, Pcl7, Ura8 and Sse1 all co-purified with Ssa1 and associated chaperones/co-chaperones Sse1, Hsp82 and Ydj1 (Figure 20C).

Hsp70 regulates activity of the HIR complex

The HIR protein complex is a nucleosome assembly complex involved in regulation of histone gene transcription. It contributes to the nucleosome formation, heterochromatic and gene silencing (33, 34). Our XL-MS analysis revealed a novel interaction between Ssa1 and HIR complex Hir1 and Hir2. We observed cross-linking between the substrate-binding domain of Ssa1 and residues of K435 of Hir1 and K452 of Hir2, adjacent to their respective nuclear localization signals (Figure 21A and 21B). To validate our XL-MS data, we queried interaction of Hir1 and Hir2 with key chaperone components Ssa1, Sse1, Hsp82 and Ydj1 by Co-IP/Western Blotting. In both cases a strong association between HIR and chaperones were observed (Figure 21C).

Given our observed interaction with the Ssa1 SBD, we examined whether Hir1 and Hir2 are *bona fide* Ssa1 clients. Inactivation of Ssa1 function (achieved via the temperature-labile mutant *ssa1-45*) resulted in Hir1 and Hir2 destabilization (Figure 21D).

To demonstrate evolutionary conservation of this chaperone-HIR interaction, we examined interaction between human Hsc70 and HIRA (the major HIR complex protein in human cells). Consistent with our results in yeast, HA-HIRA co-immunoprecipitated with Hsc70, Hsp110, Hsp90, DNAJA1 (Figure 21E). To examine dependence of HIRA on Hsc70 chaperone activity, we treated HEK293 cells with Hsp70 inhibitor JG-98 and observed HIRA abundance over time. HIRA levels rapidly decreased after JG-98 addition, with HIRA becoming undetectable after 2 hours (Figure 21F). Given that in our system HA-HIRA was expressed under the constitutive CMV promoter, we considered the possibility that the effect we observed on HIRA abundance could be explained by protein degradation. In accordance with this theory, addition of the proteasomal inhibitor bortezomib prevented JG-98 dependent HIRA loss (Figure 21F). Taken together, our results suggest that major HIR complex proteins are clients of the Hsp70 chaperone system in yeast and mammalian cells. While further studies are required, it is plausible that the acetylation site on the NLS governs Ssa1 interaction and the localization of Hir1 (Figure 21G).

Hsp70 plays a dual role in mitochondrial Pim1 protease activity

31% (55/177) of our cross-linked peptides contained a post translational modification such as acetylation, methylation or phosphorylation (see Table S4). A search for these PTMs using GPMDB revealed that 95% of these PTMs had not been previously observed. After

considering the possibility that these PTMs might be biologically relevant, we selected 3 diverse PTM-modified Xlinks for further study, Pim1, Mtw1 and Ste11.

Hsp70 plays a dual role in mitochondrial Pim1 protease activity

Pim1 is an ATP-dependent yeast Lon protease that is involved in degradation of misfolded mitochondrial proteins, required for mitochondrial maintenance and biogenesis (35). Our XL-MS data revealed an interaction between the Pim1 protease domain and N-terminal domain of Ssa1 (Figure 22A, 22B). As with our previous client examples, we validated Pim1 interaction with Ssa1 and associated co-chaperones using co-immunoprecipitation followed by Western blot analysis (Figure 22C).

The clearance of mitochondrial aggregates is important throughout life and as such, many organisms express a Pim1 homologue. To examine whether the Ssa1-Pim1 interaction was conserved in mammalian cells, we performed an equivalent experiment to that shown in 22C, using mammalian Lonp-1 as the bait. As in yeast, mammalian Lonp-1 interacted with chaperone proteins including Hsc70, Hsp110, Hsp90 and DNAJA1 (Figure 22D).

In order to determine if Lonp-1 is a client of Hsp70, we treated HEK293 cells with Hsp70 inhibitor JG-98 and observed Lonp-1 degradation after 2 hours of treatment. Treatment of HEK293 cells with bortezomib before addition of JG-98 prevented loss of Lonp-1, confirming that Lonp-1 is a client of Hsc70 (Figure 22E).

The Pim1 part of the Ssa1-Pim1 cross-linked peptide contained a previously undiscovered Pim1 phosphorylation site (S974). Given its proximity to the interaction surface between Ssa1 and Pim1, we wondered whether this site might be important for

Pim1 function. In order to study the effect of Pim1 S974 phosphorylation, we expressed Pim1 lacking this phosphorylation site (S974A) or mimicking constitutive phosphorylation (S974D) from the regulatable *CUP1* promoter in cells lacking Pim1. Although S974A cells grew at a similar rate to WT in standard growth media, S974D cells were substantially inhibited for growth (Figure 22F). To determine whether the growth defect S974D observed was due to inappropriate mitochondrial protein aggregation, we examined aggregation of a previously established mitoFluc reporter (29, 36). In accordance with the defects observed in Figure 22F, S974D cells demonstrated an inability to clear mitochondrial protein aggregates (Figure 22G, 24B). To query whether this loss of Pim1 function was due to mis localization of Pim1, we examined localization of GFP-tagged WT, S974A and S974D Pim1 proteins. Intriguingly, Pim1 localization was unaffected by S974 phosphorylation (Figure 24A).

Like many proteases, Pim1 undergoes self-cleavage to become fully mature (37). We examined Pim1 processing in WT, S974A and S974D cells. In contrast to both WT and S974A, S974D resolved as a single band on SDS-PAGE suggesting Pim1 self-cleavage* and therefore intrinsic protease activity) was compromised in S974D cells (Figure 22H, 24C). The proximity of S974 in the Ssa1-Pim1 cross-linked peptide suggested to us a potential importance in the Ssa1-Pim1 interaction. Immunoprecipitation of Pim1 variants demonstrated that although not critical for Ssa1-Pim1 interaction, S974 phosphorylation significantly enhanced the interaction between the two proteins (Figure 22I). Based on our results 22A-22I, we hypothesized that Ssa1 binds to phosphorylated Pim1 to inhibit its function. To examine Pim1 activity in an environment lacking native Ssa1 activity, we expressed recombinant yeast Pim1 (WT, S974A and S974D) in *e.coli*. In

contrast to our findings in 22H, we observed no difference in Pim1 activity based on S974 status (Figure not shown). Taken together, our findings demonstrate that fascinately, Pim1 is not only a client of Ssa1, but that Ssa1 can also act to inhibit Pim1 function in a phosphorylation-dependent manner (Figure 22J).

Ssa1 regulates kinetochore function via Mtw1

Mtw1 is an essential component of the MIND kinetochore complex and joins kinetochore subunits contacting DNA to those contacting microtubules rendering it critical to kinetochore assembly (38-41). Direct interaction between the NBD of Ssa1 and the head domain of Mtw1 was observed by XL-MS (Figure 23A, 23B). As with our previous examples, we utilized Co-IP/Western Blotting to confirm Mtw1 interaction with Hsp70 chaperone system proteins including Ssa1, Sse1, Hsp82 and Ydj1 (Figure 23C). Perturbation of Ssa1 function destabilized Mtw1 confirming its status as a new client in yeast (Figure 23D).

The mammalian equivalent of Mtw1, Mis12 is critical for correct kinetochore attachment (42). To demonstrate equivalence of the Ssa1-Mtw1 interaction in mammalian cells, we successfully co-purified Mis12 with Hsc70, Hsp110, Hsp90 and DNAJA1 (Figure 23E). Treatment of HEK293 cells with JG-98 resulted in loss of Mis12, and addition of bortezomib prevented JG-98-mediated Mis12 destruction (Figure 23F). Taken together, our results suggest that Mis12 is a novel client of Hsp70. Inhibition of Hsp70 leads to degradation of Mis12 in the proteasome.

The site of interaction between Mtw1 and Ssa1 contained a previously undiscovered phosphorylation site, Y86 on Mtw1 (Figure 23A). Although Mtw1 is an essential gene, the heterozygous deletion is still viable. In this background, cells expressing

the non-phosphorylatable (Y86F) mutation of Mtw1 were viable although were compromised for growth on benomyl, a microtubule-perturbing agent (Figure 23G, 25A and B).

We compared Mtw1 localization at the kinetochore in both WT and Y86F mutant strains. Y86F cells showed a significantly increased accumulation of Mtw1 at the kinetochore compared to wild-type cells (Figure 23H and 23I). Taken together our data suggests that Mtw1 needs to be dephosphorylated and released by Ssa1 to bind kinetochores (Figure 23J)

Ssa1 regulates the activation of Ste11 in response to osmotic stress

Ste11 is a MEK kinase involved in both the cellular response to both pheromone and hypo-osmolarity (28, 43-45) (Figure 24A). As one of the first uncovered clients of Hsp90 and potential client of Ssa1, it was an encouraging validation of our XL-MS methodology to observe direct interaction between the N-terminus of Ssa1 and the unstructured linker domain of Ste11 (Figure 24B). As with Mtw1, Pim1 and Hir1, the Ssa1-Ste11 peptide contained a previous undiscovered dimethylation on Ste11 R305. To determine the biological relevance of dimethylation of Ste11 R305, we created the non-methylatable mutant R305A and dimethylation-mimic R305F and expressed this in cells lacking Ste11. To examine the impact of R305 on the pheromone response, we assessed the ability of Ste11 R305A and R305F to form halos in response to alpha factor, activate a FUS1-LacZ reporter and promote Fus3 phosphorylation. In all 3 experiments, both R305A and R305F behaved in a similar manner to WT (Figures 24C, D, E).

Although R305 status had minimal impact on the pheromone response, previous studies have demonstrated that mutation of residues in this region lead to hyperactive

Ste20-branch hyperosmotic response signaling (44, 45). We examined the ability of R305 mutants to complement the loss of Ste11 in response to osmotic shock. As with the pheromone response, R305 status appeared to be dispensable for Ste11 function in this regard (Figure 24F). Deletion of the upstream components of the Ste11-osmotic response pathway Ssk1, Ssk22 and Ste20 render cells sensitive to media containing NaCl (43-45). Interestingly, we found that while expression of WT and R305A Ste11 in these cells had no discernible effect on osmotic resistance, R305F Ste11 rendered cells resistant to NaCl (Figure 7F). Taken together, these data suggest a role for Ste11 R305 dimethlyation in supporting the activity of the cellular response to osmotic stress.

4.4 Discussion

Towards a comprehensive Hsp70 interactome

The identification and characterization of new chaperone interactions is important to understand the fundamental process of protein folding (46). Critically it may lead to creation of novel therapies that rely on manipulation of chaperone function. While large-scale interactome analysis of chaperones have been attempted previously, each of the methods utilized have significant drawbacks (47, 48). Several of these technologies such as LUMIER are performed on purified proteins and thus discount the impacts of PTMs and scaffold proteins (49, 50). Other cell-based assays such as AP-MS, Y2H and proximity labelling lack the ability to discern direct vs bridged interactions.

XL-MS provides the ability to both stabilize transient interactions and allow characterization of the interaction surface between two proteins (15, 16). Recently, this innovative technology was used to obtain an accurate interactome of Hsp90, and its molecular dynamics (51). Here we have used XL-MS to characterize a more definitive list

of yeast direct Hsp70 interactions. We identified a total of 1512 proteins in a complex with Hsp70, out of which 238 were confirmed to direct interactors. Importantly, 121 of these interactions had never been previously, validating the use of this technology to stabilize and study Hsp70 interactions in the future. It is interesting to speculate what the remaining 1274 interactors represent. They may be bridged interactors present in Hsp70 complexes. If that is the case, it would suggest that large-scale datasets claiming chaperone interactions need to be revisited. On the hand, these interactions may be direct *bona fide* interactors that for technical reasons were unable to be cross-linked to Ssa1.

Previous *in vitro* studies suggested that the majority of interactions would be localized to the C-terminus of Hsp70, the domain recognized as being responsible for binding and processing of Hsp70 clients (4). We identified new Ssa1-interacyions using XL-MS (Fig. 23A). Unexpectedly, the majority of interactions (79%) were through the NTD of Hsp70 (Fig. 23 B and C). We initially considered that the distribution of crosslinkable lysines on Hsp70 may be skewed towards the NBD. Interestingly, even accounting for the number of crosslinkable lysines present on each domain, the NBD had over threefold the number of interactions compared to the other domains. Biologically, there may be several explanations for this result. Firstly, it is possible that during the client-binding process, there are multiple interactions between chaperone and client that traverse the entirety of Hsp70. Although this phenomenon has been observed *in vitro* between recombinant Hsp70 and single substrates, our work is the first make a similar observation at the whole interactome level (52). Alternatively, we may be detecting the interaction of Hsp70 in fully-formed protein complexes. Finally, several of the N-terminal interactions may represent novel co-chaperones/regulators of Hsp70.

Our goal was to identify a comprehensive clientome of Hsp70. To achieve this, we did not replenish ATP during the crosslinking and purification process, skewing the complexes towards co-chaperone free, client-bound Hsp70 complexes. In accordance with this, although several co-chaperones (Sse1, Cct8, Ydj1) were detected in complexes with Hsp70, very few were identified in our crosslinked samples. Although beyond the scope of this study, future experiments may entail purification of Hsp70 complexes in different stages of the folding cycle.

While proteomics methods can undoubtedly produce non-native interactions, all hits selected for follow up were confirmed to be genuine Hsp70 interactors in both yeast and mammalian cells. Given the stress-dependent nature of the Hsp70 interactome, it will be desirable to perform variations of this XL-MS experiment under different stress conditions such as heat, cell cycle stage, DNA damage response and nutrient deprivation.

Understanding novel Ssa1-Ssa1 interactions

An advantage of XL-MS is the ability to detect gain information about protein folding and structure. In the case of Hsp90, XL-MS has been previously used to understand protomer conformational changes upon ATP binding (51). In this study, we identified 177 internal Ssa1-Ssa1 crosslinks. Although the structure of full length Ssa1 has yet to be obtained, sequence similarity to bacterial and mammalian Hsp70 implies that Ssa1 probably forms highly similar ATP and ADP-bound conformations (5, 53, 54). Serving as an internal control to our experiment, the majority of obtained Ssa1-Ssa1 peptides could be matched to these structures. We were perplexed by the remaining peptides which could not be matched to any known Hsp70 structure. Deeper analysis of these peptides revealed that

many must have come from the crosslinking of *two different* Ssa1 molecules. The evidence supporting this is twofold: these cross linked peptides came from peptides further apart the the DSSO crosslinker length. Secondly, several cross linked peptides were symmetrical, that is to say that the peptides on each side of the crosslink were the same. While clearly not at the same stoichiometry as Hsp90, several studies on bacterial and human Hsp70 have demonstrated a capacity for the purified chaperone to form higher-order structures (32, 53, 55-58) Expression of a dimerization-deficient DnaK in bacteria produces viable cells that are sensitive to thermal stress, suggesting that dimerization is needed for a subset of DnaK functions (55). Through both co-immunoprecipitation and BiFC, we demonstrate for the first time that yeast Ssa1 can also form dimers in cells. Suggesting an organelle-specific function, these dimers are almost exclusively localized to the nucleus. While the role of the Ssa1 dimer remains to be explored, given that regulation of the heat shock response by HSF occurs in the nucleus, it is tempting to speculate that dimerization may be a novel way to regulate HSF activation in cells.

Using sites of Hsp70 interaction to reveal novel PTMs of biological importance on clients

Molecular chaperones are critical for supporting the activity of proteins involved in signal transduction, particularly those involved in post-translational modifications such as kinases or acetylases (59-61). These interactions are complex; some are stable, with clients requiring continuous chaperone interaction for activity (62). Others are transient, where client maturation is followed by rapid chaperone dissociation needed for full client activity (5). However, there is also a growing body of work that shows that PTMs also play an

important role in chaperone interactions. Several have been characterized that are dependent on client-phosphorylation status, as with Hsp90-Mpk1 and Hsp90-ERK5 (63). The chaperone code (PTMs on chaperones) also regulates interactions of many chaperones/co-chaperones including Hsp90, Hsp70, HSF, Cdc37 (9, 21, 64). While these PTMs have been identified on a one at a time basis, this is the first study to identify important chaperone-PTM interactions on a much larger scale.

In this work, we have followed up on four Hsp70 clients that contain novel PTMs on the site of interaction with Ssa1, Hir1, Mtw1, Pim1 and Ste11. In each of these cases, the PTMs on the clients had been previously undiscovered and yet have turned out to regulate novel (and very different) facets of client function. For Hir1 and Mtw1, their PTMs appear to regulate their localization, required for full functionality. For Pim1, S974 phosphorylation doesn't impact stability or localization, but rather self-processing and proteolytic activity. For Ste11, one the first discovered Hsp90 clients, our working model is that Ste11 demethylation regulates pathway specificity, explaining how a branched pathway with shared components can function in a selective manner.

Future studies will aim to decipher the stresses and enzymes that regulate these sites in addition to teasing apart the hierarchy of interaction between Ssa1 and these novel PTMs. We currently have two working models; in the first the presence of the PTM recruits Hsp70 to alter client interactions and therefore function. In the second, Ssa1 is acting as a "protective cover" over the novel PTM, trapping the PTM in its on/off state altering kinetics of client activation. These models, while reasonable, are hard to test given that Ssa1 plays multiple roles on these clients, is essential for cell growth and acts at multiple points in the signal transduction pathways involved.

Overall, this work meant to test just the feasibility of crosslinking Hsp70 complexes has pulled back the curtain on new regulator mechanisms for both chaperones and clients. In doing so we have created novel tools and methods for the signal transduction/chaperone communities as well as a substantial list of novel clients and biologically important PTMs to study.

4.5 Figures

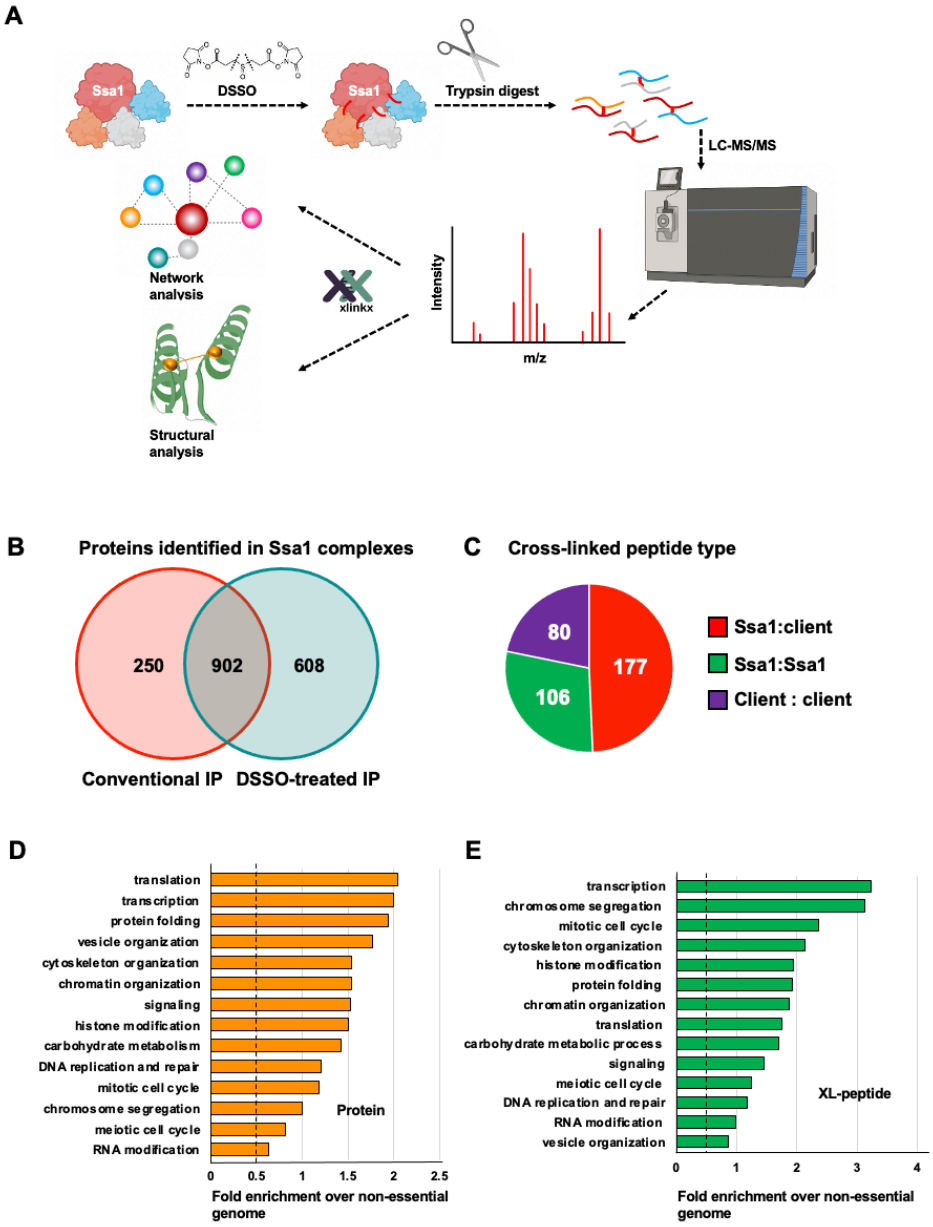

Figure 18. Cross-linking mass spectrometry of Ssa1 complexes. (A) Experimental workflow of cross-linking mass spectrometry of Ssa1 complexes purified from yeast cells. (B) Venn diagram representing Ssa1 complexes found in conventional IP and DSSO treated IP. (C) Pie chart showing types of cross links identified from XL-MS analysis. (D) and (E) Gene ontology analysis of DSSO treated Ssa1 immunoprecipitated complexes and crosslinked Ssa1 complexes.

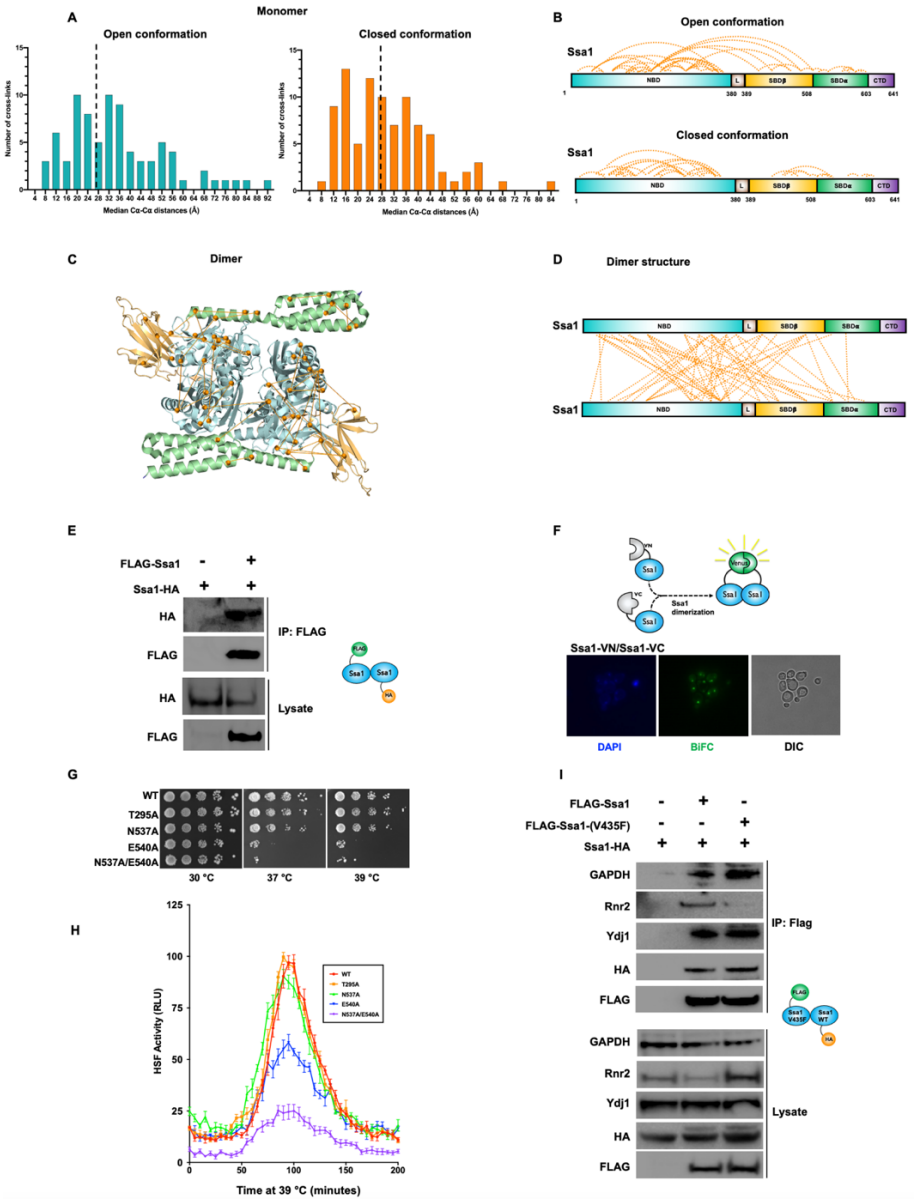

Figure 19. A proportion of Ssa1 exists as dimer. (A) Ssa1 cross links identified from XL-MS analysis mapped on the monomeric structure of Ssa1 in open and closed conformation. (B) Ssa1 cross links mapped on the domains of Ssa1 in open and closed conformation. (C) Internal and External Ssa1 cross links were mapped on the dimeric structure of Ssa1 (4JNE). (D) External cross links were mapped on the domains of Ssa1 (E) Internal and External cross links were mapped on the crystal structure of Ssa1 (4JNE). (F) Immunoblot analysis of Flag tagged Ssa1 purified from cells expressing HA-tagged Ssa1. (G) Western blot analysis of Flag-tagged Ssa1 and Flag-tagged Ssa1-V435F mutants purified from cells expressing HA-tagged Ssa1. (H) Fluorescence images of diploid cells expressing the N-terminally VN- and VC- tagged Ssa1. DAPI was used as a nuclear marker. Scale bars are10 μM.

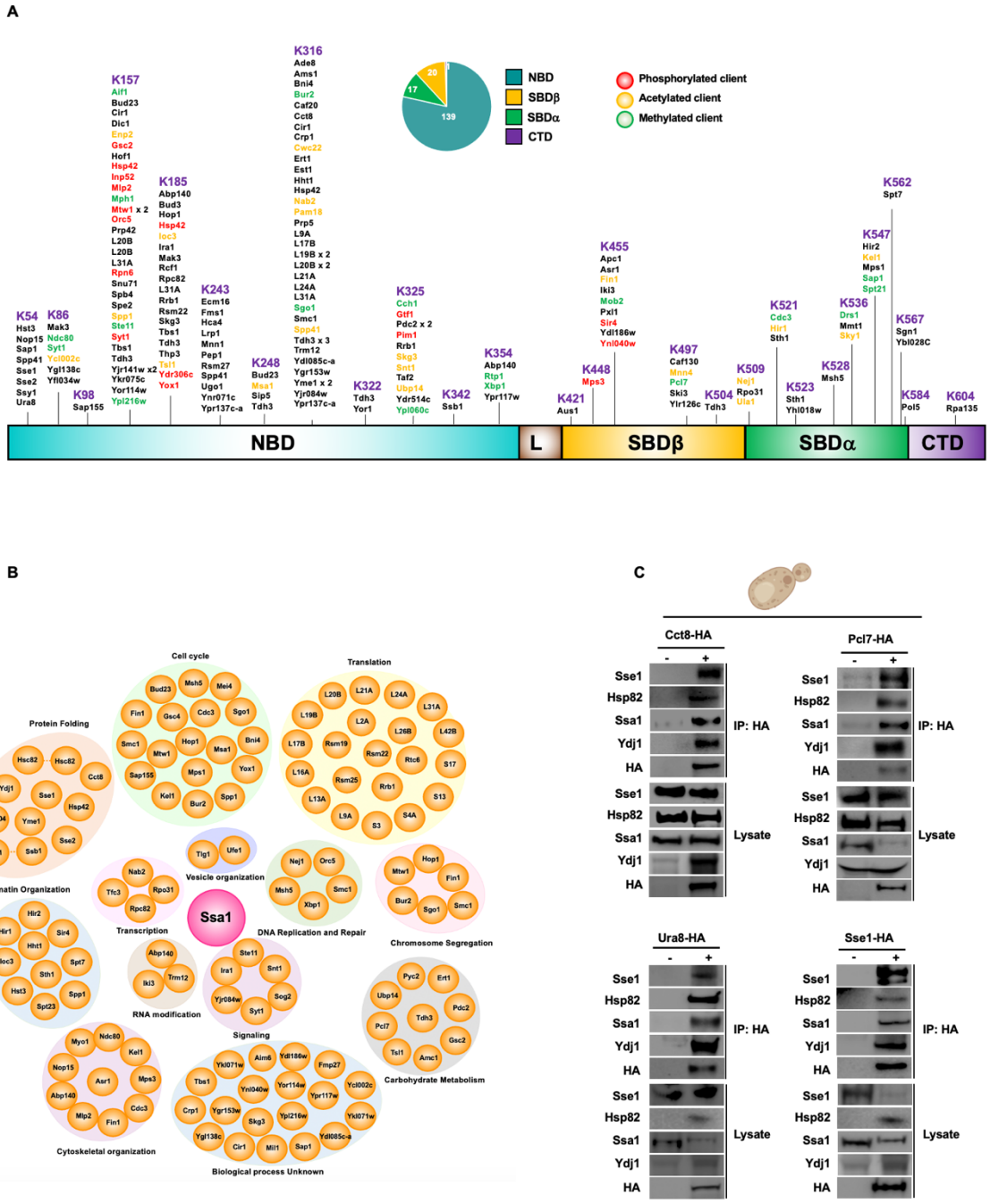

Figure 20. Novel clients and post translationally modified clients identified on yeast Hsp70 based on XL-MS. (A) Schematic representation of 177 inter-protein crosslinks and identified post translational modifications on domains of Hsp70. (B) Functional classification of direct Hsp70-client peptides. (C) Western blot analysis of HA-tag immunoprecipitated Cct8, Pcl7, Ura8 and Sse1 from yeast cells.

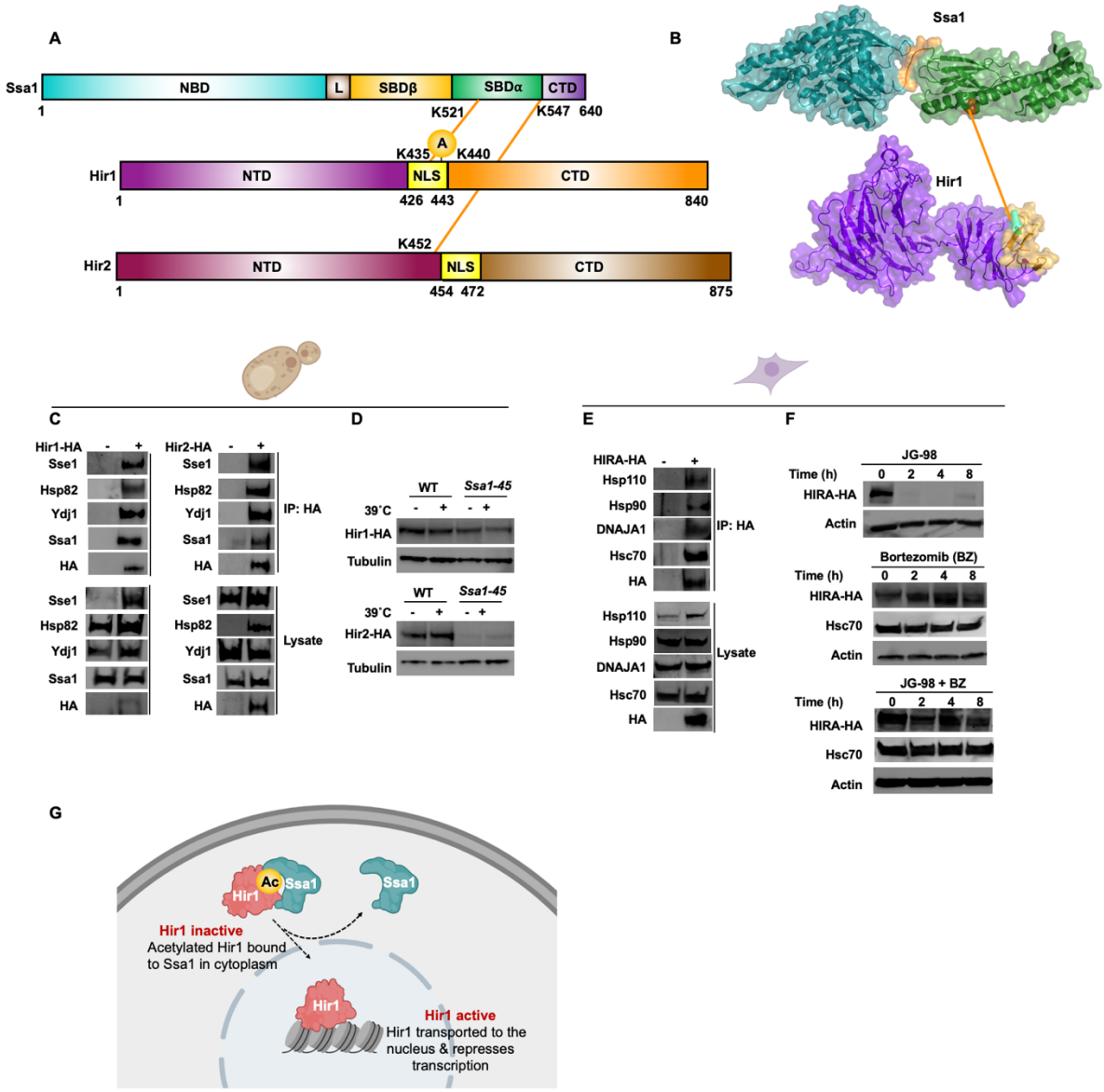

Figure 21. HIR complex is a novel client of Hsp70 in yeast and humans. (A) Schematic representation of Ssa1-Hir1/Hir2 inter protein cross-links detected on SBD of Ssa1 and NLS of Hir1 and NTD of Hir2. (B) Ssa1-Hir1/2 cross links mapped on the crystal structure of Ssa1, Hir1 and Hir2. (C) Hir complex interacts with the chaperone complex. (D) Hir1 and Hir2 are destabilized in Ssa1-45 mutant strain. (E) HIRA complex interacts with chaperone complexes in mammalian cells. IP analysis of the HIRA complex in mammalian cells. (F) Western blot analysis of HIRA upon addition of Hsp70 inhibitor JG-98 and proteasomal inhibitor Bortezomib. (G) Model of Hir1 regulation by acetylation site on the NLS.

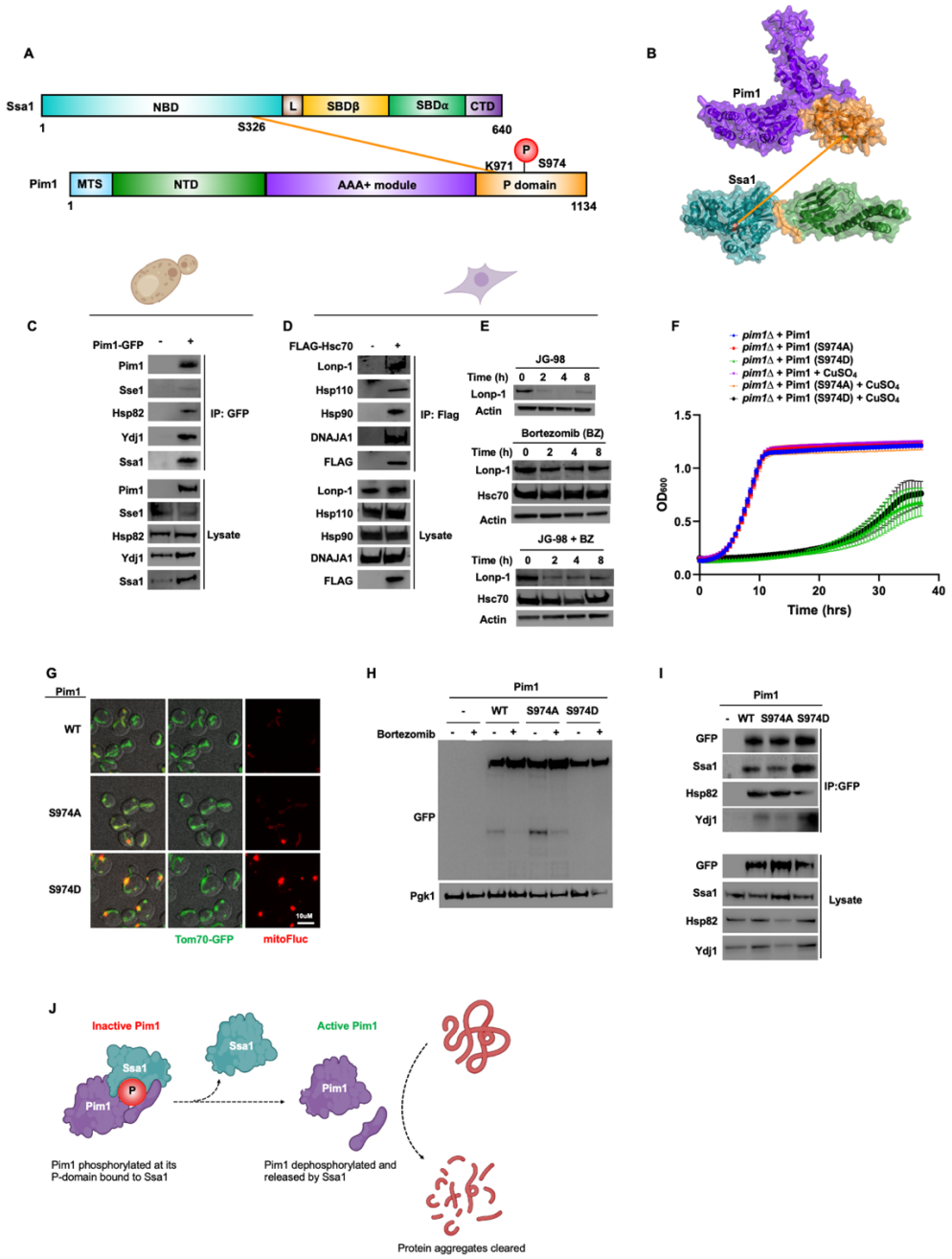

Figure 22. Pim1 phosphorylation regulates mitochondrial clearance in an Ssa1-dependent manner. (A) Schematic representation of Ssa1-Pim1 inter protein cross-links detected on NBD of Ssa1 and proteolytic domain of Pim1. (B) Ssa1-Pim1 cross links mapped on the crystal structure. (C) Pim1 interacts with the chaperone complex in yeast cells. (D) IP analysis of Lonp-1 interacts with chaperone complexes in mammalian cells. (E) Western blot analysis of Lonp-1 upon addition of Hsp70 inhibitor JG-98 and proteasomal inhibitor Bortezomib. (F) Growth assay of Pim1 phospho mutants in yeast. (G) Fluorescence images of cells expressing FlucSM–RFP and Tom70-GFP. Scale bars are 10 μM. (H) Western blot analysis of Pim1 wildtype and phosphomutants upon addition of Bortezomib. (I) IP analysis of Pim1 wildtype and phospho mutants with chaperone complex. (J) Model of the Pim1 phosphorylation regulating its aggregate clearance activity.

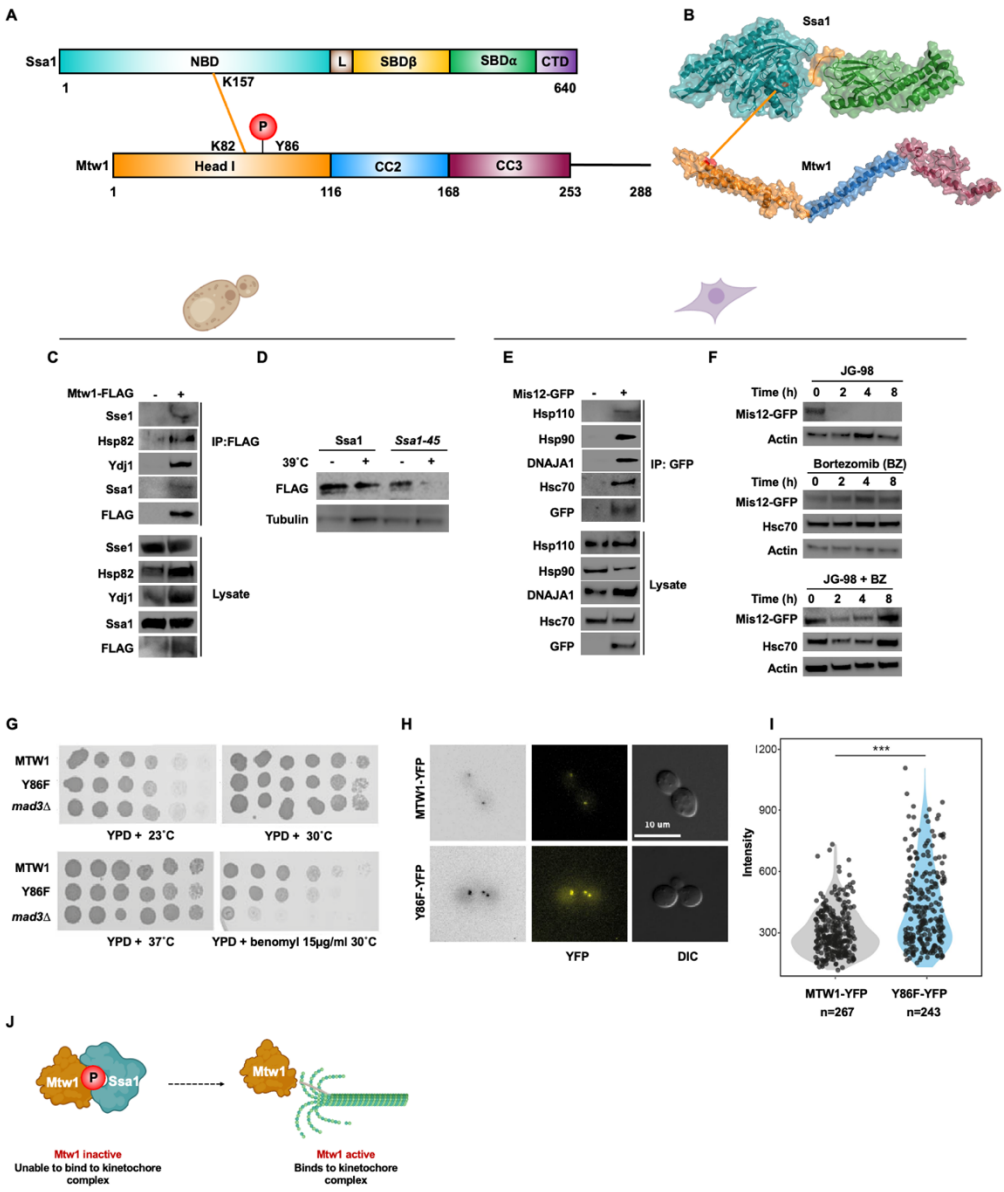

Figure 23. Mtw1 is a client of Hsp70 and is regulated by phosphorylation. (A) Schematic representation of Ssa1-Mtw1 inter protein cross-links detected on NBD of Ssa1 and head domain of Mtw1. (B) Ssa1-Mtw1 cross links mapped on the crystal structure of Ssa1 and Mtw1. (C) Mtw1 interacts with the chaperone complex. (D) Mtw1 is destabilized in Ssa1-45 mutant strain. (E) MIS12 interacts with chaperone complexes in mammalian cells. IP analysis of the MIS12 in mammalian cells. (F) Western blot analysis of MIS12 upon addition of Hsp70 inhibitor JG-98 and proteasomal inhibitor Bortezomib. (G) Growth assay analyzing the phenotype of the Mtw1 and its Y86 mutant. (H) Mtw1 was tagged with YFP in wild-type and Mtw1-Y86F mutant strains to compare Mtw1 localization at the kinetochore using Fluorescence microscopy. (I) Fluorescence intensities were quantified in wildtype and mutant Mtw1 using the semi-automated FociQuant ImageJ script (31). Intensities were compared using the Student's t-test (p-value=1.8E-12). (J) Model of Mtw1 activity regulation via its phosphorylation.

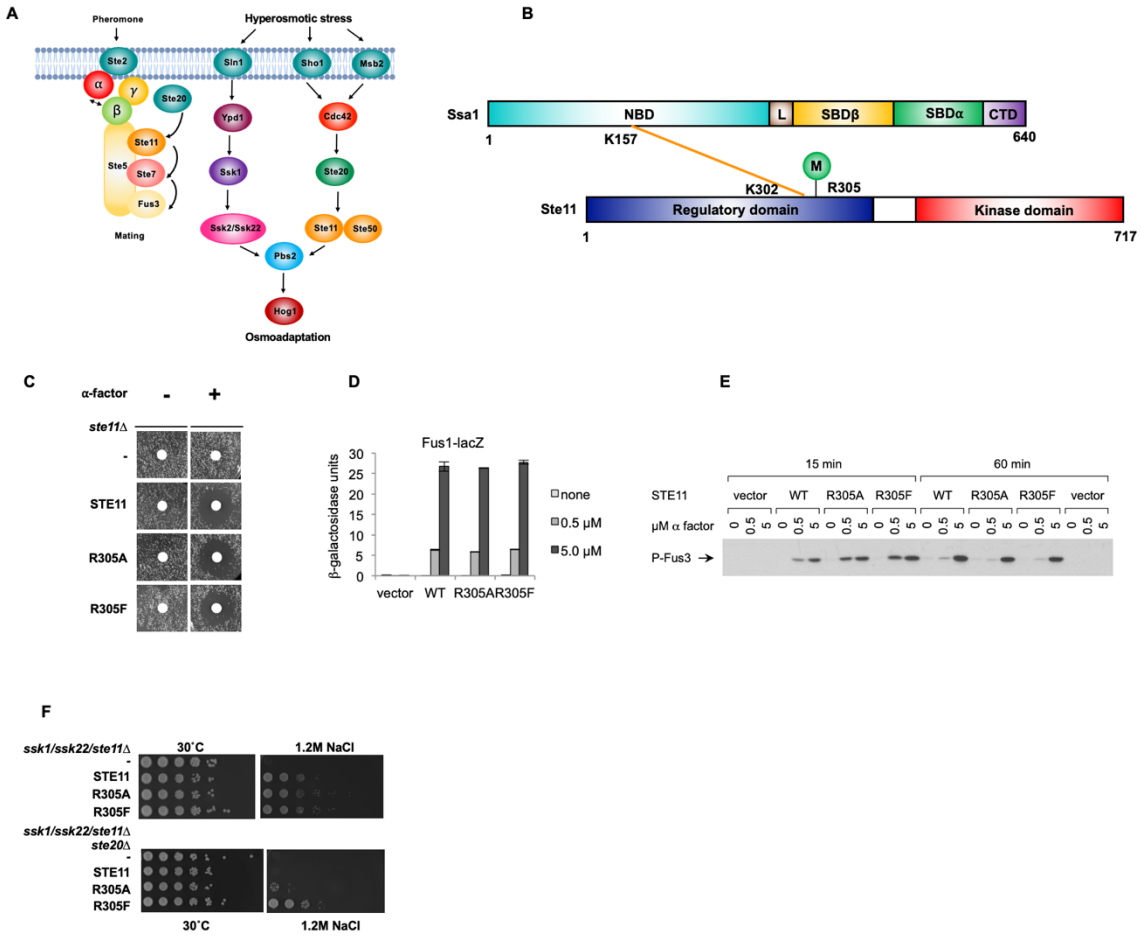

Figure 24. Ste11 dimethylation impacts the osmotic stress response in an Ssa1-dependent manner. (A) Depiction of Ste11 pathway under hyperosmotic stress. (B) Schematic representation of Ssa1-Ste11 inter protein cross-links detected on NBD of Ssa1 and regulatory domain of Ste11. (C) Halo assay analyzing the phenotype of the Ste11 wildtype and methylation mutants in response to alpha factor. (D) b-galactosidase assay of Ste11 mutants in response to pheromone. (E) Western blot analysis of the effect of Ste11 wildtype and mutants in response to pheromone signaling. (F) Growth assay analyzing the phenotype of the Ste11 wildtype and the methylation mutants in hyperosmotic stress.

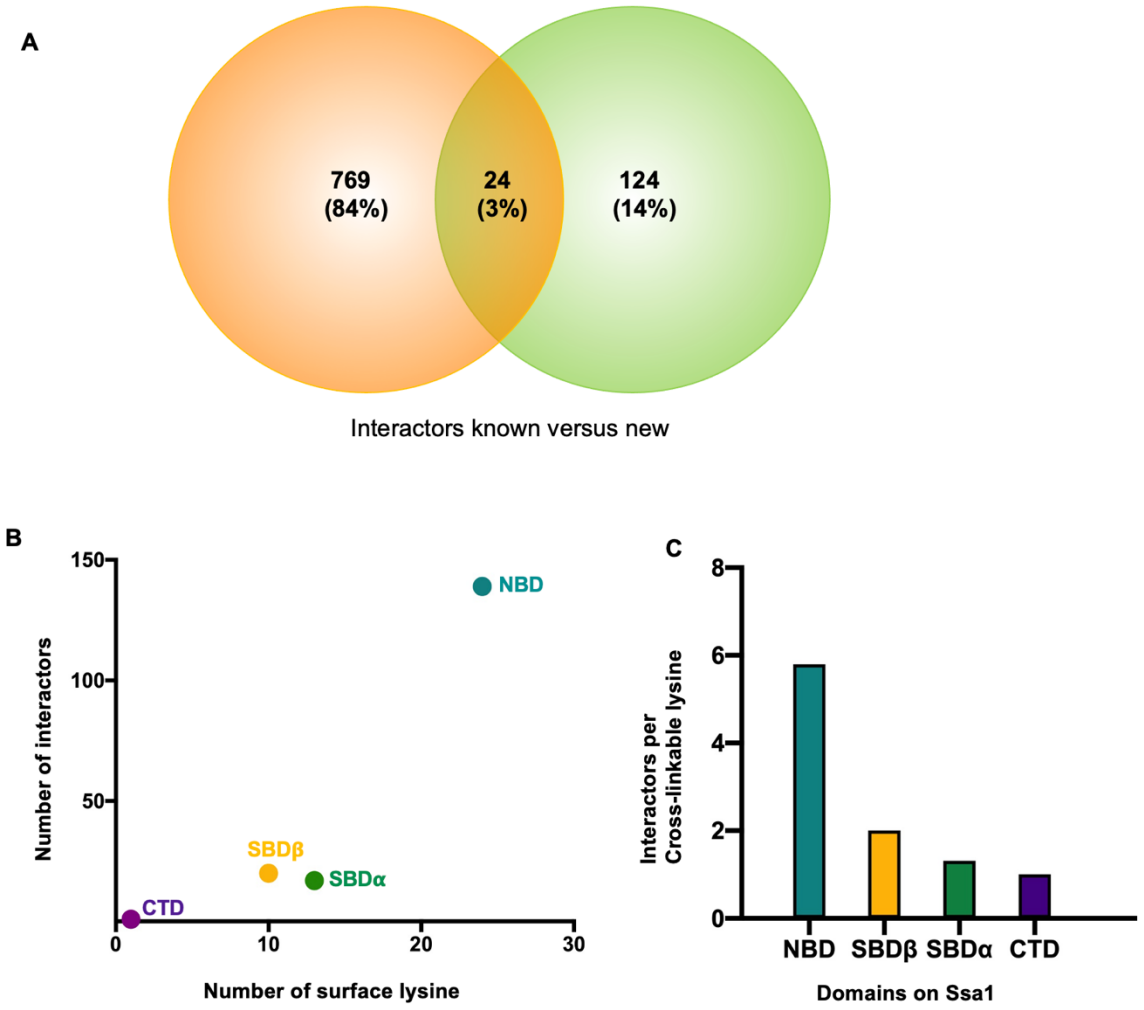

Figure 25. Supplementary 1 (A) Venn diagram representing known physical interactors of Ssa1 versus new direct interactors of Ssa1 identified in this study. (B) Scatter plot of number of interactors identified versus surface lysine on the domains of Ssa1. (C) Bar graph representing interactors per cross linkable lysine on domains of Ssa1.

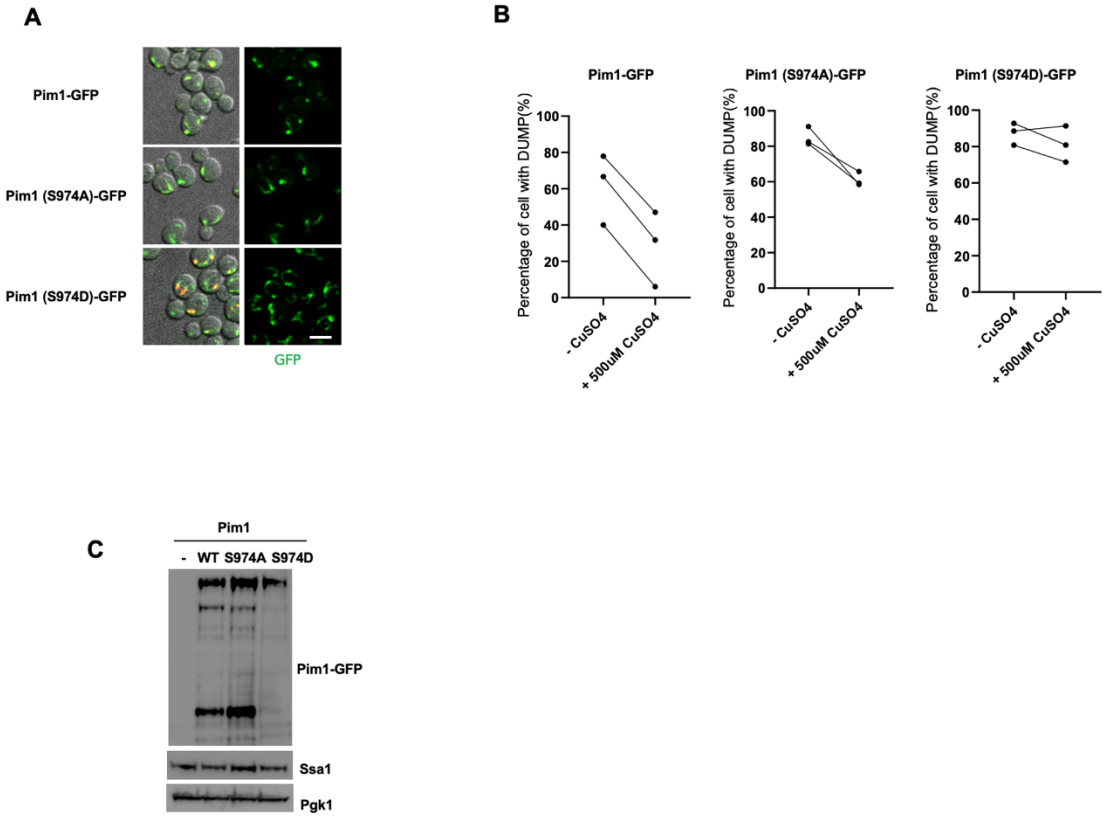

Figure 26. Supplementary 2 (A). Localization of Pim1 wildtype and the mutants in yeast cells. (B) Quantification of percentage of cell with mitoFluc labeled DUMP structures in (Figure5G). Paired t test was used for statistical analysis. (C) Western blot showing the levels of Pim1 wildtype and the mutants in yeast cells.

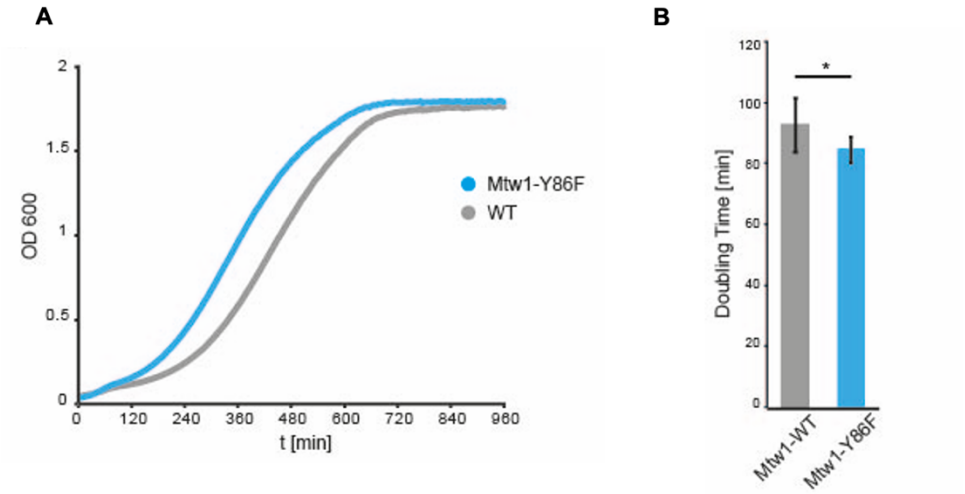

Figure 27. Supplementary 3 (A) Growth curves of wild-type (BY4741) and Mtw1-Y86F yeast strains. Cells were diluted from an overnight culture to OD600=0.03 and the OD600 was measured every 5 minutes for 16 hours using a microplate reader. Growth analysis was performed in 10 replicates per strain. (B) Doubling times for wild-type and mutant strains were calculated for each replicate and compared using Student's t-Test (mean=92.97 min, p-value=0.04).

Table S1: List of reagents used in this study.

REAGENT or RESOURCE	SOURCE	IDENTIFIER
Chemicals, Peptides, and Recombinant Proteins		
Dulbecco's Modified Eagle Medium (DMEM)	Thermo Fisher Scientific	Cat# 10313-021
Fetal Bovine Serum (FBS)	Thermo Fisher Scientific	Cat# 16000044
GlutaMAX	Thermo Fisher Scientific	Cat# 35050-061
Trypsin	Thermo Fisher Scientific	Cat# 15400-054
Penicillin/Streptomycin	Thermo Fisher Scientific	Cat# 15140-163
DSSO	Cell IDx	This study
Anti-Flag M2 magnetic beads	Sigma	Cat# M8823
HA beads	Pierce	Cat# 88836
GFP beads	ChromeTek	Cat# GTMA-20
DAPI	Invitrogen	Cat# D1306
JG-98	Kind gift from Prof. Jason Gestwicki, UCSF	
Bortezomib	LC-Laboratories	Cat# B-1408
Flag peptide	ApexBio	Cat# A6002
Benomyl	Agilent	Cat# PST-1245A100A01
α-factor	Genscript	Cat# RP01002
Copper Sulfate	Acros organics	Cat# 197711000
Luciferin	ApexBio	Cat# B6040
Antibodies		
Flag	Sigma	Cat# F3165
HA	Thermo Fisher Scientific	Cat# 26183
GAPDH	Thermo Fisher Scientific	Cat# MA5-15738
GFP	Millipore Sigma	Cat# 11814460001
Ydj1	StressMarq	Cat# SMC166
Hsp82	StressMarq	Cat# SMC-135D
Sse1	StressMarq	Cat# SPC-195
Ssa1	Enzo	Cat# BB79
Hsp90	Santa Cruz	Cat# sc-13119
Dnaja1	Thermo Fisher Scientific	Cat# MA5-12748
Hsc70	Santa Cruz	Cat# sc-7298

Actin	CST	Cat# 9774
Pgk1	Invitrogen	Cat# PA5-28612
Tubulin	Santa Cruz	Cat# sc-53030
Lonp-1	Proteintech	Cat# 66043
Secondary antibody mouse	GE	Cat# NA931V
Secondary antibody rabbit	GE	Cat# NA934V/AG
Commercial kits		
Protease Inhibitor EDTA free	Thermo Fisher Scientific	Cat# A32961
Super Signal ECL	Thermo Fisher Scientific	Cat# 34577
HisTrap HP His tag protein purification column	GE	Cat# 17524701
Lipofectamine 3000	Thermo Fisher Scientific	Cat# L3000008
NuPAGE™ LDS sample buffer	Thermo Fisher Scientific	Cat# NP0007
M-PER	Thermo Fisher Scientific	Cat# 78501
NuPAGE™ 4 to 12% Bis-Tris, Mini Protein Gel	Thermo Fisher Scientific	Cat# NP0321BOX
Restore Western Blot Stripping Buffer	Thermo Fisher Scientific	Cat# 46430
Coomassie Protein Assay Kit	Thermo Fisher Scientific	Cat# 23236
Software		
Graphpad prism	Graphpad	www.graphpad.com/scientificsoftware/prism/
PyMOL	PyMOL by Schrödinger	https://pymol.org/2/
Biorender	Biorender	https://biorender.com/
ImageLab	Bio-Rad	https://www.bio-rad.com/en-us/product/image-lab-software?ID=KRE6P5E8Z
Experimental Models: Cell Lines		
HEK293T Cell lines	ATCC	Cat# CRL-3216
Others		
96 well Nuncleon delta white microwell plates	Thermo Fisher Scientific	Cat# 136101
DMSO	Sigma	Cat# W387520

Table S2: Novel Ssa1-Ssa1 crosslinks found in this study.

Protein	Position A	Position B
Ssa1	18	65
Ssa1	54	243
Ssa1	54	316
Ssa1	54	592
Ssa1	69	316
Ssa1	86	243
Ssa1	110	316
Ssa1	126	316
Ssa1	126	185
Ssa1	157	316
Ssa1	157	504
Ssa1	157	243
Ssa1	157	509
Ssa1	157	455
Ssa1	157	185
Ssa1	157	325
Ssa1	185	509
Ssa1	185	243
Ssa1	243	322
Ssa1	243	504
Ssa1	248	316
Ssa1	248	157
Ssa1	248	185
Ssa1	248	325
Ssa1	316	322
Ssa1	316	494
Ssa1	316	504
Ssa1	316	455
Ssa1	316	110
Ssa1	316	106
Ssa1	316	126
Ssa1	316	98
Ssa1	316	185
Ssa1	316	157
Ssa1	325	157

Ssa1	325	243
Ssa1	342	421
Ssa1	342	509
Ssa1	354	157
Ssa1	354	455
Ssa1	354	536
Ssa1	354	325
Ssa1	420	157
Ssa1	420	185
Ssa1	420	316
Ssa1	420	562
Ssa1	420	316
Ssa1	421	157
Ssa1	448	316
Ssa1	455	157
Ssa1	504	185
Ssa1	504	157
Ssa1	509	342
Ssa1	509	316
Ssa1	509	536
Ssa1	536	509
Ssa1	536	54
Ssa1	556	157
Ssa1	584	528
Ssa1	54	157
Ssa1	61	65
Ssa1	69	157
Ssa1	69	126
Ssa1	69	185
Ssa1	86	69
Ssa1	86	316
Ssa1	86	106
Ssa1	126	157
Ssa1	126	110
Ssa1	136	157
Ssa1	157	509
Ssa1	157	342
Ssa1	157	98
Ssa1	157	86

Ssa1	157	54
Ssa1	157	69
Ssa1	157	98
Ssa1	185	316
Ssa1	185	354
Ssa1	185	322
Ssa1	243	248
Ssa1	243	342
Ssa1	316	243
Ssa1	316	342
Ssa1	316	354
Ssa1	316	69
Ssa1	316	54
Ssa1	316	325
Ssa1	316	86
Ssa1	342	354
Ssa1	342	322
Ssa1	342	325
Ssa1	342	157
Ssa1	342	54
Ssa1	354	185
Ssa1	420	497
Ssa1	448	504
Ssa1	448	536
Ssa1	455	504
Ssa1	504	509
Ssa1	509	523
Ssa1	528	521
Ssa1	547	562
Ssa1	547	567
Ssa1	562	562
Ssa1	568	590
Ssa1	584	592
Ssa1	592	584
Ssa1	243	316

Table S3: Novel Ssa1 crosslinked to clients found in this study

Yeast Gene	Name	Position on client	Position on Ssa1
INP52	Inositol polyphosphate 5-Phosphatase	2	157
CIR1	Changed Intracellular Redox state	4	316
CIR1	Changed Intracellular Redox state	4	157
RPN6	Regulatory Particle Non-ATPase	7	157
RPL24A	Ribosomal 60S subunit protein L24A	27	316
CAF20	Cap Associated Factor	33	316
RPL20B	Ribosomal 60S subunit protein L20B	38	157
HHT1	Histone H3	43	316
SPE2	Spermidine auxotroph	50	157
RPL31A	Ribosomal 60S subunit protein L31A	65	157
RPL31A	Ribosomal 60S subunit protein L31A	65	316
RPL31A	Ribosomal 60S subunit protein L31A	65	185
MMT1	Mitochondrial Metal Transporter	66	536
TDH3	Glyceraldehyde-3-phosphate dehydrogenase	71	316
TDH3	Glyceraldehyde-3-phosphate dehydrogenase	213	316
TDH3	Glyceraldehyde-3-phosphate dehydrogenase	331	322
TDH3	Glyceraldehyde-3-phosphate dehydrogenase	331	504
TDH3	Glyceraldehyde-3-phosphate dehydrogenase	331	316
TDH3	Glyceraldehyde-3-phosphate dehydrogenase	331	185
TDH3	Glyceraldehyde-3-phosphate dehydrogenase	331	157
TDH3	Glyceraldehyde-3-phosphate dehydrogenase	331	248
RRB1	Regulator of Ribosome Biogenesis	72	325
PRP5	Pre-mRNA Processing	75	316
MTW1	Mis Twelve-like	82	157
RPL21A	Ribosomal 60S subunit protein L21A	87	316
SAP155	Sit4 Associated Protein	789	98
YFL034W	Medium adapting-Interacting Ligand	107	86
GTF1	Glutaminyl Transamidase subunit F	119	325
AUS1	ABC protein involved in Uptake of Sterols	140	421
CRP1	Cruciform DNA-Recognizing Protein	148	316
PRP42	Pre-mRNA Processing	163	157
NOP15	Nucleolar protein	169	54
RPL19B	Ribosomal 60S subunit protein L19B	180	316
MPS3	Monopolar spindle	211	448
SIP5	Snf1 Interacting Protein	232	248
CCT8	Chaperonin Containing TCP-1	243	316

BUD23	BUD site selection	254	248
BUD23	BUD site selection	254	157
TRM12	tRNA Methyltransferase	262	316
SSE1	Stress Seventy subfamily E	262	316
SSE2	Stress Seventy subfamily E	273	54
PDC2	Pyruvate decarboxylase	280	325
HCA4	Helicase CA	293	243
HSP42	Heat shock protein 42	298	157
HSP42	Heat shock protein 42	298	185
HSP42	Heat shock protein 42	298	316
RPL17B	Ribosomal 60S subunit protein L17B	13	316
RPL20B	Ribosomal 60S subunit protein L20B	38	316
RPL19B	Ribosomal 60S subunit protein L19B	153	316
YOX1	Yeast homeobox	347	185
ORC5	Origin Recognition Complex	353	157
SMC1	Stability of mini chromosomes	432	316
AMS1	Alpha-mannosidase	483	316
ERT1	Ethanol Regulated Transcription factor	488	316
BNI4	Bud Neck Involved	511	316
RPC82	RNA polymerase III subunit C82	529	185
ABP140	Actin Binding Protein	538	185
SKI3	Super killer	573	497
SIR4	Silent Information Regulator	596	455
MLP2	Myosin-Like Protein	647	157
YME1	Yeast Mitochondrial Escape	711	316
SPP41	Suppressor of PrP4	818	54
PIM1	Proteolysis in Mitochondria	971	325
CAF130	CCR4 Associated Factor	1028	497
SYT1	Suppressor of ypt3	1134	157
RPO31	RNA Polymerase III subunit C82	1290	509
TAF2	TATA binding protein-Associated Factor	1339	325
BUR2	Cyclin for the Sgv1p (Bur1p) protein kinase;	72	316
SPB4	Suppressor of PAB1	532	157
PCL7	Pho85 cyclin	7	497
XBP1	Xho I site-Binding Protein	454	354
CCH1	Calcium Channel Homolog	273	325
RTP1	Required for the nuclear Transport of RNA Pol II	607	354
SGO1	Component of the spindle checkpoint	484	316
AIF1	Apoptosis Inducing Factor	363	157

SPT1/HIR2	Protein with a role in transcriptional silencing	452	547
CDC3	Cell division cycle 3	478	521
MPH1	DNA HELICASE	424	157
SAP1	Sin1 Associated Protein	532	54
NDC80	Nuclear Division Cycle	632	86
STE11	Signal transducing MEK kinase	302	316
HOP1	Meiosis-specific protein required for chromosome synapsis	8	185
RPL9A	Ribosomal 60S subunit protein L9A	26	316
ECM16	Essential DEAH-box ATP-dependent RNA helicase	1055	243
DRS1	Deficiency of Ribosomal Subunits	112	536
MNN4	Mannosyl phosphate transferase	244	497
ULA1	Ubiquitin-Like protein Activation	223	509
ABP140	Actin Binding protein	538	354
YOR1	Yeast Oligomycin Resistance	556	322
NAB2	Nuclear polyadenylated RNA-Binding	402	316
IOC3	Iswi One Complex	472	185
HIR1	Histone Regulation	435	521
SKY1	SR protein kinase (SRPK)	369	536
SNT1	SANT domains	472	325
ASR1	Alcohol Sensitive Ring/PHD finger	202	455
FIN1	Filaments In between Nuclei	79	455
ENP2	Essential Nuclear Protein	565	157
SPP1	Set1c, PHD finger Protein	140	157
PAM18	Pre sequence translocase-Associated Motor	88	316
MOB2	Mps1 Binder	53	455
TSL1	Trehalose Synthase Long chain	776	185
DIC1	Dicarboxylate Carrier	143	157
KEL1	Kelch repeat	882	547
IKI3	Insensitive to killer toxin	1062	455
MSA1	Activator of G1-specific transcription factors MBF	8	248
NEJ1	Nonhomologous End-Joining defective	285	509
CWC22	Complexed with Cef1p	167	316
UBP14	Ubiquitin-specific Protease	507	325
GSC2	Glucan Synthase of Cerevisiae	1404	157
RSM27	Ribosomal Small subunit of Mitochondria	107	243
MAK3	Catalytic subunit of the Nat C type N-terminal acetyltransferase (NAT)	161	185
MPS1	Monopolar Spindle	272	547
YME1	Yeast Mitochondrial Escape	711	316

POL5	DNA Polymerase phi	937	584
SPT7	Subunit of the SAGA transcriptional regulatory complex	981	562
UGO1	Outer membrane component of the mitochondrial fusion machinery	73	243
PMT4	Protein O-mannosyl transferase	630	54
PDC2	Pyruvate decarboxylase	280	325
EST1	Ever Shorter Telomeres	307	316
HOF1	Homolog of Cdc15	142	157
IRA1	Inhibitory Regulator of the RAS-cAMP pathway	1018	185
THP3	THO-related Protein	448	185
STH1	SNF Two Homolog	709	521
RPA135	RNA Polymerase A	805	604
YBL028C	Protein of unknown function	74	567
YHL018W	Putative 4a-hydroxytetrahydrobiopterin dehydratase	23	523
RCF1	Cytochrome c oxidase subunit	29	185
HST3	Homolog of SIR Two (SIR2)	168	54
RPL20B	Ribosomal 60S subunit protein L20B	38	316
STH1	SNF Two Homolog	709	523
SPP41	Protein of unknown function; involved in negative regulation of expression of spliceosome components PRP4 and PRP3	818	243
YJR141W	Protein implicated in pre-mRNA processing and proteasomal degradation	98	157
RRB1	Regulator of Ribosome Biogenesis	73	185
TBS1	Protein of unknown function	835	185
PEP1	Type I transmembrane sorting receptor for multiple vacuolar hydrolases	409	243
MNN1	Mannosyl transferase	646	243
YJR141W	cleavage and Poly Adenylation	98	157
FMS1	essential modification of translation factor eIF-5A	391	243
YHL042W	Protein of unknown function	54	584
MTW1	Mis Twelve-like	122	157
RSM22	Ribosomal Small subunit of Mitochondria	395	185
URA8	Minor CTP synthase isozyme	391	54
RPL20B	Ribosomal 60S subunit protein L20B	38	157
MAK3	Catalytic subunit of the NatC type N-terminal acetyltransferase (NAT)	161	86
YDR514C	Protein of unknown function that localizes to mitochondria	135	325
APC1	Anaphase Promoting Complex subunit	944	455
SGN1	Cytoplasmic RNA-binding protein; contains an RNA recognition motif (RRM)	219	567

LRP1	Nuclear exosome-associated nucleic acid binding protein; involved in RNA processing,	183	243
YNR071C	Putative aldose 1-epimerase	18	243
MSH5	Mut S Homolog	746	528
ADE8	Adenine requiring	70	316
YKR075C	Protein of unknown function;	239	157
SPT23	Suppressor of Ty	904	54
SNU71	Small nuclear ribonucleoprotein associated	588	157
PXL1	Paxillin-Like protein	16	455
BUD3	BUD site selection	1174	185
SSB1	Stress-Seventy subfamily B	314	342
YPR117W	Putative protein of unknown function	1483	354
YPR137C-A	Putative protein of unknown function	322	316
YPR137C-A	Transposable element gene	344	243
YGL138C	Putative protein of unknown function	344	86
YJR084W	Unknown ORF	27	316
YDL085C-A	Putative protein of unknown function	62	316
YNL040W	Protein of unknown function	79	455
YDL186W	Putative protein of unknown function	126	455
YGR153W	Putative protein of unknown function	175	316
YDR306C	F-box protein of unknown function	217	185
YPL216W	F-box protein of unknown function	60	157
AI5,	Uncharacterized ORF	455	273
YPL060C	Putative protein of unknown function		325
SKG3	Putative protein of unknown function	493	185
SPP41	Putative protein of unknown function	701	316
YCL002C	Putative protein of unknown function	260	86
TBS1	Putative protein of unknown function	835	157
YOR114W	Putative protein of unknown function	261	157
YLR126C	Putative protein of unknown function	212	497
SIP5	Snf1 Interacting Protein	232	248

Table S4: Novel Ssa1 crosslinked to post translationally clients found in this study

Protein A	**Protein function**	**Phosphosite position**	**Position on Ssa1**
MLP2	Nuclear basket protein connects the nuclear pore complex with the nuclear interior	S648	157
GSC2	Catalytic subunit of 1,3-beta-glucan synthase	T1406	157
INP52	Inositol polyphosphate 5-Phosphatase	S6	157

RPN6	Regulatory Particle Non-ATPase	S2	157
MTW1	Mis Twelve-like	Y86	157
SYT1	Guanine nucleotide exchange factor (GEF) for Arf proteins	T1135	157
ORC5	Origin Recognition Complex	S350/T353	157
HSP42	Small heat shock protein (sHsp) with chaperone activity	T300	157/185/316
YOX1	Homeobox transcriptional repressor	S340	185
YDR306C	F-box protein of unknown function	S213/S216	185
GTF1	Glutaminyl Transamidase subunit	T118	325
PIM1	ATP-dependent Lon protease; involved in degradation of misfolded proteins in mitochondria	S974	325
MPS3	Nuclear envelope protein	S207	448
YNL040W	Protein of unknown function	S76	455
SIR4	SIR protein involved in assembly of silent chromatin domains	T594	455
Protein A	**Protein function**	**Acetylation position**	**Position on Ssa1**
YCL002C	Unknown ORF	K272	86
ENP2	Essential Nuclear Protein	K581	157
SPP1	Set1c, PHD finger Protein	K150	157
IOC3	Isw1a has nucleosome-stimulated ATPase activity and represses transcription	K473	185
TSL1	Trehalose Synthase Long chain	K779	185
MSA1	Activator of G1-specific transcription factors MBF	K7	248
SPP41	Unknown ORF	K713	316
NAB2	Nuclear poly adenylated RNA-Binding	K410	316
PAM18	Pre sequence translocase-Associated Motor	K94	316
CWC22	Complexed with Cef1p	K168	316
SKG3	Unknown ORF	K495	325
SNT1	SANT domains	K475	325
UBP14	Ubiquitin-specific Protease	k513	325
FIN1	Filaments In between Nuclei	K79	455
MNN4	Putative positive regulator of mannosyl phosphate transferase	K245	497
ULA1	Protein that activates Rub1p (NEDD8) before neddylation	K224	509
NEJ1	Nonhomologous End-Joining defective	K283	509
HIR1	Histone Regulation	K440	521
SKY1	SR protein kinase (SRPK)	K373	536
KEL1	Kelch repeat	K891	547

Protein A	Protein function	Methylation position	Position on Ssa1
NDC80	Nuclear division cycle	R647	86
SYT1	Guanine nucleotide exchange factor (GEF)	K1113 K1125	86
YPL216W	Unknown ORF	K67	157
AIF1	Apoptosis inducing factor	K365 K71me2	157
MPH1	DNA helicase	K430	157
SGO1	Component of the spindle checkpoint	K485	316
BUR2	Cyclin for the Sgv1p (Bur1p) protein kinase	K76	316
STE11	Signal transducing MEK kinase	R305	157
CCH1	Calcium Channel Homolog	K274	325
YPL060C	Unknown ORF	K399	325
XBP1	Transcriptional repressor; binds promoter sequences of cyclin genes	K445	354
RTP1	Required for the nuclear Transport of RNA pol II	K609	354
MOB2	Activator of Cbk1p kinase	K48	455
PCL7	Pho85p cyclin	K9	497
CDC3	Cell Division Cycle	K474	521
DRS1	Putative ATP-dependent RNA helicase	R116	536
SPT21	Protein with a role in transcriptional silencing	K452 K61	547
SAP1	Putative ATPase of the AAA family	K533	547

Table S5: Yeast strains used in this study

Strain	Genotype	Reference
yAT143	MAT a (MH272) ssa1Δ ::trp1 ssa2::HisG ssa3:: ssa4::HisG::HisG (ssa1-4) [YCPlac33 SSA1]:: SSA1-HA-His3MX6	This study
yAT388	MAT α his3Δ1 leu2Δ0 lys2Δ0 ura3Δ0 SSA1-VC::His3MX6	This study
yAT392	MAT α his3Δ1 leu2Δ0 lys2Δ0 ura3Δ0 SSA1-VN::kanMX6	This study
yAT229	MATα his3Δ1 leu2Δ0 lys2Δ0 ura3Δ0 GFP RNR2:: His3MX6	Sluder et al., 2018 (27)
yAT543	MAT a (MH272) ssa1Δ ::trp1 ssa2::HisG ssa3:: ssa4::HisG::HisG (ssa1-4) [YCPlac33 SSA1]:: CCT8-HA-His3MX6	This study
yAT544	MAT a (MH272) ssa1Δ ::trp1 ssa2::HisG ssa3:: ssa4::HisG::HisG (ssa1-4) [YCPlac33 SSA1]:: PCL7-HA-His3MX6	This study
yAT545	MAT a (MH272) ssa1Δ ::trp1 ssa2::HisG ssa3:: ssa4::HisG::HisG (ssa1-4) [YCPlac33 SSA1]:: SSE1-HA-His3MX6	This study
yAT546	MAT a (MH272) ssa1Δ ::trp1 ssa2::HisG ssa3:: ssa4::HisG::HisG (ssa1-4) [YCPlac33 SSA1]:: URA8-HA-His3MX6	This study
yAT537	MAT α his 3-11,15,leu2-3,112,ura3-52,trp1-Δ1,lys2,SSA1, ssa2-1(LEU2), ssa3-1(TRP1), ssa4-2(LYS2)	Horton et al. 2001(65)

yAT538	MAT α his 3-11,15,leu2-3,112,ura3-52,trp1-Δ1,lys2,SSA1-45, ssa2-1(LEU2), ssa3-1(TRP1), ssa4-2(LYS2)	Horton et al. 2001(65)
yAT515	MATa his3Δ1 leu2Δ0 met15Δ0 ura3Δ0 PIM1-GFP::His3MX6	This study
yAT516	MATa his3Δ1 leu2Δ0 met15Δ0 ura3Δ0 PIM1 (S974A)-GFP::His3MX6	This study
yAT517	MATa his3Δ1 leu2Δ0 met15Δ0 ura3Δ0) PIM1 (S974D)-GFP::His3MX6	This study
yAT535	MATa his3Δ1 leu2Δ0 met15Δ0 ura3Δ0 MTW1-YFP::His3MX6	This study
yAT537	MATa his3Δ1 leu2Δ0 met15Δ0 ura3Δ0 MTW1 (Y86F)-YFP::His3MX6	This study
yAT512	MATa *ade2 his3 leu2 trp1 ura3 can1* FUS1::FUS1-lacZ::LEU2 *ste11*::ADE2	Harris et al., 2001(28)
yAT534	MATa ura3 leu2 trp1 his3 ssk2::LEU2 ste11Δ::HIS3	Tataebayashi et al., 2006 (44)
yAT535	MATa ura3 leu2 his3 ssk2::LEU2 ssk22::LEU2 ste11hisG ste20::kanMX6	Tatebayashi et al., 2006 (44)
yAT547	trp1::pGAP-MTS-FlucSM-mCherry:NatMX, Tom70-GFP:His3MX	Ruan L et al., 2020 (29)
yAT548	MATa ADE2 his3-11,15 leu2-3,112 LYS2 TRP1 ura3-1 PSH1 mad3Δ::kanMX6	Herrero et al., 2016 (39)

Table S6: Plasmids used in this study

Plasmid	**Description**	**Reference**
pAT51	pRS315-SSA2 promoter-His-SSA1	Truman et al., 2012 (17)
pAT381	pRS315-SSA2 promoter-FLAG-SSA1	This study
pAT679	pRS315-SSA2 promoter-FLAG-SSA1 (T295A)	This study
pAT685	pRS315-SSA2 promoter-FLAG-SSA1 (N537A)	This study
pAT681	pRS315-SSA2 promoter-FLAG-SSA1 (E540A)	This study
pATXX	pRS315-SSA2 promoter-FLAG-SSA1 (N537A, E540A)	This study
pAT784	pRS315-SSA2 promoter-FLAG-SSA1 (V435F)	This study
pAT385	6xHSE-Luciferase	Peffer et al., 2019 (66)
pAT654	pBG1085-GAL1 promoter-ZZ-HA-HIR1	Dharmacon
pAT655	pBG1085-GAL1 promoter-ZZ-HA-HIR2	Dharmacon
pAT691	pCMV-HIRA-HA	Ray-Gallet et al., 2018 (67)
pAT818	pcDNA3.2-LONP1-FLAG	Strauss et al., 2015 (68)

pAT812	pRS313-MTW1-WT-1x FLAG	Steger et al., 2020 (38)
pAT805	pEGFPN1-MIS12-GFP	Sivakumar et al., 2016 (69)
pAT727	pFD53-STE11-WT	Lamson et al., 2006 (70)
pAT736	pFD53-STE11-R305A	This study
pAT737	pFD53-STE11-R305F	This study

4.6 References

1. Rosenzweig R, Nillegoda NB, Mayer MP, Bukau B. The Hsp70 chaperone network. Nat Rev Mol Cell Biol. 2019.
2. Hartl FU, Bracher A, Hayer-Hartl M. Molecular chaperones in protein folding and proteostasis. Nature. 2011;475(7356):324-32.
3. Frydman J, Nimmesgern E, Ohtsuka K, Hartl FU. Folding of nascent polypeptide chains in a high molecular mass assembly with molecular chaperones. Nature. 1994;370(6485):111-7.
4. Radons J. The human HSP70 family of chaperones: where do we stand? Cell Stress Chaperones. 2016;21(3):379-404.
5. Rosenzweig R, Nillegoda NB, Mayer MP, Bukau B. The Hsp70 chaperone network. Nat Rev Mol Cell Biol. 2019;20(11):665-80.
6. Chirico WJ, Markey ML, Fink AL. Conformational changes of an Hsp70 molecular chaperone induced by nucleotides, polypeptides, and N-ethylmaleimide. Biochemistry. 1998;37(39):13862-70.
7. Artigues A, Iriarte A, Martinez-Carrion M. Binding to chaperones allows import of a purified mitochondrial precursor into mitochondria. J Biol Chem. 2002;277(28):25047-55.
8. Bush GL, Meyer DI. The refolding activity of the yeast heat shock proteins Ssa1 and Ssa2 defines their role in protein translocation. J Cell Biol. 1996;135(5):1229-37.
9. Nitika, Truman AW. Cracking the Chaperone Code: Cellular Roles for Hsp70 Phosphorylation. Trends Biochem Sci. 2017;42(12):932-5.
10. Millson SH, Truman AW, King V, Prodromou C, Pearl LH, Piper PW. A two-hybrid screen of the yeast proteome for Hsp90 interactors uncovers a novel Hsp90 chaperone requirement in the activity of a stress-activated mitogen-activated protein kinase, Slt2p (Mpk1p). Eukaryot Cell. 2005;4(5):849-60.
11. Truman AW, Kristjansdottir K, Wolfgeher D, Ricco N, Mayampurath A, Volchenboum SL, et al. Quantitative proteomics of the yeast Hsp70/Hsp90 interactomes during DNA damage reveal chaperone-dependent regulation of ribonucleotide reductase. J Proteomics. 2015;112:285-300.
12. Vidal M, Brachmann RK, Fattaey A, Harlow E, Boeke JD. Reverse two-hybrid and one-hybrid systems to detect dissociation of protein-protein and DNA-protein interactions. Proc Natl Acad Sci U S A. 1996;93(19):10315-20.
13. Zhao R, Davey M, Hsu YC, Kaplanek P, Tong A, Parsons AB, et al. Navigating the chaperone network: an integrative map of physical and genetic interactions mediated by the hsp90 chaperone. Cell. 2005;120(5):715-27.
14. Gentzel M, Pardo M, Subramaniam S, Stewart AF, Choudhary JS. Proteomic navigation using proximity-labeling. Methods. 2019;164-165:67-72.
15. Leitner A, Faini M, Stengel F, Aebersold R. Crosslinking and Mass Spectrometry: An Integrated Technology to Understand the Structure and Function of Molecular Machines. Trends Biochem Sci. 2016;41(1):20-32.
16. Liu F, Rijkers DT, Post H, Heck AJ. Proteome-wide profiling of protein assemblies by cross-linking mass spectrometry. Nat Methods. 2015;12(12):1179-84.

17. Truman AW, Kristjansdottir K, Wolfgeher D, Hasin N, Polier S, Zhang H, et al. CDK-dependent Hsp70 Phosphorylation controls G1 cyclin abundance and cell-cycle progression. Cell. 2012;151(6):1308-18.
18. Dubrez L, Causse S, Borges Bonan N, Dumetier B, Garrido C. Heat-shock proteins: chaperoning DNA repair. Oncogene. 2019.
19. Gupta A, Puri A, Singh P, Sonam S, Pandey R, Sharma D. The yeast stress inducible Ssa Hsp70 reduces alpha-synuclein toxicity by promoting its degradation through autophagy. PLoS Genet. 2018;14(10):e1007751.
20. Yang Y, Fiskus W, Yong B, Atadja P, Takahashi Y, Pandita TK, et al. Acetylated hsp70 and KAP1-mediated Vps34 SUMOylation is required for autophagosome creation in autophagy. Proc Natl Acad Sci U S A. 2013;110(17):6841-6.
21. Nitika, Porter CM, Truman AW, Truttmann MC. Post-translational modifications of Hsp70 family proteins: Expanding the chaperone code. J Biol Chem. 2020;295(31):10689-708.
22. Beltrao P, Albanese V, Kenner LR, Swaney DL, Burlingame A, Villen J, et al. Systematic functional prioritization of protein posttranslational modifications. Cell. 2012;150(2):413-25.
23. Catherman AD, Skinner OS, Kelleher NL. Top Down proteomics: facts and perspectives. Biochem Biophys Res Commun. 2014;445(4):683-93.
24. Dushukyan N, Dunn DM, Sager RA, Woodford MR, Loiselle DR, Daneshvar M, et al. Phosphorylation and Ubiquitination Regulate Protein Phosphatase 5 Activity and Its Prosurvival Role in Kidney Cancer. Cell Rep. 2017;21(7):1883-95.
25. Swaney DL, Beltrao P, Starita L, Guo A, Rush J, Fields S, et al. Global analysis of phosphorylation and ubiquitylation cross-talk in protein degradation. Nat Methods. 2013;10(7):676-82.
26. Liu F, Lossl P, Scheltema R, Viner R, Heck AJR. Optimized fragmentation schemes and data analysis strategies for proteome-wide cross-link identification. Nat Commun. 2017;8:15473.
27. Sluder IT, Nitika, Knighton LE, Truman AW. The Hsp70 co-chaperone Ydj1/HDJ2 regulates ribonucleotide reductase activity. PLoS Genet. 2018;14(11):e1007462.
28. Harris K, Lamson RE, Nelson B, Hughes TR, Marton MJ, Roberts CJ, et al. Role of scaffolds in MAP kinase pathway specificity revealed by custom design of pathway-dedicated signaling proteins. Curr Biol. 2001;11(23):1815-24.
29. Ruan L, McNamara JT, Zhang X, Chang AC, Zhu J, Dong Y, et al. Solid-phase inclusion as a mechanism for regulating unfolded proteins in the mitochondrial matrix. Sci Adv. 2020;6(32):eabc7288.
30. de Chaumont F, Dallongeville S, Chenouard N, Herve N, Pop S, Provoost T, et al. Icy: an open bioimage informatics platform for extended reproducible research. Nat Methods. 2012;9(7):690-6.
31. Ledesma-Fernandez E, Thorpe PH. Fluorescent foci quantitation for high-throughput analysis. J Biol Methods. 2015;2(2).
32. Sarbeng EB, Liu Q, Tian X, Yang J, Li H, Wong JL, et al. A functional DnaK dimer is essential for the efficient interaction with Hsp40 heat shock protein. J Biol Chem. 2015;290(14):8849-62.

33. Mazzoni C, Palermo V, Torella M, Falcone C. HIR1, the co-repressor of histone gene transcription of Saccharomyces cerevisiae, acts as a multicopy suppressor of the apoptotic phenotypes of the LSM4 mRNA degradation mutant. FEMS Yeast Res. 2005;5(12):1229-35.
34. Sharp JA, Rizki G, Kaufman PD. Regulation of histone deposition proteins Asf1/Hir1 by multiple DNA damage checkpoint kinases in Saccharomyces cerevisiae. Genetics. 2005;171(3):885-99.
35. Van Dyck L, Pearce DA, Sherman F. PIM1 encodes a mitochondrial ATP-dependent protease that is required for mitochondrial function in the yeast Saccharomyces cerevisiae. J Biol Chem. 1994;269(1):238-42.
36. Ruan L, Zhou C, Jin E, Kucharavy A, Zhang Y, Wen Z, et al. Cytosolic proteostasis through importing of misfolded proteins into mitochondria. Nature. 2017;543(7645):443-6.
37. Ondrovicova G, Liu T, Singh K, Tian B, Li H, Gakh O, et al. Cleavage site selection within a folded substrate by the ATP-dependent lon protease. J Biol Chem. 2005;280(26):25103-10.
38. Ghodgaonkar-Steger M, Potocnjak M, Zimniak T, Fischbock-Halwachs J, Solis-Mezarino V, Singh S, et al. C-Terminal Motifs of the MTW1 Complex Cooperatively Stabilize Outer Kinetochore Assembly in Budding Yeast. Cell Rep. 2020;32(13):108190.
39. Herrero E, Thorpe PH. Synergistic Control of Kinetochore Protein Levels by Psh1 and Ubr2. PLoS Genet. 2016;12(2):e1005855.
40. Olafsson G, Thorpe PH. Synthetic physical interactions map kinetochore regulators and regions sensitive to constitutive Cdc14 localization. Proc Natl Acad Sci U S A. 2015;112(33):10413-8.
41. Pinsky BA, Tatsutani SY, Collins KA, Biggins S. An Mtw1 complex promotes kinetochore biorientation that is monitored by the Ipl1/Aurora protein kinase. Dev Cell. 2003;5(5):735-45.
42. Petrovic A, Pasqualato S, Dube P, Krenn V, Santaguida S, Cittaro D, et al. The MIS12 complex is a protein interaction hub for outer kinetochore assembly. J Cell Biol. 2010;190(5):835-52.
43. Nishimura A, Yamamoto K, Oyama M, Kozuka-Hata H, Saito H, Tatebayashi K. Scaffold Protein Ahk1, Which Associates with Hkr1, Sho1, Ste11, and Pbs2, Inhibits Cross Talk Signaling from the Hkr1 Osmosensor to the Kss1 Mitogen-Activated Protein Kinase. Mol Cell Biol. 2016;36(7):1109-23.
44. Tatebayashi K, Yamamoto K, Tanaka K, Tomida T, Maruoka T, Kasukawa E, et al. Adaptor functions of Cdc42, Ste50, and Sho1 in the yeast osmoregulatory HOG MAPK pathway. EMBO J. 2006;25(13):3033-44.
45. Tatebayashi K, Yamamoto K, Tomida T, Nishimura A, Takayama T, Oyama M, et al. Osmostress enhances activating phosphorylation of Hog1 MAP kinase by mono-phosphorylated Pbs2 MAP2K. EMBO J. 2020;39(5):e103444.
46. Bohen SP, Kralli A, Yamamoto KR. Hold 'em and fold 'em: chaperones and signal transduction. Science. 1995;268(5215):1303-4.
47. Koegl M, Uetz P. Improving yeast two-hybrid screening systems. Brief Funct Genomic Proteomic. 2007;6(4):302-12.

48. Yugandhar K, Gupta S, Yu H. Inferring Protein-Protein Interaction Networks From Mass Spectrometry-Based Proteomic Approaches: A Mini-Review. Comput Struct Biotechnol J. 2019;17:805-11.
49. Taipale M, Tucker G, Peng J, Krykbaeva I, Lin ZY, Larsen B, et al. A quantitative chaperone interaction network reveals the architecture of cellular protein homeostasis pathways. Cell. 2014;158(2):434-48.
50. Taipale M. Quantitative Profiling of Chaperone/Client Interactions with LUMIER Assay. Methods Mol Biol. 2018;1709:47-58.
51. Chavez JD, Schweppe DK, Eng JK, Bruce JE. In Vivo Conformational Dynamics of Hsp90 and Its Interactors. Cell Chem Biol. 2016;23(6):716-26.
52. Mashaghi A, Bezrukavnikov S, Minde DP, Wentink AS, Kityk R, Zachmann-Brand B, et al. Alternative modes of client binding enable functional plasticity of Hsp70. Nature. 2016;539(7629):448-51.
53. Bertelsen EB, Chang L, Gestwicki JE, Zuiderweg ER. Solution conformation of wild-type E. coli Hsp70 (DnaK) chaperone complexed with ADP and substrate. Proc Natl Acad Sci U S A. 2009;106(21):8471-6.
54. Zhu X, Zhao X, Burkholder WF, Gragerov A, Ogata CM, Gottesman ME, et al. Structural analysis of substrate binding by the molecular chaperone DnaK. Science. 1996;272(5268):1606-14.
55. Liu Q, Li H, Yang Y, Tian X, Su J, Zhou L, et al. A disulfide-bonded DnaK dimer is maintained in an ATP-bound state. Cell Stress Chaperones. 2017;22(2):201-12.
56. Morgner N, Schmidt C, Beilsten-Edmands V, Ebong IO, Patel NA, Clerico EM, et al. Hsp70 forms antiparallel dimers stabilized by post-translational modifications to position clients for transfer to Hsp90. Cell Rep. 2015;11(5):759-69.
57. Trcka F, Durech M, Vankova P, Chmelik J, Martinkova V, Hausner J, et al. Human Stress-inducible Hsp70 Has a High Propensity to Form ATP-dependent Antiparallel Dimers That Are Differentially Regulated by Cochaperone Binding. Mol Cell Proteomics. 2019;18(2):320-37.
58. Takakuwa JE, Nitika, Knighton LE, Truman AW. Oligomerization of Hsp70: Current Perspectives on Regulation and Function. Front Mol Biosci. 2019;6(81):81.
59. Tao Y, Messer JS, Goss KH, Hart J, Bissonnette M, Chang EB. Hsp70 exerts oncogenic activity in the Apc mutant Min mouse model. Carcinogenesis. 2016;37(7):731-9.
60. O'Regan L, Sampson J, Richards MW, Knebel A, Roth D, Hood FE, et al. Hsp72 is targeted to the mitotic spindle by Nek6 to promote K-fiber assembly and mitotic progression. J Cell Biol. 2015;209(3):349-58.
61. Chen YJ, Lai KC, Kuo HH, Chow LP, Yih LH, Lee TC. HSP70 colocalizes with PLK1 at the centrosome and disturbs spindle dynamics in cells arrested in mitosis by arsenic trioxide. Arch Toxicol. 2014;88(9):1711-23.
62. Kim YE, Hipp MS, Bracher A, Hayer-Hartl M, Hartl FU. Molecular chaperone functions in protein folding and proteostasis. Annu Rev Biochem. 2013;82:323-55.
63. Piper PW, Truman AW, Millson SH, Nuttall J. Hsp90 chaperone control over transcriptional regulation by the yeast Slt2(Mpk1)p and human ERK5 mitogen-activated protein kinases (MAPKs). Biochem Soc Trans. 2006;34(Pt 5):783-5.

64. Cloutier P, Coulombe B. Regulation of molecular chaperones through post-translational modifications: decrypting the chaperone code. Biochim Biophys Acta. 2013;1829(5):443-54.
65. Horton LE, James P, Craig EA, Hensold JO. The yeast hsp70 homologue Ssa is required for translation and interacts with Sis1 and Pab1 on translating ribosomes. J Biol Chem. 2001;276(17):14426-33.
66. Peffer S, Goncalves D, Morano KA. Regulation of the Hsf1-dependent transcriptome via conserved bipartite contacts with Hsp70 promotes survival in yeast. J Biol Chem. 2019;294(32):12191-202.
67. Ray-Gallet D, Ricketts MD, Sato Y, Gupta K, Boyarchuk E, Senda T, et al. Functional activity of the H3.3 histone chaperone complex HIRA requires trimerization of the HIRA subunit. Nat Commun. 2018;9(1):3103.
68. Strauss KA, Jinks RN, Puffenberger EG, Venkatesh S, Singh K, Cheng I, et al. CODAS syndrome is associated with mutations of LONP1, encoding mitochondrial AAA+ Lon protease. Am J Hum Genet. 2015;96(1):121-35.
69. Sivakumar S, Janczyk PL, Qu Q, Brautigam CA, Stukenberg PT, Yu H, et al. The human SKA complex drives the metaphase-anaphase cell cycle transition by recruiting protein phosphatase 1 to kinetochores. Elife. 2016;5.
70. Lamson RE, Takahashi S, Winters MJ, Pryciak PM. Dual role for membrane localization in yeast MAP kinase cascade activation and its contribution to signaling fidelity. Curr Biol. 2006;16(6):618-23.

CHAPTER 5: CONCLUSIONS

Molecular chaperones are multifunctional proteins that are essential for cellular homeostasis across all kingdoms of life (194). Importantly, Hsp70 plays an important role in progression of many important human illnesses including cancer and various neurodegenerative diseases such as Alzheimer's and Huntington's disease (195, 196). The intrinsic instability in many cancer-driving proteins mean that cancer cells rely heavily on Hsp70 for their survival and function (197-200). Main challenges in studying chaperone networks in mammalian cells involve purifying complexes at native stoichiometry, determining which interactors are direct vs indirect ("bridged") and understanding how Hsp70 co-chaperones fine tune this interaction.

To address the issues of purifying chaperone complexes at native stoichiometry, we utilized CRISPR-CAS9 to integrate a FLAG-HIS at the N-terminus of the *HSC70* locus. This offers several benefits to traditional technologies including expression of the tagged protein under native promoter control, high stability (no requirement for continuous selection in antibiotic-containing media) and the tagged form of Hsc70 as the only form present in cells. This is the first example of a molecular chaperone being tagged in this way and is a useful (free) tool for the chaperone community. It is our hope that the chaperone researchers will also create similar cell lines for other chaperones and co-chaperones such as Hsp90 and the various J-proteins allowing the "epichaperome" to be studied under a myriad of different conditions.

The majority of small molecule inhibitors developed for molecular chaperones have failed clinical trials due to patient toxicity (201). The chaperone field is gradually beginning to accept that complete silencing of Hsp70 or Hsp90 function is not a viable path

forward. Rather than targeting Hsp70 itself, here we have examined the feasibility of inhibiting the Hsp70 co-chaperone DNAJA1 as a novel anticancer strategy. After performing a high throughput chemogenomic screen using NIH approved oncology drug collection cancer, we found that over 30% of tested small molecules displayed (several fold) increased potency upon loss of DNAJA1. Intriguingly, several molecules became less potent, possibly due to roles of chaperones in stabilizing negative regulators of signal transduction pathways. One interesting outcome of this work was the differential response of drugs thought to target the same proteins/pathways. Our study suggests that in fact many of these molecules are not as specific as currently thought. Overall, our data resolve nicely the apparently paradoxical role for DNAJA1 in cancer, underpinning its major function in anticancer drug resistance. Going forward, the drug combinations identified in our study may be tested in *in vivo*, in mouse models and eventually in human clinical trials. In light of the opposing effects of DNAJA1 on different anticancer molecules, this study also indicates the potential of using patient DNAJA1 status as a personalized medicine approach to design an effective anticancer therapy plan for prostate cancer patients. This study is the first in kind to examine the role of a co-chaperone in anticancer drug resistance on a larger scale. Perhaps future studies will extend this type of analysis to all co-chaperones, allowing a comprehensive understanding of the interplay between chaperones and cancer.

The majority of current large-scale interactomic technologies lack the ability to distinguish between direct and bridged interactions. This is especially problematic for delineating chaperone interactions where the protein is highly abundant, expressed throughout the cell and potentially interacts with a large number of regulators and clients. To navigate these issues, we have pioneered the use of cross-linking-based mass

spectrometry to detect the direct interactors of Hsp70 in yeast cells. Using this method, we have been able to gain fundamental new insights into Hsp70 function, including definitive evidence of Hsp70 self-association as well as multipoint client interaction. In defining a novel set of direct Hsp70 interactors which can be used to probe Hsp70 function in cells, we have also identified a suite of PTM-associated interactions. The majority of these client PTMs have not been previously observed and appear to be critical in regulation of client function. We believe that in addition to understanding chaperone function, this technology can be used to identify new low abundance, biologically important PTMs. This work forms the basis for future studies in which the direct clientome of Hsp70 (another chaperones) may be characterized under a variety of stress conditions and in disease models. Understanding the exact binding surface of chaperones with disease-causing proteins may allow the creation of novel therapies that block this interaction. Finally, in light of our work on the Chaperone code, it will be interesting to examine whether predictions can be made upon which chaperone PTMs may impact specific interactions.

Taken together, the work in this thesis provides a set of useful molecular tools and mechanistic insight in chaperone function that can be used to expand our ability to pinpoint ways to selectively manipulate chaperone function in cancer.

REFERENCES

1. Mayer MP, Bukau B. Hsp70 chaperones: cellular functions and molecular mechanism. Cell Mol Life Sci. 2005;62(6):670-84.
2. Rosenzweig R, Nillegoda NB, Mayer MP, Bukau B. The Hsp70 chaperone network. Nat Rev Mol Cell Biol. 2019.
3. Kampinga HH, Craig EA. The HSP70 chaperone machinery: J proteins as drivers of functional specificity. Nat Rev Mol Cell Biol. 2010;11(8):579-92.
4. Karakashev S, Zhu H, Yokoyama Y, Zhao B, Fatkhutdinov N, Kossenkov AV, et al. BET Bromodomain Inhibition Synergizes with PARP Inhibitor in Epithelial Ovarian Cancer. Cell Rep. 2017;21(12):3398-405.
5. Kaushik S, Cuervo AM. The coming of age of chaperone-mediated autophagy. Nature Reviews Molecular Cell Biology. 2018;19(6):365-81.
6. Sanchez E, Darvish H, Mesias R, Taghavi S, Firouzabadi SG, Walker RH, et al. Identification of a Large DNAJB2 Deletion in a Family with Spinal Muscular Atrophy and Parkinsonism. Hum Mutat. 2016;37(11):1180-9.
7. Olgiati S, Quadri M, Fang M, Rood JP, Saute JA, Chien HF, et al. DNAJC6 Mutations Associated With Early-Onset Parkinson's Disease. Ann Neurol. 2016;79(2):244-56.
8. Vilarino-Guell C, Rajput A, Milnerwood AJ, Shah B, Szu-Tu C, Trinh J, et al. DNAJC13 mutations in Parkinson disease. Hum Mol Genet. 2014;23(7):1794-801.
9. Gagliardi M, Annesi G, Procopio R, Morelli M, Iannello G, Bonapace G, et al. DNAJC13 mutation screening in patients with Parkinson's disease from South Italy. Parkinsonism Relat Disord. 2018;55:134-7.
10. Synofzik M, Haack TB, Kopajtich R, Gorza M, Rapaport D, Greiner M, et al. Absence of BiP co-chaperone DNAJC3 causes diabetes mellitus and multisystemic neurodegeneration. Am J Hum Genet. 2014;95(6):689-97.
11. Dorard C, de Thonel A, Collura A, Marisa L, Svrcek M, Lagrange A, et al. Expression of a mutant HSP110 sensitizes colorectal cancer cells to chemotherapy and improves disease prognosis. Nat Med. 2011;17(10):1283-9.
12. Norton N, Li D, Rieder MJ, Siegfried JD, Rampersaud E, Zuchner S, et al. Genome-wide studies of copy number variation and exome sequencing identify rare variants in BAG3 as a cause of dilated cardiomyopathy. Am J Hum Genet. 2011;88(3):273-82.
13. Villard E, Perret C, Gary F, Proust C, Dilanian G, Hengstenberg C, et al. A genome-wide association study identifies two loci associated with heart failure due to dilated cardiomyopathy. Eur Heart J. 2011;32(9):1065-76.
14. Cloutier P, Coulombe B. Regulation of molecular chaperones through post-translational modifications: decrypting the chaperone code. Biochim Biophys Acta. 2013;1829(5):443-54.
15. Nitika, Truman AW. Cracking the Chaperone Code: Cellular Roles for Hsp70 Phosphorylation. Trends Biochem Sci. 2017;42(12):932-5.
16. Truttmann MC, Ploegh HL. rAMPing Up Stress Signaling: Protein AMPylation in Metazoans. Trends Cell Biol. 2017;27(8):608-20.
17. Velasco L, Dublang L, Moro F, Muga A. The Complex Phosphorylation Patterns that Regulate the Activity of Hsp70 and Its Cochaperones. Int J Mol Sci. 2019;20(17).

18. Griffith AA, Holmes W. Fine Tuning: Effects of Post-Translational Modification on Hsp70 Chaperones. Int J Mol Sci. 2019;20(17).
19. Borchiellini C, Boury-Esnault N, Vacelet J, Le Parco Y. Phylogenetic analysis of the Hsp70 sequences reveals the monophyly of Metazoa and specific phylogenetic relationships between animals and fungi. Mol Biol Evol. 1998;15(6):647-55.
20. Gupta RS, Singh B. Phylogenetic analysis of 70 kD heat shock protein sequences suggests a chimeric origin for the eukaryotic cell nucleus. Curr Biol. 1994;4(12):1104-14.
21. Wu B, Hunt C, Morimoto R. Structure and expression of the human gene encoding major heat shock protein HSP70. Mol Cell Biol. 1985;5(2):330-41.
22. Werner-Washburne M, Stone DE, Craig EA. Complex interactions among members of an essential subfamily of hsp70 genes in Saccharomyces cerevisiae. Mol Cell Biol. 1987;7(7):2568-77.
23. Lotz SK, Knighton LE, Nitika, Jones GW, Truman AW. Not quite the SSAme: unique roles for the yeast cytosolic Hsp70s. Curr Genet. 2019;65(5):1127-34.
24. Boorstein WR, Craig EA. Structure and regulation of the SSA4 HSP70 gene of Saccharomyces cerevisiae. J Biol Chem. 1990;265(31):18912-21.
25. Boorstein WR, Craig EA. Transcriptional regulation of SSA3, an HSP70 gene from Saccharomyces cerevisiae. Mol Cell Biol. 1990;10(6):3262-7.
26. Werner-Washburne M, Becker J, Kosic-Smithers J, Craig EA. Yeast Hsp70 RNA levels vary in response to the physiological status of the cell. J Bacteriol. 1989;171(5):2680-8.
27. Nelson RJ, Ziegelhoffer T, Nicolet C, Werner-Washburne M, Craig EA. The translation machinery and 70 kd heat shock protein cooperate in protein synthesis. Cell. 1992;71(1):97-105.
28. Kabani M, Martineau CN. Multiple hsp70 isoforms in the eukaryotic cytosol: mere redundancy or functional specificity? Curr Genomics. 2008;9(5):338-248.
29. Brocchieri L, Conway de Macario E, Macario AJ. hsp70 genes in the human genome: Conservation and differentiation patterns predict a wide array of overlapping and specialized functions. BMC Evol Biol. 2008;8:19.
30. Vos MJ, Hageman J, Carra S, Kampinga HH. Structural and functional diversities between members of the human HSPB, HSPH, HSPA, and DNAJ chaperone families. Biochemistry. 2008;47(27):7001-11.
31. Zhu X, Zhao X, Burkholder WF, Gragerov A, Ogata CM, Gottesman ME, et al. Structural analysis of substrate binding by the molecular chaperone DnaK. Science. 1996;272(5268):1606-14.
32. Daugaard M, Rohde M, Jaattela M. The heat shock protein 70 family: Highly homologous proteins with overlapping and distinct functions. FEBS Lett. 2007;581(19):3702-10.
33. Rohde M, Daugaard M, Jensen MH, Helin K, Nylandsted J, Jaattela M. Members of the heat-shock protein 70 family promote cancer cell growth by distinct mechanisms. Genes Dev. 2005;19(5):570-82.
34. Alderson TR, Kim JH, Markley JL. Dynamical Structures of Hsp70 and Hsp70-Hsp40 Complexes. Structure. 2016;24(7):1014-30.
35. Liu T, Singh R, Rios Z, Bhushan A, Li M, Sheridan PP, et al. Tyrosine phosphorylation of HSC70 and its interaction with RFC mediates methotrexate resistance in murine L1210 leukemia cells. Cancer Lett. 2015;357(1):231-41.

36. Takakuwa JE, Nitika, Knighton LE, Truman AW. Oligomerization of Hsp70: Current Perspectives on Regulation and Function. Front Mol Biosci. 2019;6:81.
37. Trcka F, Durech M, Vankova P, Chmelik J, Martinkova V, Hausner J, et al. Human Stress-inducible Hsp70 Has a High Propensity to Form ATP-dependent Antiparallel Dimers That Are Differentially Regulated by Cochaperone Binding. Mol Cell Proteomics. 2019;18(2):320-37.
38. Sarbeng EB, Liu Q, Tian X, Yang J, Li H, Wong JL, et al. A functional DnaK dimer is essential for the efficient interaction with Hsp40 heat shock protein. J Biol Chem. 2015;290(14):8849-62.
39. Kelley WL. Molecular chaperones: How J domains turn on Hsp70s. Curr Biol. 1999;9(8):R305-8.
40. Voisine C, Craig EA, Zufall N, von Ahsen O, Pfanner N, Voos W. The protein import motor of mitochondria: unfolding and trapping of preproteins are distinct and separable functions of matrix Hsp70. Cell. 1999;97(5):565-74.
41. Takayama S, Reed JC. Molecular chaperone targeting and regulation by BAG family proteins. Nat Cell Biol. 2001;3(10):E237-41.
42. Hohfeld J, Minami Y, Hartl FU. Hip, a novel cochaperone involved in the eukaryotic Hsc70/Hsp40 reaction cycle. Cell. 1995;83(4):589-98.
43. Bascos NAD, Mayer MP, Bukau B, Landry SJ. The Hsp40 J-domain modulates Hsp70 conformation and ATPase activity with a semi-elliptical spring. Protein Sci. 2017;26(9):1838-51.
44. Malinverni D, Jost Lopez A, De Los Rios P, Hummer G, Barducci A. Modeling Hsp70/Hsp40 interaction by multi-scale molecular simulations and coevolutionary sequence analysis. Elife. 2017;6.
45. Kityk R, Kopp J, Mayer MP. Molecular Mechanism of J-Domain-Triggered ATP Hydrolysis by Hsp70 Chaperones. Mol Cell. 2018;69(2):227-37 e4.
46. Hohfeld J, Jentsch S. GrpE-like regulation of the hsc70 chaperone by the anti-apoptotic protein BAG-1. EMBO J. 1997;16(20):6209-16.
47. Nelson GM, Prapapanich V, Carrigan PE, Roberts PJ, Riggs DL, Smith DF. The heat shock protein 70 cochaperone hip enhances functional maturation of glucocorticoid receptor. Mol Endocrinol. 2004;18(7):1620-30.
48. Chen S, Smith DF. Hop as an adaptor in the heat shock protein 70 (Hsp70) and hsp90 chaperone machinery. J Biol Chem. 1998;273(52):35194-200.
49. Alvira S, Cuellar J, Rohl A, Yamamoto S, Itoh H, Alfonso C, et al. Structural characterization of the substrate transfer mechanism in Hsp70/Hsp90 folding machinery mediated by Hop. Nat Commun. 2014;5:5484.
50. Carrigan PE, Sikkink LA, Smith DF, Ramirez-Alvarado M. Domain:domain interactions within Hop, the Hsp70/Hsp90 organizing protein, are required for protein stability and structure. Protein Sci. 2006;15(3):522-32.
51. Meacham GC, Lu Z, King S, Sorscher E, Tousson A, Cyr DM. The Hdj-2/Hsc70 chaperone pair facilitates early steps in CFTR biogenesis. EMBO J. 1999;18(6):1492-505.
52. Hernando R, Manso R. Muscle fibre stress in response to exercise: synthesis, accumulation and isoform transitions of 70-kDa heat-shock proteins. Eur J Biochem. 1997;243(1-2):460-7.

53. Melling CW, Thorp DB, Milne KJ, Noble EG. Myocardial Hsp70 phosphorylation and PKC-mediated cardioprotection following exercise. Cell Stress Chaperones. 2009;14(2):141-50.
54. Gonzalez B, Manso R. Induction, modification and accumulation of HSP70s in the rat liver after acute exercise: early and late responses. J Physiol. 2004;556(Pt 2):369-85.
55. Beltrao P, Albanese V, Kenner LR, Swaney DL, Burlingame A, Villen J, et al. Systematic functional prioritization of protein posttranslational modifications. Cell. 2012;150(2):413-25.
56. Cvoro A, Dundjerski J, Trajkovic D, Matic G. The level and phosphorylation of Hsp70 in the rat liver cytosol after adrenalectomy and hyperthermia. Cell Biol Int. 1999;23(4):313-20.
57. Truman AW, Kristjansdottir K, Wolfgeher D, Hasin N, Polier S, Zhang H, et al. CDK-dependent Hsp70 Phosphorylation controls G1 cyclin abundance and cell-cycle progression. Cell. 2012;151(6):1308-18.
58. Muller P, Ruckova E, Halada P, Coates PJ, Hrstka R, Lane DP, et al. C-terminal phosphorylation of Hsp70 and Hsp90 regulates alternate binding to co-chaperones CHIP and HOP to determine cellular protein folding/degradation balances. Oncogene. 2013;32(25):3101-10.
59. Hornbeck PV, Zhang B, Murray B, Kornhauser JM, Latham V, Skrzypek E. PhosphoSitePlus, 2014: mutations, PTMs and recalibrations. Nucleic Acids Res. 2015;43(Database issue):D512-20.
60. Craig R, Cortens JP, Beavis RC. Open source system for analyzing, validating, and storing protein identification data. J Proteome Res. 2004;3(6):1234-42.
61. Pawson T, Scott JD. Protein phosphorylation in signaling--50 years and counting. Trends Biochem Sci. 2005;30(6):286-90.
62. Verghese J, Abrams J, Wang Y, Morano KA. Biology of the heat shock response and protein chaperones: budding yeast (Saccharomyces cerevisiae) as a model system. Microbiol Mol Biol Rev. 2012;76(2):115-58.
63. Eckerdt F, Strebhardt K. Polo-like kinase 1: target and regulator of anaphase-promoting complex/cyclosome-dependent proteolysis. Cancer Res. 2006;66(14):6895-8.
64. Chen YJ, Lai KC, Kuo HH, Chow LP, Yih LH, Lee TC. HSP70 colocalizes with PLK1 at the centrosome and disturbs spindle dynamics in cells arrested in mitosis by arsenic trioxide. Arch Toxicol. 2014;88(9):1711-23.
65. O'Regan L, Sampson J, Richards MW, Knebel A, Roth D, Hood FE, et al. Hsp72 is targeted to the mitotic spindle by Nek6 to promote K-fiber assembly and mitotic progression. J Cell Biol. 2015;209(3):349-58.
66. Gong X, Luo T, Deng P, Liu Z, Xiu J, Shi H, et al. Stress-induced interaction between p38 MAPK and HSP70. Biochem Biophys Res Commun. 2012;425(2):357-62.
67. Lim S, Kim DG, Kim S. ERK-dependent phosphorylation of the linker and substrate-binding domain of HSP70 increases folding activity and cell proliferation. Exp Mol Med. 2019;51(9):1-14.
68. Songyang Z, Lu KP, Kwon YT, Tsai LH, Filhol O, Cochet C, et al. A structural basis for substrate specificities of protein Ser/Thr kinases: primary sequence preference of casein kinases I and II, NIMA, phosphorylase kinase, calmodulin-dependent kinase II, CDK5, and Erk1. Mol Cell Biol. 1996;16(11):6486-93.

69. Carlson SM, Chouinard CR, Labadorf A, Lam CJ, Schmelzle K, Fraenkel E, et al. Large-scale discovery of ERK2 substrates identifies ERK-mediated transcriptional regulation by ETV3. Sci Signal. 2011;4(196):rs11.
70. Sheridan DL, Kong Y, Parker SA, Dalby KN, Turk BE. Substrate discrimination among mitogen-activated protein kinases through distinct docking sequence motifs. J Biol Chem. 2008;283(28):19511-20.
71. Miyata Y, Rauch JN, Jinwal UK, Thompson AD, Srinivasan S, Dickey CA, et al. Cysteine reactivity distinguishes redox sensing by the heat-inducible and constitutive forms of heat shock protein 70. Chem Biol. 2012;19(11):1391-9.
72. Hanahan D, Weinberg RA. Hallmarks of cancer: the next generation. Cell. 2011;144(5):646-74.
73. Matherly LH, Hou Z, Deng Y. Human reduced folate carrier: translation of basic biology to cancer etiology and therapy. Cancer Metastasis Rev. 2007;26(1):111-28.
74. Liu T, Dean A, Ashwini S, Sheridan PP, Bhushan A, Lai JC, et al. Identification and characterization of a 66-68-kDa protein as a methotrexate-binding protein in murine leukemia L1210 cells. Cell Stress Chaperones. 2013;18(2):223-34.
75. Ding CL, Xu G, Tang HL, Zhu SY, Zhao LJ, Ren H, et al. Anchoring of both PKA-RIIalpha and 14-3-3theta regulates retinoic acid induced 16 mediated phosphorylation of heat shock protein 70. Oncotarget. 2015;6(17):15540-50.
76. Fernandez-Fernandez MR, Gragera M, Ochoa-Ibarrola L, Quintana-Gallardo L, Valpuesta JM. Hsp70 - a master regulator in protein degradation. FEBS Lett. 2017;591(17):2648-60.
77. Ballinger CA, Connell P, Wu Y, Hu Z, Thompson LJ, Yin LY, et al. Identification of CHIP, a novel tetratricopeptide repeat-containing protein that interacts with heat shock proteins and negatively regulates chaperone functions. Mol Cell Biol. 1999;19(6):4535-45.
78. Zemanovic S, Ivanov MV, Ivanova LV, Bhatnagar A, Michalkiewicz T, Teng RJ, et al. Dynamic Phosphorylation of the C Terminus of Hsp70 Regulates the Mitochondrial Import of SOD2 and Redox Balance. Cell Rep. 2018;25(9):2605-16 e7.
79. Finsel I, Hilbi H. Formation of a pathogen vacuole according to Legionella pneumophila: how to kill one bird with many stones. Cell Microbiol. 2015;17(7):935-50.
80. Weissman Z, Pinsky M, Wolfgeher DJ, Kron SJ, Truman AW, Kornitzer D. Genetic analysis of Hsp70 phosphorylation sites reveals a role in Candida albicans cell and colony morphogenesis. Biochim Biophys Acta Proteins Proteom. 2020;1868(3):140135.
81. Alonso-Morales A, Gonzalez-Lopez L, Cazares-Raga FE, Cortes-Martinez L, Torres-Monzon JA, Gallegos-Perez JL, et al. Protein phosphorylation during Plasmodium berghei gametogenesis. Exp Parasitol. 2015;156:49-60.
82. Hendershot LM, Ting J, Lee AS. Identity of the immunoglobulin heavy-chain-binding protein with the 78,000-dalton glucose-regulated protein and the role of posttranslational modifications in its binding function. Mol Cell Biol. 1988;8(10):4250-6.
83. Freiden PJ, Gaut JR, Hendershot LM. Interconversion of three differentially modified and assembled forms of BiP. EMBO J. 1992;11(1):63-70.
84. Satoh M, Nakai A, Sokawa Y, Hirayoshi K, Nagata K. Modulation of the phosphorylation of glucose-regulated protein, GRP78, by transformation and inhibition of glycosylation. Exp Cell Res. 1993;205(1):76-83.

85. Woolery AR, Luong P, Broberg CA, Orth K. AMPylation: Something Old is New Again. Front Microbiol. 2010;1:113.
86. Khater S, Mohanty D. In silico identification of AMPylating enzymes and study of their divergent evolution. Sci Rep. 2015;5:10804.
87. Yarbrough ML, Li Y, Kinch LN, Grishin NV, Ball HL, Orth K. AMPylation of Rho GTPases by Vibrio VopS disrupts effector binding and downstream signaling. Science. 2009;323(5911):269-72.
88. Sreelatha A, Yee SS, Lopez VA, Park BC, Kinch LN, Pilch S, et al. Protein AMPylation by an Evolutionarily Conserved Pseudokinase. Cell. 2018;175(3):809-21 e19.
89. Kingdon HS, Shapiro BM, Stadtman ER. Regulation of glutamine synthetase. 8. ATP: glutamine synthetase adenylyltransferase, an enzyme that catalyzes alterations in the regulatory properties of glutamine synthetase. Proc Natl Acad Sci U S A. 1967;58(4):1703-10.
90. Dudkiewicz M, Szczepinska T, Grynberg M, Pawlowski K. A novel protein kinase-like domain in a selenoprotein, widespread in the tree of life. PLoS One. 2012;7(2):e32138.
91. Engel P, Goepfert A, Stanger FV, Harms A, Schmidt A, Schirmer T, et al. Adenylylation control by intra- or intermolecular active-site obstruction in Fic proteins. Nature. 2012;482(7383):107-10.
92. Casey AK, Moehlman AT, Zhang J, Servage KA, Kramer H, Orth K. Fic-mediated deAMPylation is not dependent on homodimerization and rescues toxic AMPylation in flies. J Biol Chem. 2017;292(51):21193-204.
93. Preissler S, Rato C, Perera L, Saudek V, Ron D. FICD acts bifunctionally to AMPylate and de-AMPylate the endoplasmic reticulum chaperone BiP. Nat Struct Mol Biol. 2017;24(1):23-9.
94. Sanyal A, Zbornik EA, Watson BG, Christoffer C, Ma J, Kihara D, et al. Kinetic And Structural Parameters Governing Fic-Mediated Adenylylation/AMPylation of the Hsp70 chaperone, BiP/GRP78. bioRxiv. 2018:494930.
95. Perera LA, Rato C, Yan Y, Neidhardt L, McLaughlin SH, Read RJ, et al. An oligomeric state-dependent switch in the ER enzyme FICD regulates AMPylation and deAMPylation of BiP. EMBO J. 2019;38(21):e102177.
96. Preissler S, Rato C, Chen R, Antrobus R, Ding S, Fearnley IM, et al. AMPylation matches BiP activity to client protein load in the endoplasmic reticulum. Elife. 2015;4:e12621.
97. Preissler S, Rohland L, Yan Y, Chen R, Read RJ, Ron D. AMPylation targets the rate-limiting step of BiP's ATPase cycle for its functional inactivation. Elife. 2017;6.
98. Ham H, Woolery AR, Tracy C, Stenesen D, Kramer H, Orth K. Unfolded protein response-regulated Drosophila Fic (dFic) protein reversibly AMPylates BiP chaperone during endoplasmic reticulum homeostasis. J Biol Chem. 2014;289(52):36059-69.
99. Rahman M, Ham H, Liu X, Sugiura Y, Orth K, Kramer H. Visual neurotransmission in Drosophila requires expression of Fic in glial capitate projections. Nat Neurosci. 2012;15(6):871-5.
100. Moehlman AT, Casey AK, Servage K, Orth K, Kramer H. Adaptation to constant light requires Fic-mediated AMPylation of BiP to protect against reversible photoreceptor degeneration. Elife. 2018;7.

101. Truttmann MC, Zheng X, Hanke L, Damon JR, Grootveld M, Krakowiak J, et al. Unrestrained AMPylation targets cytosolic chaperones and activates the heat shock response. Proc Natl Acad Sci U S A. 2017;114(2):E152-E60.
102. Truttmann MC, Cruz VE, Guo X, Engert C, Schwartz TU, Ploegh HL. The Caenorhabditis elegans Protein FIC-1 Is an AMPylase That Covalently Modifies Heat-Shock 70 Family Proteins, Translation Elongation Factors and Histones. PLoS Genet. 2016;12(5):e1006023.
103. Evans CG, Wisen S, Gestwicki JE. Heat shock proteins 70 and 90 inhibit early stages of amyloid beta-(1-42) aggregation in vitro. J Biol Chem. 2006;281(44):33182-91.
104. Fonte V, Kapulkin WJ, Taft A, Fluet A, Friedman D, Link CD. Interaction of intracellular beta amyloid peptide with chaperone proteins. Proc Natl Acad Sci U S A. 2002;99(14):9439-44.
105. Truttmann MC, Pincus D, Ploegh HL. Chaperone AMPylation modulates aggregation and toxicity of neurodegenerative disease-associated polypeptides. Proc Natl Acad Sci U S A. 2018;115(22):E5008-E17.
106. Klucken J, Shin Y, Masliah E, Hyman BT, McLean PJ. Hsp70 Reduces alpha-Synuclein Aggregation and Toxicity. J Biol Chem. 2004;279(24):25497-502.
107. Sanyal A, Chen AJ, Nakayasu ES, Lazar CS, Zbornik EA, Worby CA, et al. A novel link between Fic (filamentation induced by cAMP)-mediated adenylylation/AMPylation and the unfolded protein response. J Biol Chem. 2015;290(13):8482-99.
108. Krakowiak J, Zheng X, Patel N, Feder ZA, Anandhakumar J, Valerius K, et al. Hsf1 and Hsp70 constitute a two-component feedback loop that regulates the yeast heat shock response. Elife. 2018;7.
109. Kielkowski P, Buchsbaum IY, Kirsch VC, Bach NC, Drukker M, Cappello S, et al. FICD activity and AMPylation remodelling modulate human neurogenesis. Nature Communications. 2020;11(1):517.
110. Luscher B, Butepage M, Eckei L, Krieg S, Verheugd P, Shilton BH. ADP-Ribosylation, a Multifaceted Posttranslational Modification Involved in the Control of Cell Physiology in Health and Disease. Chem Rev. 2018;118(3):1092-136.
111. Cohen MS, Chang P. Insights into the biogenesis, function, and regulation of ADP-ribosylation. Nat Chem Biol. 2018;14(3):236-43.
112. Carlsson L, Lazarides E. ADP-ribosylation of the Mr 83,000 stress-inducible and glucose-regulated protein in avian and mammalian cells: modulation by heat shock and glucose starvation. Proc Natl Acad Sci U S A. 1983;80(15):4664-8.
113. Ledford BE, Leno GH. ADP-ribosylation of the molecular chaperone GRP78/BiP. Mol Cell Biochem. 1994;138(1-2):141-8.
114. Ledford BE, Jacobs DF. Translational control of ADP-ribosylation in eucaryotic cells. Eur J Biochem. 1986;161(3):661-7.
115. Dani N, Stilla A, Marchegiani A, Tamburro A, Till S, Ladurner AG, et al. Combining affinity purification by ADP-ribose-binding macro domains with mass spectrometry to define the mammalian ADP-ribosyl proteome. Proc Natl Acad Sci U S A. 2009;106(11):4243-8.
116. Rack JGM, Palazzo L, Ahel I. (ADP-ribosyl)hydrolases: structure, function, and biology. Genes Dev. 2020;34(5-6):263-84.

117. Leno GH, Ledford BE. Reversible ADP-ribosylation of the 78 kDa glucose-regulated protein. FEBS Lett. 1990;276(1-2):29-33.
118. Laitusis AL, Brostrom MA, Brostrom CO. The dynamic role of GRP78/BiP in the coordination of mRNA translation with protein processing. J Biol Chem. 1999;274(1):486-93.
119. Chambers JE, Petrova K, Tomba G, Vendruscolo M, Ron D. ADP ribosylation adapts an ER chaperone response to short-term fluctuations in unfolded protein load. J Cell Biol. 2012;198(3):371-85.
120. Staddon JM, Bouzyk MM, Rozengurt E. Interconversion of GRP78/BiP. A novel event in the action of Pasteurella multocida toxin, bombesin, and platelet-derived growth factor. J Biol Chem. 1992;267(35):25239-45.
121. Leutert M, Menzel S, Braren R, Rissiek B, Hopp AK, Nowak K, et al. Proteomic Characterization of the Heart and Skeletal Muscle Reveals Widespread Arginine ADP-Ribosylation by the ARTC1 Ectoenzyme. Cell Rep. 2018;24(7):1916-29 e5.
122. Leno GH, Ledford BE. ADP-ribosylation of the 78-kDa glucose-regulated protein during nutritional stress. Eur J Biochem. 1989;186(1-2):205-11.
123. Ouyang C, Huang TF. Inhibition of platelet aggregation by 5'-nucleotidase purified from Trimeresurus gramineus snake venom. Toxicon. 1983;21(4):491-501.
124. Rankin PW, Jacobson EL, Benjamin RC, Moss J, Jacobson MK. Quantitative studies of inhibitors of ADP-ribosylation in vitro and in vivo. J Biol Chem. 1989;264(8):4312-7.
125. Grunfeld C, Shigenaga JK. Nicotinamide and other inhibitors of ADP-ribosylation block deoxyglucose uptake in cultured cells. Biochem Biophys Res Commun. 1984;123(2):785-91.
126. Banasik M, Ueda K. Inhibitors and activators of ADP-ribosylation reactions. Mol Cell Biochem. 1994;138(1-2):185-97.
127. Narita T, Weinert BT, Choudhary C. Functions and mechanisms of non-histone protein acetylation. Nat Rev Mol Cell Biol. 2019;20(3):156-74.
128. Zheng X, Krakowiak J, Patel N, Beyzavi A, Ezike J, Khalil AS, et al. Dynamic control of Hsf1 during heat shock by a chaperone switch and phosphorylation. Elife. 2016;5.
129. Xu L, Nitika, Hasin N, Cuskelly DD, Wolfgeher D, Doyle S, et al. Rapid deacetylation of yeast Hsp70 mediates the cellular response to heat stress. Sci Rep. 2019;9(1):16260.
130. Seo JH, Park JH, Lee EJ, Vo TT, Choi H, Kim JY, et al. ARD1-mediated Hsp70 acetylation balances stress-induced protein refolding and degradation. Nat Commun. 2016;7:12882.
131. Yang Y, Fiskus W, Yong B, Atadja P, Takahashi Y, Pandita TK, et al. Acetylated hsp70 and KAP1-mediated Vps34 SUMOylation is required for autophagosome creation in autophagy. Proc Natl Acad Sci U S A. 2013;110(17):6841-6.
132. Sun F, Jiang X, Wang X, Bao Y, Feng G, Liu H, et al. Vincristine ablation of Sirt2 induces cell apoptosis and mitophagy via Hsp70 acetylation in MDA-MB-231 cells. Biochem Pharmacol. 2019;162:142-53.
133. Gao WW, Xiao RQ, Peng BL, Xu HT, Shen HF, Huang MF, et al. Arginine methylation of HSP70 regulates retinoid acid-mediated RARbeta2 gene activation. Proc Natl Acad Sci U S A. 2015;112(26):E3327-36.

134. Guo A, Gu H, Zhou J, Mulhern D, Wang Y, Lee KA, et al. Immunoaffinity enrichment and mass spectrometry analysis of protein methylation. Molecular & cellular proteomics : MCP. 2014;13(1):372-87.
135. Larsen SC, Sylvestersen KB, Mund A, Lyon D, Mullari M, Madsen MV, et al. Proteome-wide analysis of arginine monomethylation reveals widespread occurrence in human cells. Sci Signal. 2016;9(443):rs9.
136. Jakobsson ME, Moen A, Bousset L, Egge-Jacobsen W, Kernstock S, Melki R, et al. Identification and characterization of a novel human methyltransferase modulating Hsp70 protein function through lysine methylation. J Biol Chem. 2013;288(39):27752-63.
137. Cloutier P, Lavallee-Adam M, Faubert D, Blanchette M, Coulombe B. A newly uncovered group of distantly related lysine methyltransferases preferentially interact with molecular chaperones to regulate their activity. PLoS Genet. 2013;9(1):e1003210.
138. Cho HS, Shimazu T, Toyokawa G, Daigo Y, Maehara Y, Hayami S, et al. Enhanced HSP70 lysine methylation promotes proliferation of cancer cells through activation of Aurora kinase B. Nat Commun. 2012;3:1072.
139. Biggar KK, Li SS. Non-histone protein methylation as a regulator of cellular signalling and function. Nat Rev Mol Cell Biol. 2015;16(1):5-17.
140. Blanc RS, Richard S. Arginine Methylation: The Coming of Age. Mol Cell. 2017;65(1):8-24.
141. Shimazu T, Barjau J, Sohtome Y, Sodeoka M, Shinkai Y. Selenium-based S-adenosylmethionine analog reveals the mammalian seven-beta-strand methyltransferase METTL10 to be an EF1A1 lysine methyltransferase. PLoS One. 2014;9(8):e105394.
142. Jakobsson ME, Moen A, Falnes PO. Correspondence: On the enzymology and significance of HSPA1 lysine methylation. Nat Commun. 2016;7:11464.
143. Sieber J, Wieder N, Ostrosky-Frid M, Dvela-Levitt M, Aygun O, Udeshi ND, et al. Lysine trimethylation regulates 78-kDa glucose-regulated protein proteostasis during endoplasmic reticulum stress. J Biol Chem. 2017;292(46):18878-85.
144. Wang C, Arrington J, Ratliff AC, Chen J, Horton HE, Nie Y, et al. Methyltransferase-like 21c methylates and stabilizes the heat shock protein Hspa8 in type I myofibers in mice. J Biol Chem. 2019;294(37):13718-28.
145. Zhang H, Amick J, Chakravarti R, Santarriaga S, Schlanger S, McGlone C, et al. A bipartite interaction between Hsp70 and CHIP regulates ubiquitination of chaperoned client proteins. Structure. 2015;23(3):472-82.
146. Caslavka Zempel KE, Vashisht AA, Barshop WD, Wohlschlegel JA, Clarke SG. Determining the Mitochondrial Methyl Proteome in Saccharomyces cerevisiae using Heavy Methyl SILAC. J Proteome Res. 2016;15(12):4436-51.
147. Kerscher O, Felberbaum R, Hochstrasser M. Modification of proteins by ubiquitin and ubiquitin-like proteins. Annu Rev Cell Dev Biol. 2006;22:159-80.
148. Zheng N, Shabek N. Ubiquitin Ligases: Structure, Function, and Regulation. Annual review of biochemistry. 2017;86:129-57.
149. Xu P, Duong DM, Seyfried NT, Cheng D, Xie Y, Robert J, et al. Quantitative proteomics reveals the function of unconventional ubiquitin chains in proteasomal degradation. Cell. 2009;137(1):133-45.
150. Iwai K. Diverse roles of the ubiquitin system in NF-kappaB activation. Biochim Biophys Acta. 2014;1843(1):129-36.

151. Iwai K. Diverse ubiquitin signaling in NF-kappaB activation. Trends Cell Biol. 2012;22(7):355-64.
152. Thrower JS, Hoffman L, Rechsteiner M, Pickart CM. Recognition of the polyubiquitin proteolytic signal. EMBO J. 2000;19(1):94-102.
153. Kim W, Bennett EJ, Huttlin EL, Guo A, Li J, Possemato A, et al. Systematic and quantitative assessment of the ubiquitin-modified proteome. Mol Cell. 2011;44(2):325-40.
154. Shi Y, Chan DW, Jung SY, Malovannaya A, Wang Y, Qin J. A data set of human endogenous protein ubiquitination sites. Molecular & cellular proteomics : MCP. 2011;10(5):M110 002089.
155. Wagner SA, Beli P, Weinert BT, Nielsen ML, Cox J, Mann M, et al. A proteome-wide, quantitative survey of in vivo ubiquitylation sites reveals widespread regulatory roles. Molecular & cellular proteomics : MCP. 2011;10(10):M111 013284.
156. Gendron JM, Webb K, Yang B, Rising L, Zuzow N, Bennett EJ. Using the Ubiquitin-modified Proteome to Monitor Distinct and Spatially Restricted Protein Homeostasis Dysfunction. Molecular & cellular proteomics : MCP. 2016;15(8):2576-93.
157. Jiang J, Ballinger CA, Wu Y, Dai Q, Cyr DM, Hohfeld J, et al. CHIP is a U-box-dependent E3 ubiquitin ligase: identification of Hsc70 as a target for ubiquitylation. J Biol Chem. 2001;276(46):42938-44.
158. Kundrat L, Regan L. Identification of residues on Hsp70 and Hsp90 ubiquitinated by the cochaperone CHIP. J Mol Biol. 2010;395(3):587-94.
159. Morales JL, Perdew GH. Carboxyl terminus of hsc70-interacting protein (CHIP) can remodel mature aryl hydrocarbon receptor (AhR) complexes and mediate ubiquitination of both the AhR and the 90 kDa heat-shock protein (hsp90) in vitro. Biochemistry. 2007;46(2):610-21.
160. Qian SB, McDonough H, Boellmann F, Cyr DM, Patterson C. CHIP-mediated stress recovery by sequential ubiquitination of substrates and Hsp70. Nature. 2006;440(7083):551-5.
161. Soss SE, Rose KL, Hill S, Jouan S, Chazin WJ. Biochemical and Proteomic Analysis of Ubiquitination of Hsc70 and Hsp70 by the E3 Ligase CHIP. PLoS One. 2015;10(5):e0128240.
162. Moore DJ, West AB, Dikeman DA, Dawson VL, Dawson TM. Parkin mediates the degradation-independent ubiquitination of Hsp70. J Neurochem. 2008;105(5):1806-19.
163. Lin DI, Barbash O, Kumar KG, Weber JD, Harper JW, Klein-Szanto AJ, et al. Phosphorylation-dependent ubiquitination of cyclin D1 by the SCF(FBX4-alphaB crystallin) complex. Mol Cell. 2006;24(3):355-66.
164. Wang Y, Gibney PA, West JD, Morano KA. The yeast Hsp70 Ssa1 is a sensor for activation of the heat shock response by thiol-reactive compounds. Mol Biol Cell. 2012;23(17):3290-8.
165. Siegenthaler KD, Pareja KA, Wang J, Sevier CS. An unexpected role for the yeast nucleotide exchange factor Sil1 as a reductant acting on the molecular chaperone BiP. Elife. 2017;6.
166. Yang J, Zhang H, Gong W, Liu Z, Wu H, Hu W, et al. S-Glutathionylation of human inducible Hsp70 reveals a regulatory mechanism involving the C-terminal alpha-helical lid. J Biol Chem. 2020;295(24):8302-24.

167. Wang J, Sevier CS. Formation and Reversibility of BiP Protein Cysteine Oxidation Facilitate Cell Survival during and post Oxidative Stress. J Biol Chem. 2016;291(14):7541-57.
168. Poole LB. The basics of thiols and cysteines in redox biology and chemistry. Free Radic Biol Med. 2015;80:148-57.
169. Wei PC, Hsieh YH, Su MI, Jiang X, Hsu PH, Lo WT, et al. Loss of the oxidative stress sensor NPGPx compromises GRP78 chaperone activity and induces systemic disease. Mol Cell. 2012;48(5):747-59.
170. Wang J, Pareja KA, Kaiser CA, Sevier CS. Redox signaling via the molecular chaperone BiP protects cells against endoplasmic reticulum-derived oxidative stress. Elife. 2014;3:e03496.
171. Olahova M, Taylor SR, Khazaipoul S, Wang J, Morgan BA, Matsumoto K, et al. A redox-sensitive peroxiredoxin that is important for longevity has tissue- and stress-specific roles in stress resistance. Proc Natl Acad Sci U S A. 2008;105(50):19839-44.
172. Kumsta C, Thamsen M, Jakob U. Effects of oxidative stress on behavior, physiology, and the redox thiol proteome of Caenorhabditis elegans. Antioxid Redox Signal. 2011;14(6):1023-37.
173. Knoefler D, Thamsen M, Koniczek M, Niemuth NJ, Diederich AK, Jakob U. Quantitative in vivo redox sensors uncover oxidative stress as an early event in life. Mol Cell. 2012;47(5):767-76.
174. Hendriks IA, Lyon D, Su D, Skotte NH, Daniel JA, Jensen LJ, et al. Site-specific characterization of endogenous SUMOylation across species and organs. Nat Commun. 2018;9(1):2456.
175. Weinert BT, Scholz C, Wagner SA, Iesmantavicius V, Su D, Daniel JA, et al. Lysine succinylation is a frequently occurring modification in prokaryotes and eukaryotes and extensively overlaps with acetylation. Cell Rep. 2013;4(4):842-51.
176. Munk S, Sigurethsson JO, Xiao Z, Batth TS, Franciosa G, von Stechow L, et al. Proteomics Reveals Global Regulation of Protein SUMOylation by ATM and ATR Kinases during Replication Stress. Cell Rep. 2017;21(2):546-58.
177. Hendriks LEL, Dingemans AC. Heat shock protein antagonists in early stage clinical trials for NSCLC. Expert Opin Investig Drugs. 2017;26(5):541-50.
178. Bailly AP, Perrin A, Serrano-Macia M, Maghames C, Leidecker O, Trauchessec H, et al. The Balance between Mono- and NEDD8-Chains Controlled by NEDP1 upon DNA Damage Is a Regulatory Module of the HSP70 ATPase Activity. Cell Rep. 2019;29(1):212-24 e8.
179. Enchev RI, Schulman BA, Peter M. Protein neddylation: beyond cullin-RING ligases. Nat Rev Mol Cell Biol. 2015;16(1):30-44.
180. Serlidaki D, van Waarde M, Rohland L, Wentink AS, Dekker SL, Kamphuis MJ, et al. Functional diversity between HSP70 paralogs caused by variable interactions with specific co-chaperones. J Biol Chem. 2020;295(21):7301-16.
181. Khachatoorian R, Ganapathy E, Ahmadieh Y, Wheatley N, Sundberg C, Jung CL, et al. The NS5A-binding heat shock proteins HSC70 and HSP70 play distinct roles in the hepatitis C viral life cycle. Virology. 2014;454-455:118-27.
182. Reidy M, Miot M, Masison DC. Prokaryotic chaperones support yeast prions and thermotolerance and define disaggregation machinery interactions. Genetics. 2012;192(1):185-93.

183. Sharma D, Masison DC. Hsp70 structure, function, regulation and influence on yeast prions. Protein Pept Lett. 2009;16(6):571-81.
184. Sharma D, Masison DC. Single methyl group determines prion propagation and protein degradation activities of yeast heat shock protein (Hsp)-70 chaperones Ssa1p and Ssa2p. Proc Natl Acad Sci U S A. 2011;108(33):13665-70.
185. Knighton LE, Saa LP, Reitzel AM, Truman AW. Analyzing the Functionality of Non-native Hsp70 Proteins in Saccharomyces cerevisiae. Bio Protoc. 2019;9(19).
186. Morgner N, Schmidt C, Beilsten-Edmands V, Ebong IO, Patel NA, Clerico EM, et al. Hsp70 forms antiparallel dimers stabilized by post-translational modifications to position clients for transfer to Hsp90. Cell Rep. 2015;11(5):759-69.
187. Knowlton AA, Grenier M, Kirchhoff SR, Salfity M. Phosphorylation at tyrosine-524 influences nuclear accumulation of HSP72 with heat stress. Am J Physiol Heart Circ Physiol. 2000;278(6):H2143-9.
188. Woodford MR, Truman AW, Dunn DM, Jensen SM, Cotran R, Bullard R, et al. Mps1 Mediated Phosphorylation of Hsp90 Confers Renal Cell Carcinoma Sensitivity and Selectivity to Hsp90 Inhibitors. Cell Rep. 2016;14(4):872-84.
189. Rigo MM, Borges TJ, Lang BJ, Murshid A, Nitika, Wolfgeher D, et al. Host expression system modulates recombinant Hsp70 activity through post-translational modifications. FEBS J. 2020.
190. Sager RA, Woodford MR, Backe SJ, Makedon AM, Baker-Williams AJ, DiGregorio BT, et al. Post-translational Regulation of FNIP1 Creates a Rheostat for the Molecular Chaperone Hsp90. Cell Rep. 2019;26(5):1344-56 e5.
191. Gregorich ZR, Ge Y. Top-down proteomics in health and disease: challenges and opportunities. Proteomics. 2014;14(10):1195-210.
192. Bertelsen EB, Chang L, Gestwicki JE, Zuiderweg ER. Solution conformation of wild-type E. coli Hsp70 (DnaK) chaperone complexed with ADP and substrate. Proc Natl Acad Sci U S A. 2009;106(21):8471-6.
193. Larkin MA, Blackshields G, Brown NP, Chenna R, McGettigan PA, McWilliam H, et al. Clustal W and Clustal X version 2.0. Bioinformatics. 2007;23(21):2947-8.
194. Radons J. The human HSP70 family of chaperones: where do we stand? Cell Stress Chaperones. 2016;21(3):379-404.
195. Ciechanover A, Kwon YT. Protein Quality Control by Molecular Chaperones in Neurodegeneration. Front Neurosci. 2017;11:185.
196. Brehme M, Voisine C. Model systems of protein-misfolding diseases reveal chaperone modifiers of proteotoxicity. Dis Model Mech. 2016;9(8):823-38.
197. Nitika, Blackman JS, Knighton LE, Takakuwa JE, Calderwood SK, Truman AW. Chemogenomic screening identifies the Hsp70 co-chaperone DNAJA1 as a hub for anticancer drug resistance. Sci Rep. 2020;10(1):13831.
198. Knighton LE, Delgado LE, Truman AW. Novel insights into molecular chaperone regulation of ribonucleotide reductase. Curr Genet. 2019;65(2):477-82.
199. Wu J, Liu T, Rios Z, Mei Q, Lin X, Cao S. Heat Shock Proteins and Cancer. Trends Pharmacol Sci. 2017;38(3):226-56.
200. Sherman MY, Gabai VL. Hsp70 in cancer: back to the future. Oncogene. 2015;34(32):4153-61.
201. Schlecht R, Scholz SR, Dahmen H, Wegener A, Sirrenberg C, Musil D, et al. Functional analysis of Hsp70 inhibitors. PLoS One. 2013;8(11):e78443.

APPENDIX- CONTRIBUTIONS, HONORS AND AWARDS

PEER-REVIEWED PUBLICATIONS:

1) **Nitika**, Blackman, J.S., Knighton, L.E., Takakuwa, J. E., Calderwood S.K. and Truman A. W.* Chemogenomic screening identifies the Hsp70 co-chaperone HDJ2 as a hub for anticancer drug resistance. Scientific Reports, 2020. doi.org/10.1038/s41598-020-70764-x. (**Impact factor: 4.0**)

2) **Nitika**, Porter C.M., Truman A.W**.** and Truttmann M.C. Hsp70 post-translational modifications: Expanding the chaperone code. Journal of Biological Chemistry, 2020. doi: 10.1074/jbc.REV120.011666. (**Impact factor: 4.2**)

3) Jeffries A.M., **Nitika**, Truman A.W. and Marriott I. The intracellular DNA sensors cGAS and IFI16 do not mediate effective antiviral immune responses to HSV-1 in human microglial cells. Journal of Neurovirology, 2020. doi:10.1007/s13365-020-00852-1. (**Impact factor: 2.5**)

4) Rigo M.M, Borges T.J., Murshid A., **Nitika**, Wolfgeher D., Calderwood S.K., Truman A.W., Bonorino C. Host expression system modulates recombinant Hsp70 activity through post-translational modifications. FEBS Journal, 2020. doi.org/10.1111/febs.15279 (Published Cover Illustration). (**Impact factor: 4.7**)

5) Xu L., **Nitika**, Hasin N., Cuskelly D.D., Doyle S., Moynagh P., Perrett S., Truman A.W., Jones G.W. Rapid deacetylation of yeast Hsp70 mediates the cellular response to heat stress. Scientific Reports, November 2019. doi:10.1038/s41598-019-52545-3. Recommended on *Faculty of 1000* (https://f1000.com/prime/736877290). (**Impact factor: 4.0**)

6) Knighton L.E., **Nitika**, Wolfgeher D., Reitzel A.M., Truman A.W. Dataset of Nematostella vectensis Hsp70 isoform interactomes upon heat shock. Data in Brief 2019. (**Impact factor: 0.9**)

7) Takakuwa J., **Nitika**, Knighton L. E., and Truman A.W. Oligomerization of Hsp70: current perspectives on regulation and function. Frontiers in Molecular Biosciences, 2019. doi:10.3389/fmolb.2019.00081. (**Impact factor: 3.5**)

8) Knighton L. K., **Nitika**, Waller S.J., Storm O., Reitzel A.M. and Truman A.W. Dynamic remodeling of the interactomes of *Nematostella vectensis* Hsp70 isoforms under heat shock. Journal of Proteomics, 2019. doi: 10.1016/j.jprot.2019.103416. (**Impact factor: 3.5**)

9) Lotz S.K., Knighton L.E., **Nitika**, and A.W. Truman. Not quite the SSAme: unique roles for the yeast cytosolic Hsp70s.Current Genetics, 2019. doi: 10.1007/s00294-019-00978-8. (**Impact factor: 3.4**)

10) Sluder I.T.*, **Nitika***, Knighton L.E., and Truman A.W. The Ydj1/HDJ2 co-chaperone is a novel regulator of ribonucleotide reductase activity. PLOS Genetics, 2018.doi: 10.1371/journal.pgen.1007462. (*authors contributed equally). (**Impact factor: 5.5**)

11) **Nitika** and Truman A.W. Cracking the chaperone code: cellular roles for Hsp70 phosphorylation. Trends in Biochemical Sciences, 2017.doi: 10.1016/j.tibs.2017.10.002. 2017. (**Impact factor: 14.2**)

12) **Nitika** and Truman A.W. Endogenous Epitope Tagging of Heat Shock Protein 70 Isoform Hsc70 using CRISPR/Cas9. Cell Stress Chaperones, 2017.doi: 10.1007/s12192-017-0845-2. (**Impact factor: 2.7**)

Works in Progress

1. Grover P., Nath S., Bose M., Sanders A.J., Brouwer C., **Nitika**, Zhou R., Yazdanifar M., Ahmad M., Wu, S.T., Truman A.W. and P. Mukherjee. Tumor-Associated MUC1 Regulates TGF-β signaling and function in Pancreatic Ductal Adenocarcinoma.(https://www.biorxiv.org/content/10.1101/2020.04.29.068577v1.abstract)

2. Knighton, L.E.†, **Nitika**†, Shrader C. and Truman A.W. Hsp70 isoform-specific regulation of Ribonucleotide reductase. (†authors contributed equally) (Expected submission: May 2021*)*

3. **Nitika**, Sikora J., Thomas P., Fornelli L., Knighton, L.E. , Ruan L., Li R., Almouzni G., Kelleher N. and Truman A.W. An Atlas of Diverse PTM-Mediated Hsp70 Functions Uncovered Using Structural Proteomics. (Expect submission: April 2021)

Published Abstracts

Nitika, Donald J. Wolfgeher, Pinku Mukherjee, Andrew W. Truman. Alterations in the HSP70 interactome are induced by overexpression of MUC1 in pancreatic cancer [abstract]. In: Proceedings of the American Association for Cancer Research Annual Meeting 2018; 2018 Apr 14-18; Chicago, IL. Philadelphia (PA): AACR; Cancer Res 2018;78(13 Suppl): Abstract nr 2697.

RECENT HONORS AND AWARDS:

2020: Finalist for Three Minute Thesis Competition, UNCC
2020: The Graduate School Summer Fellowship, UNCC
2020: UNCC Outstanding Graduate Teaching Assistant Award
2019: Nominated for NIH F99/K00 fellowship from UNCC
2019: Noteworthy research project Laura Bassi Scholarship
2019: The Graduate School Summer Fellowship, UNCC
2019: AAUW Doctoral Dissertation Fellowship Program (Alternate)
2019: **2nd Prize**, Postdoctoral and Graduate Student Category, Poster Competition Annual North Carolina Research Campus Catalyst Spring Symposium, NC
2019: UNCC Graduate and Professional Student Government Travel Award
2018: UNCC Graduate and Professional Student Government Travel Award
2018: Sigma Xi Grants-in-Aid of Research Award
2018: Awarded Excellence in Research Award in the Department of Biological Sciences
2018: Nominated for Best Graduate Teaching Assistant Award at UNCC
2018: **2nd Prize**, Postdoctoral and Graduate Student Category, Poster Competition North Carolina Research Campus Catalyst Spring Symposium, NC, USA
2018: The Center for Biomedical Engineering and Science Graduate Travel Award
2017: UNCC Fellowship Application Incentive Program Award
2017: UNCC Graduate and Professional Student Government Travel Award
2017: Best Teaching Assistant in Department of Biological Sciences

Professional Memberships:

2019-present: Member of American Society for Cell Biology.
2019-present: Member of Genetics Society of America.
2018-present: Member of Graduate Women in Science.
2017-present: Member of American Association for Cancer Research.
2016-present: Member of Society for In vitro Biology.
2016-present: Member of North Carolina Academy of Sciences.
2016-present: Member of Cell Stress and Chaperone Society International.

Service:

2021-present: Reviewer for Cell Stress and Chaperone Society International.
2021-present: Reviewer for Frontiers in Molecular Biosciences.
2019-present: Reviewer for Dove Press Medical Journals.
2018-present: Reviewer for PLOS ONE.

Outreach:

2019-present: Founder and President, UNCC Career Ladder Program

• Provide graduate students with a step-by-step approach to career development, and to encourage a peer support network.

• Coordinated weekly seminars and workshops that centered on career development such as panel discussions, networking and mock interview sessions.

05/2018-present: Guest Speaker

• Teaching science and research to elementary, middle and high school students in Mecklenberg county, NC area.

• Teaching High school students including women and underrepresented students for Project GENES summer camp at Pfeiffer University.

08/2018-08/2020:

• Volunteer for SPARC program (STEM Persistence and Retention via Curricula, Centralization, Cohorts and Collaboration Project)

• Assisting community college transfer students who enter college with aspirations for biomedical careers prepare for the processes of science.

Media Coverage:

https://inside.uncc.edu/featured-stories/cancer-research-hands

https://graduateschool.uncc.edu/news/biology-geography-graduate-students-honored-top-teaching-assistants